

Manuscript Number: JMPG-D-19-01287R3

Title: Geological settings and controls of fluid migration and associated seafloor seepage features in the north Irish Sea

Article Type: Full Length Article

Keywords: pockmark, seabed mounds, fluid seepage, MDAC, mud diapir, geohazards, ecological conservation, offshore infrastructure

Corresponding Author: Dr. Mark Coughlan,

Corresponding Author's Institution: Irish Centre for Research in Applied Geoscience

First Author: Mark Coughlan

Order of Authors: Mark Coughlan; Srikumar Roy; Conor O'Sullivan; Annika Clements; Ronan O'Toole; Ruth Plets

Abstract: Shallow gas accumulation in unconsolidated Quaternary sediments, and associated seepage at the seafloor, is widespread in the north Irish Sea. This study integrates high-resolution seafloor bathymetry and sub-surface geophysical data to investigate shallow gas accumulations and possible fluid (gas and/or liquids) migration pathways to the seafloor in the northern part of the Irish Sea. Shallow gas occurs broadly in two geological settings: the Codling Fault Zone and the Western Irish Sea Mud Belt. The gas has been recognised to accumulate in both sandy and muddy Quaternary marine near-surface sediments and is characterised by three characteristic sub-bottom acoustic features: i) enhanced reflections, ii) acoustic turbid zones, and iii) acoustic blanking. The seepage of shallow gas at the seafloor has resulted in the formation of morphological features including methane-derived authigenic carbonates, seabed mounds and pockmarks. In many instances, the evidence for this gas as biogenic or thermogenic in origin is inconclusive. Two distinct types of pockmarks are recorded in the Western Irish Mud Belt: pockmarks with a relatively flat centre, and pockmarks with a central mound. Based on our observation and existing models, we infer that the formation of a carbonate crust at the seabed surface, is needed as a precursor for the creation of such mounds within pockmarks. The formation processes are interpreted to be different for sandy versus muddy sediments, due to variability in erodibility and sealing capacities of the substrate. We suggest that the origin of these features is linked to the presence of deeper hydrocarbon source rocks with existing and reactivated faults forming fluid migration pathways to the surface. This in turn could indicate a mixed thermogenic-biogenic origin for seep-related structures in the study area. These features have significant implications for the future development of offshore infrastructure including marine renewable energy as well as for seabed ecology and conservation efforts in the Irish Sea.

Research Data Related to this Submission

There are no linked research data sets for this submission. The following reason is given:
Data will be made available on request

Dublin, 13th October 2020

1 Dear Editor,
2

3
4 Having put considerable effort into addressing the previous set of comments, my co-authors and I are
5 disappointed that the manuscript has not been accepted in its current format. However, we appreciate
6 the efforts of both you and your reviewers and thank you for the time taken in making our manuscript
7 ultimately more robust.
8

9
10 Having reviewed and approached the latest set of comments, we feel there is either a degree of confusion
11 on behalf of the reviewers, or miscommunication on our part, with regard to the aims and objectives of
12 the study, as well as the limitations of the dataset we have. As we reiterate later, currently relating to the
13 Irish Sea there are a number of separate papers which focus on morphological features at the seabed that
14 represent fluid/gas seepage and expulsion, as well as shallow expressions of gas accumulation (e.g.
15 O'Reilly et al. (2014) and Van Landeghem et al. (2015)). These papers generally suggest a mixed
16 biogenic and thermogenic component to the gas-related feature that is described. With regard to the
17 thermogenic component, it is generally proposed and accepted that hydrocarbons generated at depth
18 migrate along structural lineaments (i.e. faults) to the shallow subsurface. To our knowledge, there is no
19 current geological model that integrates bedrock geology, hydrocarbon sources, structural geology,
20 Quaternary geology and seafloor morphology in the Irish Sea. This manuscript aims to do just that in
21 order to create a framework in which to study further aspects of the fluid migration process and feature
22 formation. The reviewers all make relevant observations and suggestions of further work which, we feel,
23 this framework will facilitate as part of future studies, but are currently outside the scope of this
24 particular study.
25
26

27
28 With that in mind, we have endeavored to address each of the comments made by both reviewers, whilst
29 more clearly detailing our aims and objectives as well as the limitations of our data with
30 recommendations for further work. Below we make specific responses to each comment raised.
31

32
33 We hope that this will be agreeable with you and your reviewers and we would implore you to make a
34 decision on this manuscript either way.
35
36

37 Kind Regards

38
39 Mark Coughlan (on behalf of the co-authors)
40
41
42
43
44
45
46
47
48
49
50
51
52
53
54
55
56
57
58
59
60
61
62
63
64
65

1
2
3
4 **Reviewer 3**
5

- 6 1) *Rev3 feels that the paper still lacks of clear evidence of fluid flow to support the arguments. To Rev3,*
7 *most of the evidence is not related to migration of gas (such as the seismic amplitude anomalies)*
8 *and most of the seabed features are enhanced by using contrasting color.*
9

10
11 This paper illustrates sub-surface acoustic anomalies and seabed morphological features, which are
12 remnants of fluid flow, migration, and seepage at the seafloor. Our study certainly lacks concrete
13 evidence of fluid flow and seepage such as geochemical and ROV video/image grabs. However, the
14 geophysical datasets used in this study have provided several sites of interest which we anticipate will
15 be the target of future sampling cruises in the coming years. There are several scientific publications
16 which, showcase acoustic and geomorphological analysis of fluid flow and seepage features.
17 Addressing to Rev3's comments on "seabed features are enhanced by using contrasting color", we fail
18 to see how they are considering we use standard colour schemes. Furthermore, we provide bathymetric
19 profiles of the seabed features discussed to exhibit their cross-sectional geometry. Nevertheless, if the
20 Editor agrees we can change the colour-scale.
21
22

23
24 With regards to seismic amplitude anomalies (presumably referring to the seabed brightening in Fig.
25 3), this is evident locally above the termination of the faults. Moreover, the entire section is presented
26 to highlight extent of the brightening in proximity to the faults and shows the difference between
27 normal-amplitude and high- amplitude zones within the same stratigraphic horizon. This was done with
28 the express intention to demonstrate that this is not a lithological feature and to not mislead the reader.
29 We would appreciate if the Editor would make a decision on whether the evidence presented is
30 sufficient.
31
32

- 33
34 2) *Rev3 also states that most of the pockmarks, mounds and depressions are less than a meter in height*
35 *and several hundreds of meters wide ("the authors cite works, e.g., O'Reilly et al., 2014 where*
36 *carbonate mounds of 5-10 meters are shown in the same area, so I am wondering why they do not*
37 *take into account those studies to verify their interpretation").*
38
39

40 Most of the pockmarks are less than a metre in height, which is consistent with other descriptions of
41 pockmarks in Irish waters referenced in the text (Line 97: Croker et al., 2005; Games, 2001; Szpak
42 et al., 2015, 2012). In the tabulated data regarding pockmark morphology, it is clear that all pockmarks
43 bar one are under 200 m in diameter with the majority under 100 m. Only one pockmark is hundreds
44 of metres wide, and in Fig. 11 its outline has been marked by contoured lines to highlight its elliptical
45 morphology. However, we have decided to remove this figure and related text from this manuscript,
46 after critical comments from Rev3.
47
48

49
50 With regards to the carbonate mounds, we clearly refer to the interpretation documented by O'Reilly
51 et al. (2014) and Van Landeghem et al. (2015) in lines 252-254 (of our previous submission) while
52 drawing our interpretations on the carbonate mounds. It seems that Rev3 might have missed these
53 lines. The mounds we illustrate in this study are not less than a meter, but 8-16 m high and 60 m in
54 diameter.
55
56

- 57 3) *The authors just imply that all of the features observed are gas related, with a proposed model that*
58 *does not take into account any sort of mechanism for which gas migrate along fault (focused) and*
59 *then suddenly as a front.*
60
61
62
63
64
65

1
2
3
4
5
6 Yes, we do propose that reactivated faults allow fluids to migrate from depth to the near surface. This
7 migration of fluids (including gas), along faults is a well-described and generally accepted process,
8 owing to factors such as, higher permeability along faults, buoyancy, and differential pressure. These
9 faults are Cenozoic or older in age, therefore they typically terminated at or near the boundary with
10 the base of the Quaternary units. Therefore, the continued migration of gas, or any fluid, towards the
11 surface or laterally within the Quaternary units will depend on the petrophysical and geomechanical
12 properties of those younger units.
13

14
15 We appreciate that in Lines 108-111 and 345-348 we could have been clearer in our objectives, scope
16 and the limitations of this study. To date in the Irish Sea, numerous studies have described seabed
17 morphological features linked to gas/fluid expulsion or seepage. The majority of these studies
18 propose a thermogenic gas component and reference possible migratory pathways (i.e. faults) from
19 deeper stratigraphic layers (source or reservoir rocks) to the surface, without offering actual evidence
20 of fault systems (fluid migration pathways). Ultimately, the aim of this paper is the establishment of a
21 geological framework incorporating bedrock geology, hydrocarbon source rocks, structural geology
22 (faults), Quaternary geology and seafloor morphology in the Irish Sea which would allow
23 investigation of subsurface fluid flow mechanisms.
24
25

26
27 We mention in the Introduction of the manuscript, that there is a mixed thermogenic and biogenic
28 signatures documents in the CFZ and the WISMB. We also mention the thermogenic origin of the gas
29 in the CFZ area which has migrated along faults to reach shallow stratigraphic layers and results in
30 gas fronts and other seepage features. So, it was already evident that fluids (thermogenic gas) had a
31 deeper source and used fault conduits to reach shallow sub-seabed sediments. However, as suggested
32 by Rev3 and the Editor, we have now added this in the discussion of the proposed model for the
33 formation of mounds and pockmarks.
34
35

- 36
37 4) *Lastly, the author simply do not explain that pockmarks and mounds and other features are related to*
38 *different type of fluid migration.*
39

40 We have now discussed the alternative formation mechanisms of pockmarks, i.e., seepage of pore-
41 water (Harrington, 1985) – this is likely possible – particularly due to the lack of geochemical data at
42 present to support gas seepage from the pockmarks; and fresh-water ice rafting (Paull et al., 1999) –
43 which is unlikely in the current geological setting.
44
45

46
47 Reviewer 3 in-manuscript comments
48

49 *Line 80-81: gas is more compressible than water. sediments might compact more if a substantial amount*
50 *of water is replaced by gas....*

51 - We are merely highlighting what is mentioned in that reference. This is not our theory.
52

53
54 *Line 98-99: I am wondering whether other references for the formation of pockmark can be used...*

55 - This reference refers specifically to Irish Sea pockmarks previously studied, we are happy to consider
56 other references offered by the reviewer.
57

58 *Line 312-313: this depression has just a 0.8 m relief over a distance of 850...this is not a pockmark!*

59 - Again, we feel this fits with the range of previously described pockmarks referenced in the text.
60
61
62
63
64
65

1
2
3
4
5
6 *Line 314-316: I disagree*

7 - Subjective, but we have removed this inference for the sake of progressing the manuscript.
8

9 *Line 395-396: This is very speculative. The seabed shows a clear subsidence that can produce space and*
10 *increase the thickness of the near-seabed sediments, and from here produce tuning anomalies. If long*
11 *migration from the deeper part of the basin is invoked, I am wondering why no gas is visible underneath*
12 *these amplification. This is to me a very weak argument.*
13

14 - The text has been amended to address this in Lines 402-407
15

16 *Line 419: No, it does not!*

17 - Text amended
18
19

20 **Reviewer 5**

21
22 1) *It is important to clarify the processing strategy which has been used for those seismic data: if some*
23 *amplitude preservation type processing has not been applied (excluding any modification of the*
24 *amplitude calibration or NMO) to me the amplitude analysis through the stacked trace can produce*
25 *ambiguities. I will clarify my comments a bit more precisely further on point “xy”.*
26

27 To reiterate, the sub-bottom profiler data presented is single-channel. All processing steps have been
28 outlined in the “Sub-bottom acoustic data” section of the manuscript, including the velocity values
29 used
30

31
32 2) Figure 6b

33 - *Multibeam : The proportion of acoustic energy reflected back from the seabed is determined by the*
34 *impedance contrast, sometimes referred to as 'hardness' and apparent surface roughness scale. the*
35 *question is how the dB intensity variation can be correlated to gas content other than hardness or*
36 *roughness of the seabed. and this is where i believe the author should better discuss their results.*
37 *There is a huge lot of literature which generally assign high backscatter intensity with rock or*
38 *coarse-grained sediment, and low backscatter intensity characterizes finer grained sediments. But*
39 *given the nature of the seabed and the physics nature of the backscatter variation a dB relative scale*
40 *is not enough to add petrophysics values to the images. without ground-truthing it is not possible to*
41 *determine the exact nature of the specific substrates. So Fig 6B i am questioning what in reality*
42 *figure 6b is telling to us. While the other images included in Fig 6 are seabed morphological maps 6b*
43 *it is not simply that. The authors should make some effort to clarify the nature of this backscattered*
44 *signal or not include this figures. In fact if the two mound , at seabed condition where compaction is*
45 *excluded, are saturated by gas..they should soften the p sonar impedance and therefore i expect to*
46 *have the way around in term of signal: not shadowing. so it has to be a hardening but the fluid*
47 *content being secondary here. To me the nature of the mounds remains very speculative..*
48
49

50
51 To be clear, in this study we use the multibeam backscatter data as a means to identify areas of seabed
52 hardness relative to surrounding softer substrate (coarse-grained sediments vs. soft sediments), and
53 not a means to identify gas-saturated sediments. We agree with Reviewer 5 in that, ultimately, these
54 features need to be ground-truth. But, in the absence of such data (ROV images of the mounds), we
55 refer to previous studies where similar mounds in the vicinity of our study area have been confirmed
56 as remnants of gas seepage (i.e. O'Reilly et al., (2014); Van Landeghem et al., 2015). Hence, our
57 interpretation of the features in Figure 6 is in keeping with those of O'Reilly et al. (2014); Van
58 Landeghem et al. (2015) for this area, as indicated in the main text of the manuscript.
59
60
61
62
63
64
65

- 1
2
3
4
5
6 3) *Fig 11 B. the same consideration apply to figure 11 B. But I do not exclude the proposed*
7 *interpretation, of carbonate precipitation which geologically (given the strat context given by the*
8 *authors) and petrophysically is plausible.*
9

10 Again we agree that, ideally, this would be groundtruthed, but we have no such data at present. In any
11 case Fig. 11 has been removed to negate further confusion.
12

- 13
14 4) *Fig 9 ; how is it produce the surface with colour scale in mbsf (so in depth). ? what are the data*
15 *source for this surface? the author refer to 2D seismic and sparkers line..buty no other 3D source of*
16 *data*
17

18 The 3D surface of the depth to the top of shallow gas displayed in Fig. 9 was generated from a
19 sparker seismic grid detailed in Fig. 1 of Coughlan et al. (2019). We hope that the editor would agree
20 to the fact that we can generate a 3D surface from a dense grid of 2D sparker seismic lines. We have
21 added additional text in the figure caption of Fig. 9 to emphasize the same. To avoid unnecessary
22 replication, the reader is referred to that paper for details of the data used and processing steps (Lines
23 292-294).
24
25

- 26
27 5) *Figs 10 ; those to me represent crucial images. they are sparker seismic lines crossing the potential*
28 *top of a gas cumulations surrounded by pockmarks. What I do not find that convincing is the seismic*
29 *expression of what the authors call Enhanced reflections:*
30 *the enhanced reflection in figure 10b are all of the same polarity of the seabed..which is not what i*
31 *expect in case of gas cumulation in a shallow environment whenre unconsolidated shale/sand should*
32 *roughly respond with shale stronger than sand and therefore any sand saturated by gas produce*
33 *reflector with reverse polarity respect to the seabed. I am not sure they represent a convincing*
34 *stacked reflection (or what in the literature Foschi et al., define amplitude anomalies stacked*
35 *structure) deriving from gas anomalies. I believe the authors should more precisely discuss all the*
36 *options out of the what the data proposed are indicating. Moreover i believe that some sort of partial*
37 *stack or AVO should be added in one of those enhanced reflectors and cross the major mounds as gas*
38 *has in the shallow context a crystal clear footprint in the AVO.*
39
40
41
42

43 Firstly, in relation to Fig. 10, it is important to note that the data presented here is shallow (<50 m)
44 single-channel sparker data, and not conventional 2D multichannel seismic data – where we look for
45 polarity reversals as an indicator to the presence of shallow gas or gas hydrates. AVO analysis is not
46 feasible on single-channel sparker data, as far as we are aware of.
47

48
49 With regards to the enhanced reflectors, these occur within localised areas of acoustic turbidity, and
50 above zones of acoustic blanking on the seismic profile. This is consistent across a number of seismic
51 profiles from this area presented in this paper and Coughlan et al. (2019). The presence of acoustic
52 turbidity and blanking infer the presence of shallow gas, which is why we are presenting this
53 evidence. Our identification of features as “enhanced reflection” horizons is consistent with other
54 work (i.e. Judd and Hovland, 1992), but if Reviewer 5 wishes to direct us towards additional literature
55 in this area we will gladly review and consider it. For now, our main concern would be that there is
56 agreement on the presence of shallow gas, enhanced reflections notwithstanding.
57
58
59
60
61
62
63
64
65

1
2
3
4 6) *the only image that i found convincing is figure 14. it shows the only clear potential gas chimney and*
5 *acoustic blanketing..suggesting that some of those feature imaged in figure 13 may represent*
6 *pockmark out of other (the linea sequence of seabed mounds may still represent sedimentary*
7 *features..) which are not that convincing*
8
9

10 We are slightly confused by this comment. Our understanding is that the reviewer is satisfied with our
11 interpretation of shallow gas at Queenie Corner from the seismic profile and that of gas chimneys
12 (which clearly cause seabed mounds on the same profiles), but maintains the corresponding features
13 on bathymetric data may still be sedimentary (Location of seismic line Fig. 14 is shown on Fig. 13
14 clearly). We feel that there is enough evidence to spatially link the subsurface gas accumulation
15 (imaged as enhanced reflections and turbidity zones) and gas migration (imaged as gas chimneys) in
16 Fig. 14 to the seafloor mounds in Fig. 13. Of course they may still represent sedimentary features as
17 the reviewer suggests, but again we suggest the evidence of shallow gas beneath the mounds is
18 compelling, and in lieu of other available data, this interpretation is the most plausible in our view. As
19 the reviewer mentions about the linearity of the mounds, similar seabed mound features, 2-6 km long
20 seabed mounds have been documented in the Alboran Sea owing to thermogenic fluid migration
21 (Comas and Pinheiro, 2007)
22
23
24
25

26 7) *So i believe that the authors at this stage should put some more effort at describing the data*
27 *proposed and on that ground discuss all the potential implication of those ambiguities*
28 *Overall the paper is extremely interesting, in fact I like the discussion of the implication of the*
29 *interpretation and seismic within a site survey approach which should in fact , if this is the message*
30 *the authors would like to convey, have been introduced at the start: an overview of the issues with*
31 *reconnaissance of the shallow gas but also the application of those techniques in a contest of site*
32 *surveying and de risking. there a few paper on that subject and in the future more will appear. In this*
33 *context a failure by the authors in convincing that all those mound or enhanced reflections features*
34 *may really represent gas intrusion should not hinder the paper: in fact it should remain a nice*
35 *rigorous case history showing the problem of ambiguities in a shallow context where the data*
36 *available are multibeam sonar, sparkers and only a limited amount of good conventional seismic*
37 *data may not be crystal clear.*
38
39
40

41 We agree with Reviewer 5 on this point and appreciate their comments and suggestions. We have
42 taken these under consideration and made the following revisions accordingly:
43

- 44 1. We have added a section in the Discussion on “Data and geological model limitations” where
45 we discuss the limitations of the data used and the ambiguities introduced;
- 46 2. Made recommendations on future data collection in the Conclusions and Recommendations
47 section to overcome these ambiguities.
48
49

50 The Lead Author would also like to offer that, on the basis of the limitations of the data highlighted,
51 an additional survey in this area was undertaken in July 2020 using targeted site investigation
52 techniques (including multichannel sparker seismic) which should clarify some of the ambiguities
53 mentioned in this study. The data from this survey is part of an ongoing project, analysis of the
54 acquired data would take considerable amount of time, and cannot be completed in the near future
55 (hence not be included in this study).
56
57

58 References
59
60
61
62
63
64
65

1
2
3
4
5
6
7
8
9
10
11
12
13
14
15
16
17
18
19
20
21
22
23
24
25
26
27
28
29
30
31
32
33
34
35
36
37
38
39
40
41
42
43
44
45
46
47
48
49
50
51
52
53
54
55
56
57
58
59
60
61
62
63
64
65

Comas, M., and Pinheiro, L. M., Discovery of carbonate mounds in the Alboran Sea: the Melilla mound field, *in* Proceedings 1st International Conference of the Moroccan Association of Petroleum Geologists (MAPG) in association with the American Association of Petroleum Geologists (AAPG), Marrakesh, October 2007, p. 28-31.

Harrington, P. K., 1985, Formation of pockmarks by pore-water escape: *Geo-Marine Letters*, v. 5, no. 3, p. 193-197.

Paull, C. K., Ussler III, W., and Borowski, W. S., 1999, Freshwater ice rafting: an additional mechanism for the formation of some high-latitude submarine pockmarks: *Geo-Marine Letters*, v. 19, no. 1, p. 164-168.

***Highlights (for review)**

1
2
3
4
5
6
7
8
9
10
11
12
13
14
15
16
17
18
19
20
21
22
23
24
25
26
27
28
29
30
31
32
33
34
35
36
37
38
39
40
41
42
43
44
45
46
47
48
49
50
51
52
53
54
55
56
57
58
59
60
61
62
63
64
65

- An integrated methodology is used to assess fluid flow in the north Irish Sea
- Characterisation of a previously undocumented accumulation of shallow gas in Quaternary sediments, 17 new pockmarks and an area of seabed mounds
- New mechanisms proposed for pockmark and seabed mound formation for this location
- Cenozoic faulting and re-activation of older faults generates pathways for deep fluids to migrate to the shallow sub-surface
- At the seabed, sediment properties play a strong role in the morphological expression of fluid seepage structures

1
2
3
4
5
6
7
8
9
10
11
12
13
14
15
16
17
18
19
20
21
22
23
24
25
26
27
28
29
30
31
32
33
34
35
36
37
38
39
40
41
42
43
44
45
46
47
48
49
50
51
52
53
54
55
56
57
58
59
60
61
62
63
64
65

1 Geological settings and controls of fluid migration and associated seafloor 2 seepage features in the north Irish Sea

3
4 Mark Coughlan^{1,3*}, Srikumar Roy^{2,3}, Conor O’Sullivan^{2,3}, Annika Clements⁴, Ronan O’Toole⁵, Ruth Plets^{6,7}

5
6 ¹School of Civil Engineering, University College Dublin, Newstead, Belfield, Dublin 4, Ireland.
7 ²School of Earth Sciences, Science Centre West, University College Dublin, Belfield, Dublin 4, Ireland.
8 ³Irish Centre for Research in Applied Geosciences, O’Brien Centre for Science East, University College
9 Dublin, Belfield, Dublin 4, Ireland
10 ⁴Seafish, 18 Logie Mill, Logie Green Road, Edinburgh.
11 ⁵Geological Survey of Ireland, Beggars Bush, Dublin, Ireland
12 ⁶School of Geography and Environmental Sciences, Ulster University, Coleraine, Northern Ireland.
13 ⁷Flanders Marine Institute, Wandelaarkaai 7, 8400 Ostend, Belgium

15 ABSTRACT

16
17 Shallow gas accumulation in unconsolidated Quaternary sediments, and associated seepage at the
18 seafloor, is widespread in the north Irish Sea. This study integrates high-resolution seafloor bathymetry
19 and sub-surface geophysical data to investigate shallow gas accumulations and possible fluid (gas and/or
20 liquids) migration pathways to the seafloor in the northern part of the Irish Sea. Shallow gas occurs
21 broadly in two geological settings: the Codling Fault Zone and the Western Irish Sea Mud Belt. The gas
22 has been recognised to accumulate in both sandy and muddy Quaternary marine near-surface
23 sediments and is characterised by three characteristic sub-bottom acoustic features: i) enhanced
24 reflections, ii) acoustic turbid zones, and iii) acoustic blanking. The seepage of shallow gas at the
25 seafloor has resulted in the formation of morphological features including methane-derived authigenic
26 carbonates, seabed mounds and pockmarks. In many instances, the evidence for this gas as biogenic or
27 thermogenic in origin is inconclusive. Two distinct types of pockmarks are recorded in the Western Irish
28 Mud Belt: pockmarks with a relatively flat centre, and pockmarks with a central mound. Based on our
29 observation and existing models, we infer that the formation of a carbonate crust at the seabed surface,
30 is needed as a precursor for the creation of such mounds within pockmarks. The formation processes

1
2
3
4
5
6
7
8
9
10
11
12
13
14
15
16
17
18
19
20
21
22
23
24
25
26
27
28
29
30
31
32
33
34
35
36
37
38
39
40
41
42
43
44
45
46
47
48
49
50
51
52
53
54
55
56
57
58
59
60
61
62
63
64
65

31 are interpreted to be different for sandy versus muddy sediments, due to variability in erodibility and
32 sealing capacities of the substrate. We suggest that the origin of these features is linked to the presence
33 of deeper hydrocarbon source rocks with existing and reactivated faults forming fluid migration
34 pathways to the surface. This in turn could indicate a mixed thermogenic-biogenic origin for seep-
35 related structures in the study area. These features have significant implications for the future
36 development of offshore infrastructure including marine renewable energy as well as for seabed ecology
37 and conservation efforts in the Irish Sea.

38
39 **Keywords:** pockmark, seabed mounds, fluid seepage, MDAC, mud diapir, geohazards, ecological
40 conservation, offshore infrastructure

41 **INTRODUCTION**

42 The accumulation of gas in shallow, unconsolidated marine sediments is a global phenomenon
43 (Andreassen et al., 2007; Dondurur et al., 2011; Ergün et al., 2002; Hovland and Judd, 1992; Karisiddaiah
44 and Veerayya, 1994; Mazumdar et al., 2009). It represents an important tool for frontier hydrocarbon
45 exploration, while also posing a significant geohazard, affecting sediment engineering properties
46 (Andreassen et al., 2007; Hovland et al., 2002; Sills and Wheeler, 1992). The impacts of shallow gas and
47 seepage on seabed ecology has also gained importance over the recent years (Jordan et al., 2019; Kiel,
48 2010; Rathburn et al., 2000). To date in the Irish Sea (Fig. 1), a number of areas associated with shallow
49 gas and fluid seepage have been designated as Special Areas of Conservation (SAC) due to the unique
50 habitats they form as “Submarine structures made by leaking gases”, according to the Annex I / II of the
51 E.U. Habitats Directive (National Parks and Wildlife, 2015). These can form two described habitat types:
52 Bubbling Reefs and Structures within Pockmarks. In the Irish Sea, the SAC areas are predominantly
53 related to Methane-Derived Authigenic Carbonates (MDAC) and are known locally as the Codling Fault
54 Zone (CFZ) SAC and Croker Carbonate Slabs (CCS) SAC (Fig. 1). Further north, Queenie Corner is an
55 offshore site within the Western Irish Sea Mud Belt (WISMB) that was designated as a UK Marine
56 Conservation Zone (MCZ) in 2019 for its subtidal mud habitat and sea-pen and burrowing megafauna
57 communities (Clements and Service, 2016).

58
59 Shallow gas in unconsolidated marine sediments can have a biogenic or thermogenic origin. Bulk
60 isotopic analysis on samples from the CFZ by O’Reilly et al. (2014) indicate a biogenic origin of the
61 seeping gas, with some possible thermogenic contribution from underlying Carboniferous coal deposits.

1
2
3
4
5
6
7
8
9
10
11
12
13
14
15
16
17
18
19
20
21
22
23
24
25
26
27
28
29
30
31
32
33
34
35
36
37
38
39
40
41
42
43
44
45
46
47
48
49
50
51
52
53
54
55
56
57
58
59
60
61
62
63
64
65

62 Methanogenesis of organic-rich Quaternary sediments has been proposed as a source for shallow gas in
63 Bantry Bay (Jordan et al., 2019) and Dunmanus Bay (Szpak et al., 2015) elsewhere in Irish waters.
64 Evidence for shallow gas accumulations and seepage in the Irish Sea has been detected from geophysical
65 observations on seismic lines as gas chimneys, enhanced reflectors and acoustic turbidity (e.g. Judd and
66 Hovland (1992)). Where fluids (e.g. methane gas) emanate from the seabed, morphological features
67 such as mounds and pockmarks have formed in the Western Irish Sea (Croker et al., 2005).

68
69 Mounds are elevated bathymetric features which can form due to upward migrating fluids exerting
70 pressure on overlying relatively impermeable layers or precipitation of carbonates due to prolonged
71 methane gas seepage. Owing to their different formation mechanism, they are known as seabed domes,
72 mud diapirs, and carbonate mounds, all of which have been found in the Irish Sea (Croker et al., 2005).
73 Hovland and Curzi (1989) documented seabed domes and mud diapirs in the Adriatic Sea offshore Italy,
74 where gas bubbles concentrating in plastic clay caused local density reversals, resulting in the upward
75 buoyant flow of the clay and deformation of overlying unlithified layers, thus forming elevated
76 bathymetric features at the seafloor and associated gas seepages. Such seabed domes and mud diapirs
77 have also been found offshore India (Ramprasad et al., 2011), in Norwegian Arctic fjords (Roy et al.,
78 2014), and offshore New Zealand (Koch et al., 2015). Croker et al. (2005) previously mapped mounds
79 (referred to as “seabed doming”) in the WISMB, and suggested that they may have formed due to the
80 replacement of water in the pore space with gas causing an increase in sediment volume in the upper
81 sediment layers. For this to occur, fine-grained, relatively impermeable sediments are required. Croker
82 et al. (2005) also suggested that seabed doming might be an initial stage of pockmark formation.
83 Mounds can also form when prolonged methane gas seepage at the seabed chemically interacts with
84 surrounding minerals to form a carbonate precipitate cement (MDAC), binding the sediment matrix and
85 forming hard, resistive rocks (Judd et al., 2019). With continued seepage over time, MDACs can continue
86 to precipitate and grow into sizeable features up to 10 m high and 250 m in length, as found at the CFZ
87 in the western Irish Sea (O’Reilly et al., 2014).

88
89 Pockmarks are the most common manifestations of fluid seepage on the seafloor and are formed by
90 fluids escaping through the seafloor sediments (Hovland and Judd, 1988). Unconsolidated sediments at
91 the seafloor are lifted and winnowed by the escaping fluids (pore water or gas) forming crater-like
92 depressions. Their shapes are typically circular to sub-circular, however, asymmetric, elongated and
93 trough-like pockmarks have also been documented (Judd and Hovland, 2007; Roy et al., 2015).

1
2
3
4
5
6
7
8
9
10
11
12
13
14
15
16
17
18
19
20
21
22
23
24
25
26
27
28
29
30
31
32
33
34
35
36
37
38
39
40
41
42
43
44
45
46
47
48
49
50
51
52
53
54
55
56
57
58
59
60
61
62
63
64
65

94 Pockmark diameters range from < 5m (unit-pockmarks) to > 1500m (mega-pockmarks) (Hovland et al.,
95 2010; Sun et al., 2011). Pockmarks found in Irish waters vary in size with smaller features typically 2 – 3
96 m in diameter (unit-pockmarks) and tens of centimetres deep. Relatively larger pockmarks offshore
97 Ireland are approximately 20 m in diameter and up to 2 m in depth (Croker et al., 2005; Games, 2001;
98 Szpak et al., 2015, 2012). What is imperative for their formation is a fine-grained, clay to silt, substrate at
99 the seafloor (Croker et al., 2005).

100
101 Seafloor and sub-seabed evidence for shallow gas and fluid migration in the Irish Sea, specifically the CFZ
102 and WISMB, has been previously documented (e.g. Croker et al. (2005)). Geochemical analysis of the
103 seep and mound locations suggest mixed biogenic and thermogenic signatures (Judd et al., 2019;
104 O’Reilly et al., 2014). However, factors such as structural and stratigraphic features responsible for the
105 migration of fluids responsible for a thermogenic signature are still poorly understood. Furthermore,
106 models applicable to the formation mechanisms of the seep-related seafloor features in the Irish Sea are
107 lacking. With this in mind, the aims of this study are:

- 108 (i) To spatially map and characterise geophysical evidence for shallow gas, fluid migration and
109 seafloor seepage in the north Irish Sea;
- 110 (ii) To establish a geological framework incorporating bedrock geology, hydrocarbon source
111 rocks, structural geology (faults), Quaternary geology and seafloor morphology in the Irish
112 Sea which will facilitate further studies into subsurface fluid flow mechanisms;
- 113 (iii) To suggest theories of seabed mound and pockmark formation in the WISMB.

114
115 To achieve this, we provide an integrated analysis of shallow high-resolution datasets (sub-bottom
116 acoustic, multibeam echosounder bathymetry and backscatter data) and deep 2D multichannel seismic
117 datasets from the north Irish Sea. Inferences are made on the formation mechanisms of seep-related
118 seabed features which can be used to better predict their distribution elsewhere in the region. Finally,
119 the implications of shallow gas and fluid-seepage at the seafloor are considered in the context of marine
120 infrastructure siting and ecological conservation.

121 **BACKGROUND GEOLOGY**

122
123 The bedrock geology of the Irish Sea is characterised by a series of rift basins with several kilometres of
124 Carboniferous, Permian and Triassic sedimentary fill. These basins formed through a series of

1
2
3
4
5
6
7
8
9
10
11
12
13
14
15
16
17
18
19
20
21
22
23
24
25
26
27
28
29
30
31
32
33
34
35
36
37
38
39
40
41
42
43
44
45
46
47
48
49
50
51
52
53
54
55
56
57
58
59
60
61
62
63
64
65

125 extensional events in the Carboniferous, Permian and Jurassic, punctuated by episodes of uplift during
126 the Late Carboniferous Variscan Orogeny and more recently the Alpine Orogeny during the Cenozoic.
127 During the Cenozoic event, the Irish Sea experienced kilometre-scale uplift resulting in the present-day
128 configuration of erosional outliers, which are remnants of a much larger rift system (Jackson and
129 Mullholland, 1993). These rift basins include the Kish Bank Basin and Peel Basin, both of which have
130 been the focus of hydrocarbon exploration during the last fifty years (Fig. 1) (Dunford et al., 2001;
131 Newman, 1999). Lithologies capable of generating hydrocarbons have been encountered in the
132 Carboniferous, including the gas-prone Pennine Coal Measures Group and the oil-prone Bowland Shale
133 Formation (Fig. 2). These source rocks have generated significant quantities of hydrocarbons, with an
134 estimated 1.8 BBOE (Billion Barrels of Oil Equivalent) discovered in the East Irish Sea Basin (Bunce,
135 2018). Similar exploration activities took place in the western Irish Sea, primarily in the Kish Bank Basin,
136 with four wells drilled between 1977 and 1997. While no commercial discoveries were made, the
137 presence of the Pennine Coal Measures Group was proven in the 33/22-1 well on the southern margin
138 of the Kish Bank Basin (Thomas, 1978).

140 The bedrock in the Irish Sea has largely been blanketed with Quaternary sediments, collectively referred
141 to as the Brython Glacigenic Group (Fig. 2). Subglacial sediments deposited by the Irish Sea Ice Stream
142 (ISIS) during the Last Glacial Maximum are referred to as the Upper Till (UT) member (Fig. 2), and
143 comprise a till containing stiff or hard clay with clasts ranging in size from sand-grade to boulders up to 1
144 m (Jackson et al., 1995). Overlying the UT are a series of units deposited in a glaciomarine to marine
145 environment as the ISIS retreated, referred to as the Western Irish Sea Formation (WISMF) (Fig. 2)
146 (Jackson et al., 1995). Included in this formation, at the base, is the Chaotic Facies (CF). This unit consists
147 of ice-proximal sediments, dominated by gravels with silts, sands and cobble-grade components
148 (Coughlan et al., 2019; Jackson et al., 1995). The overlying Prograding Facies (PF) is composed of fine- to
149 medium-grained sands that are tabular stratified, having been deposited in a marine environment in
150 front of the retreating Irish Sea Ice Stream (ISIS) (Coughlan et al., 2019; Jackson et al., 1995). The Mud
151 Facies (MF) is characterised by stratified grey-brown muddy sands with silts and clays and is interpreted
152 as being deposited in a fully marine environment (Coughlan et al., 2019; Woods et al., 2019). The
153 organic-rich sediments of the MF have been identified as a potential source of shallow gas (biogenic-
154 origin) in the north Irish Sea in the Western Irish Sea Mud Belt. The anaerobic decomposition of the
155 organic-rich sediments followed by rapid burial under high sedimentation rates during marine
156 transgression in the Early Holocene produced biogenic gas in the shallow sediments (Yuan et al., 1992).

1
2
3
4 157 The UT and WISF deposits have been reworked during marine transgression and sea-level rise in the
5
6 158 Holocene forming a complex distribution of sediments and bedforms, collectively referred to as the
7
8 159 Surface Sands Formation (SSF) (Fig. 2) (Jackson et al., 1995; Ward et al., 2015).
9

10 160 **DATA AND METHODS**

11 161
12
13 161
14 162 This study uses a variety of shallow and deep geophysical datasets. The shallow datasets used in this
15
16 163 study include multibeam echosounder (MBES) bathymetry and backscatter data as well as shallow
17
18 164 sparker and pinger seismic data from a variety of surveys (Table 1). They were acquired primarily as part
19
20 165 of the Integrated Mapping for the Sustainable Development of Ireland's Marine Resource (INFOMAR)
21
22 166 programme, delivered by the Geological Survey of Ireland (GSI) and Marine Institute of Ireland. Data
23
24 167 collected by the Agri-Food and Biosciences Institute (AFBI) in collaboration with GSI and by a Natural
25
26 168 Environment Research Council (NERC) sponsored survey (NE/H02431/1) is accessed for Queenie Corner.
27
28 169 A combination of ArcGIS, IVS Fledermaus, IHS Kingdom and Petrel software were used to analyse and
29
30 170 integrate these datasets for a complete sub-surface to seafloor analysis.
31

31 172 *Multibeam echosounder data*

32 173
33
34 174 The high-resolution multibeam datasets were collected with the EM3002D multibeam echosounder
35
36 175 (MBES) onboard the *RV Celtic Voyager* (dual head) and *RV Corystes* (single head) acquiring bathymetry
37
38 176 data in the 300 kHz range using dynamically focused beams. The horizontal accuracy (x, y) was usually
39
40 177 less than 50 cm with a vertical accuracy (z) of <15 cm obtained for the processed bathymetry data. Data
41
42 178 processing was performed on board with the CARIS HIPS and SIPS software package to remove
43
44 179 erroneous pings and correcting for tidal and water displacement offsets. The output from the CARIS
45
46 180 HIPS and SIPS software consisted of un-gridded, tidally corrected XYZ data that was subsequently
47
48 181 gridded using QPS Fledermaus v.7 to a 2 m cell resolution. Gridded raster data was then exported to
49
50 182 ArcGIS v10 and Fledermaus v.7.7.6 for 3D visualization and morphological analysis of seafloor features.
51
52 183 Relative backscatter values were obtained from the strength of the return signal during MBES
53
54 184 acquisition. Data were processed using Geocoder in CARIS HIPS and SIPS and exported into ESRI ArcGIS
55
56 185 in gridded formats.
57

58 187 *Sub-bottom acoustic data*

59 188
60
61
62
63
64
65

1
2
3
4
5
6
7
8
9
10
11
12
13
14
15
16
17
18
19
20
21
22
23
24
25
26
27
28
29
30
31
32
33
34
35
36
37
38
39
40
41
42
43
44
45
46
47
48
49
50
51
52
53
54
55
56
57
58
59
60
61
62
63
64
65

189 Seismic sparker data were gathered using a Geo-Source 400 sparker system. The system consisted of a 6
190 kJ pulsed power supply operating predominantly at a frequency of 0.5 - 2 kHz. The unfiltered return
191 signal was picked up using a Geo-Sense single channel hydrophone array. A maximum penetration of 50
192 m below the seabed was achieved with a vertical resolution of up to 30 cm. Seismic sparker data were
193 incorporated into IHS Kingdom software in SEG-Y format and merged with ASCII navigation data before
194 being processed and interpreted. A trapezoid bandpass filter was applied (low pass value 0.9 - 1.2 kHz,
195 high pass value 5 - 6 kHz) and an automatic gain control of 50 and 100 ms. Horizons were picked
196 manually, and seismic depths were converted from two-way travel time to metres using an acoustic
197 internal velocity of 1600 m s⁻¹ through shallow marine sediments. Seismic pinger data were collected
198 from Queenie Corner using a hull-mounted SES 5000 3.5kHz pinger system with a 200 ms duration. Data
199 were acquired using the CODA system and processed using IHS Kingdom.

200

201 *2D multichannel seismic data*

202

203 The 2D multichannel reflection seismic data used in this study consisted of a multi-vintage database of
204 six surveys acquired as part of the hydrocarbon exploration activities in the Irish sea. These seismic
205 surveys were acquired between 1983 and 1995, comprising over 2,800 kilometres of data, and
206 processed as per industry standards (Yilmaz, 2001). The majority of the seismic data are centred on the
207 Kish Bank Basin, with five 2D seismic surveys not extending significantly beyond the bounds of the basin.
208 Coverage of the remainder of the study area is provided by a single reconnaissance survey acquired by
209 WesternGeco in 1983, which covers the entirety of the Irish sector of the Irish Sea. Stratigraphic control
210 is provided by four deep boreholes drilled to test for hydrocarbons in the Kish Bank Basin. Data
211 associated with these boreholes consists of wireline logs (gamma ray, caliper, neutron-density, sonic,
212 and resistivity logs), well completion reports, formation tops, and time-depth relationship data in the
213 form of checkshots. Seismic interpretation of key stratigraphic horizons and seismic to well tie was
214 carried out in Petrel software.

215 **RESULTS AND INTERPRETATION**

216

217 *2D multichannel seismic data*

218

1
2
3
4
5
6
7
8
9
10
11
12
13
14
15
16
17
18
19
20
21
22
23
24
25
26
27
28
29
30
31
32
33
34
35
36
37
38
39
40
41
42
43
44
45
46
47
48
49
50
51
52
53
54
55
56
57
58
59
60
61
62
63
64
65

219 A 2D multichannel reflection seismic dataset, consisting of several discrete surveys, was used to
220 investigate the bedrock geology of the region, structural lineaments and gas related features. Six key
221 horizons were mapped in the vicinity of the Lambay Deep and Kish Bank Basin where formation tops
222 from four hydrocarbon exploration boreholes provided stratigraphic control: (i) Seabed; (ii) Base-
223 Quaternary; (iii) Base-Cenozoic; (iv) Top Lower Triassic; (v) Top Permian; (vi) Top Basement
224 (Carboniferous & older) (Fig. 1 and Fig. 3).

226 Where the Codling Fault Zone transects the Kish Bank Basin, a number of seismic amplitude anomalies
227 are observed in the upper Cenozoic section. These seismic amplitudes are locally distributed, including
228 distinct seabed brightening and widespread reverse-polarity anomalies (Fig. 3). These features are
229 confined to the Codling Fault Zone and are not observed in other areas of the Kish Bank Basin. They
230 cause acoustic blanking of the deeper section, either due to absorption or reflection of acoustic energy,
231 significantly reducing seismic image quality at depth. Absorption of acoustic energy can be caused due
232 to presence of gas in the upper stratigraphic sediments, whereas reflection could be attributed to the
233 presence of high-density rocks such as igneous bodies. The latter is unlikely, as igneous bodies have not
234 been documented in the upper Cenozoic sediments in this part of the Irish Sea.

236 There is limited stratigraphic control beyond the Kish Bank Basin, towards the Peel Basin (Fig. 1). Data
237 quality is poor here, owing to the limited reflectivity within the Palaeozoic section. Therefore, only the
238 Base-Cenozoic unconformity could be reliably interpreted. A small half-graben was identified in the
239 north of the study area (i.e. the WISMB; Fig. 1 and Fig. 4) which at present remains undrilled. Owing to
240 its location along strike from the Peel Basin in the UK sector of the Irish Sea, this minor graben is
241 interpreted as an erosional outlier, and the stratigraphy is inferred to be Permian and Triassic, similar to
242 that of the Peel Basin (Floodpage et al., 2001). The bounding faults of this small graben are observed to
243 offset the Base-Cenozoic surface, indicating relatively recent tectonic activity, and the areal extent of
244 this graben correlates with the extent of the acoustic turbidity mapped on sub-bottom profiler sections
245 (Fig. 4).

247 Further east within the WISMB, underlying the Queenie Corner area, a 2D reflection seismic line images
248 folded Carboniferous rocks at depth, overlain by Cenozoic sediments (Fig. 5). Similar to structures
249 observed in Fig. 3, several minor faults are observed offsetting the Base-Cenozoic Unconformity and
250 represent relatively recent tectonic activity (Fig. 5).

1
2
3
4
5
6
7
8
9
10
11
12
13
14
15
16
17
18
19
20
21
22
23
24
25
26
27
28
29
30
31
32
33
34
35
36
37
38
39
40
41
42
43
44
45
46
47
48
49
50
51
52
53
54
55
56
57
58
59
60
61
62
63
64
65

251

252 *Multibeam and Sub-bottom acoustic data*

253

254 Codling Fault Zone

255

256 The seabed in the Codling Fault Zone is dynamic with extensive sediment waves (Croker et al., 2005)

257 (Fig. 6). Also prominent are mounds, which form distinctive bathymetric highs relative to the

258 surrounding seafloor. Approximately 23 mounds have been described previously by O'Reilly et al. (2014)

259 and Van Landeghem et al. (2015) and been interpreted as carbonate mounds. This study identified a

260 further two mounds which exhibit a roughly circular morphology and have an approximate diameter of

261 60 m (Fig. 6). They protrude 8 and 16 m respectively from the seabed and have a higher backscatter

262 than the surrounding seafloor. Based on their morphological similarity and proximity with the carbonate

263 mounds identified Van Landeghem et al. (2015), we infer that these two mounds are probably also

264 carbonate mounds (MDAC) formed due to prolonged seepage of methane gas from the seafloor.

265 However, geochemical sampling and ROV image grabs would be required to ground-truth their

266 association with gas seepage.

267

268 Lambay Deep

269

270 The Lambay Deep itself is a pronounced bathymetric low on the seabed, forming a linear trough-like

271 feature broadly oriented NW-SE that is approximately 11 km long. The Deep is 135 mbsl at its deepest

272 point and is generally 50 m deeper than the surrounding seabed (Fig. 7). The northern extent of the

273 Lambay Deep is bound by an area of exposed bedrock, identified by its rugged seafloor morphology and

274 high backscatter. At its southern extent, the Deep is bound by a sediment wave field. Located near the

275 centre of the Deep is a prominent mound forming a bathymetric high with a clear backscatter contrast

276 to the surrounding seabed (Fig. 7).

277

278 The sparker data acquired over the Lambay Deep cover the area above the mound, where we observe

279 an acoustically transparent 24 m thick unit, above an enhanced reflection (LD-1, Fig. 8). The western

280 flank exhibits acoustic turbidity. These acoustic anomalies are possibly attributed to the accumulation of

281 shallow gas beneath the mound, which was earlier described by Croker et al. (2005) as the Lambay Deep

282 Mud Diapir (LDMD). To the east of the LDMD, low-amplitude parallel to sub-parallel reflections

1
2
3
4
5
6
7
8
9
10
11
12
13
14
15
16
17
18
19
20
21
22
23
24
25
26
27
28
29
30
31
32
33
34
35
36
37
38
39
40
41
42
43
44
45
46
47
48
49
50
51
52
53
54
55
56
57
58
59
60
61
62
63
64
65

283 characterise the sedimentary sequence. The acoustic turbidity zone is imaged on a second
284 representative seismic line across the Deep, and further illustrates an upper acoustic unit displaying an
285 almost transparent seismic signature with faint, horizontal, parallel laminations overlying an enhanced
286 reflection in the centre of the deep (LD-2, Fig. 8). The enhanced reflections imaged in both these sparker
287 lines could be possibly attributed to the sharp acoustic impedance contrast between the underlying gas
288 charged sediments and the overlying lithology. Hence, the enhanced reflections are interpreted as top
289 of shallow gas accumulation. The flanks exhibit a more complex stratigraphy with chaotic acoustic units
290 bounded by moderate to strong internal reflectors. The acoustic turbid zones are possibly caused due to
291 scattering of acoustic energy by gas which is finely disseminated within impervious clay-rich sediments.
292 The sedimentary strata on either side of the LDMD exhibit onlapping structures, which is typical at mud
293 diapir locations (Fig. 8). Onlapping stratigraphy on either side of the LDMD suggest uplifting due to the
294 structure (Fig. 8).

296 Western Irish Sea Mud Belt

297
298 As described earlier, the enhanced reflection is interpreted as the top of the shallow gas accumulation
299 in the WISMB, which lies between 8 and 18 mbsf and extends across an area of approximately 90 km²
300 (Fig. 9). The accumulation has an inverted bowl topography with the rims climbing down towards its
301 edges, and an enhanced reflection marks the top (Fig. 10). The upper layers in the gas-charged zone are
302 lenticular, and characterized by an acoustically turbid zone, while exhibiting a sharp contrast to the
303 surrounding sediments (Fig. 10). Sub-bottom acoustic anomalies related to shallow gas accumulation in
304 this area of the WISMB and details on the shallow seismic stratigraphy have previously been
305 documented by Coughlan et al. (2019).

306
307 Circular to sub-circular crater like features were identified on bathymetry data, which were interpreted
308 as pockmarks which are direct indicators of fluid seepage at the seafloor. A total of seventeen
309 pockmarks (P1-17) were identified using the slope tool in ArcGIS to highlight slope changes along
310 pockmark walls. All pockmarks in this study (with the exception of P12) were found in water depths
311 greater than 40 m (Fig. 9). Information on calculated dimensions and morphology for each pockmark is
312 presented in the supplementary material (S1). Two separate morphologies were identified: pockmarks
313 with central mounds within them and pockmarks without any central mounds.

314

1
2
3
4
5
6
7
8
9
10
11
12
13
14
15
16
17
18
19
20
21
22
23
24
25
26
27
28
29
30
31
32
33
34
35
36
37
38
39
40
41
42
43
44
45
46
47
48
49
50
51
52
53
54
55
56
57
58
59
60
61
62
63
64
65

315 P1, P2 and P3 are clustered with a distance of 355 m between P1 and P2 and a further 420 m between
316 P2 and P3 in a northerly direction. Other pockmarks along this trend are more widely spaced. Pockmarks
317 P1 to P12 are sub-circular in shape, although P5-P8 are more elongate. The alignments of the long-axis
318 of the elongate pockmarks are in different orientations suggesting no influence of bottom currents on
319 the morphological evolution of the pockmarks. Relief relative to the seabed varies between 0.6m (P3)
320 and 1.6m (P10) with pockmarks becoming generally larger and deeper to the northwest. P12 is a typical
321 giant irregular pockmark, as documented in the UK North Sea (Cole et al., 2000). It is elliptical in plan-
322 view, and at least 5 times larger than any of the other pockmarks in this group, the short and long axis
323 being c. 500 m and 1000 m.

324
325 Most pockmarks in this study are between 74 and 153 m wide with P7, P10 and P11 being 171 to 268 m
326 wide. P4 and the larger P10 and P11 pockmarks contain small mounds at their centre being 0.1 m, 0.2 m
327 and 0.4 m high respectively (Fig. 11). P14, P15, P16 and P17 are all circular with a depth typically of 0.4
328 m to 1 m relative to the seabed. P15 also has a mound about 0.1 m in height at its centre. Maximum
329 diameters vary from 54.5 m to 90 m across with the larger-diameter pockmarks tending to be deeper.

330
331 Queenie Corner

332
333 Analysis of the MBES data from the Queenie Corner MCZ suggests largely the same flat topography as
334 seen in the WISMB with notable mound structures. The mounds occur in isolation as well as part of a
335 linear chain, which is approximately 2 km in length (Fig. 12). They exhibit a maximum relief of 1 m
336 compared to the regular seabed (Fig. 12). Backscatter data from these mounds also indicate higher
337 reflectance compared to the surrounding sediments (Fig. 12).

338
339 A single Pinger line from the Queenie Corner site revealed acoustic turbidity, indicating shallow gas, at
340 its western end, coinciding with the mounds observed on MBES data (Fig. 12 and 14). The top of the
341 acoustic turbidity occurs within 1 m of the seabed with clear evidence for gas chimneys reaching the
342 seabed rooted from the acoustic turbid zone. The gas chimneys emanating from the acoustic turbid
343 zone precisely underlie the mounds observed on the MBES data. Further east, we observe a sharp
344 boundary of the turbidity zone which is interpreted as the gas front (Fig. 13B).

1
2
3
4 346 **DISCUSSION**

5
6 347
7 348 *Revised geological model with inferences on gas origin and controls on fluid migration*

9 349
10 350 Structural lineaments (i.e. faults) and the properties of Quaternary sediments in the Irish Sea play a
11 351 significant role in fluid migration from deep seated hydrocarbon source rocks to the shallow sub-
12 352 seafloor stratigraphic layers, and eventually in subsequent seepage at the seafloor. In this section we
13 353 discuss an individual, revised geological model for the CFZ and WISMB to elucidate the potential origins
14 354 for hydrocarbon fluids in both areas and the pathways that would allow for the migration of such fluids
15 355 to the sub-seabed and seafloor. This is not to suggest that there is no biogenic component to any
16 356 shallow gas in these areas. The data presented demonstrates that a thermogenic source cannot be
17 357 excluded, and it is accepted that mixing of sources can occur.
18
19
20
21
22
23
24
25
26

27 359 Codling Fault Zone (incl. Lambay Deep)

28 360
29 361 Gas-prone source rocks have been proven throughout the Irish Sea with the most prolific being the gas-
30 362 prone Pennine Coal Measures Group and the oil-prone Bowland Shale Formation, both of Carboniferous
31 363 age (Pharaoh et al., 2016). Within the study area, the Pennine Coal Measures Group has been proven in
32 364 the 33/22-1 borehole on the southern margin of the Kish Bank Basin where 17 metres of coal were
33 365 encountered with associated methane gas being detected within these coal horizons (Thomas, 1978).
34 366 These coal-bearing horizons are interpreted throughout the Kish Bank Basin and are observed as the
35 367 high-amplitude reflectors visible beneath the Base-Permian Unconformity (Fig. 3). Analysis of vitrinite
36 368 reflectance data at the 33/22-1 borehole indicates these gas-prone source rocks have reached the
37 369 pressure and temperature conditions to generate gas at present-day, suggesting that these same
38 370 horizons at deeper, down-dip positions have generated hydrocarbons (Thomas, 1978). The Bowland
39 371 Shale Formation has not been encountered in the 33/22-1 borehole, where the Pennine Coal Measures
40 372 Group sits unconformably upon Lower Palaeozoic metasediments, although erosional outliers may be
41 373 preserved elsewhere in the study area.
42
43
44
45
46
47
48
49
50
51
52
53

54 374 In addition to the presence of gas-prone source rocks, several indicators of an active petroleum system
55 375 have been encountered in the vicinity of the Kish Bank Basin, in the form of both liquid and gaseous
56 376 hydrocarbons. Both the previously mentioned 33/22-1 borehole and the 33/17-1 borehole on the
57 377 eastern margin of the Kish Bank Basin encountered residual oil, the former in Carboniferous sandstones
58
59
60
61
62
63
64
65

1
2
3
4
5
6
7
8
9
10
11
12
13
14
15
16
17
18
19
20
21
22
23
24
25
26
27
28
29
30
31
32
33
34
35
36
37
38
39
40
41
42
43
44
45
46
47
48
49
50
51
52
53
54
55
56
57
58
59
60
61
62
63
64
65

378 and the latter in Triassic sandstones (Charterhouse, 1986; Thomas, 1978). The 33/22-1 borehole
379 reported tentative oil-staining in Lower Pleistocene sands which may indicate the remigration of liquid
380 hydrocarbons from within the bedrock to these shallow, unconsolidated sediments. Previous authors
381 have also presented a proprietary seep dataset which shows the location of present-day oil seeps, with a
382 strong correlation between the location of seeps and distribution of both large faults and where source-
383 rocks sub-crop at the seabed (e.g. Anderson, 2013; Dunford et al., 2001).

384 Remigration of hydrocarbons from the bedrock to the shallow seabed can be facilitated by recent
385 tectonic activity, which creates fluid conduits in the form of faults, which either breach existing
386 hydrocarbon accumulations at depth or allow hydrocarbons to migrate directly from source rocks to
387 seabed sediments (Anka et al., 2012; Corcoran and Doré, 2002). In the study area, the Codling Fault
388 Zone is the most recent tectonic feature, being a NNW-SSE trending strike-slip fault and offshore
389 extension of the Newry and Camlough Faults of Northern Ireland (Fig. 1). Kilometre-scale dextral motion
390 on the fault has been recorded by several previous studies (e.g. Dunford et al., 2001) with the most
391 recent research indicating displacement of 8.7 kilometres, incorporating up to 2 kilometres of normal
392 movement on the basin-bounding fault along the northern margin of the Kish Bank Basin (Anderson,
393 2013). The timing of this fault activity is poorly constrained due to the attenuated Cenozoic section
394 preserved in the study area but has been inferred to have a component of both Paleocene and
395 Oligocene movement (Anderson, 2013; Dunford et al., 2001).

396 Several observations from 2D multichannel seismic data recorded in this study correlate spatially with
397 the location of the Codling Fault Zone. Within the confines of the Kish Bank Basin, amplitude brightening
398 is observed above the fault zone within the Quaternary units, with a sharp western boundary directly
399 above the trend of one of main fault splays and a more diffuse contact to the east (Fig. 3). Additionally,
400 reverse polarity anomalies are observed in the Cenozoic section directly above the fault zone. While
401 none of the available boreholes penetrate these anomalies, correlation with those seismic intervals
402 along-strike indicate these sediments consist of poorly consolidated sandstones interbedded with thin
403 layers of mudstone (Charterhouse, 1986; Thomas, 1978). These anomalies may represent local charging
404 of these sands with re-migrated gaseous hydrocarbons which have migrated up the main fault plane of
405 the Codling Fault Zone (e.g. Løseth et al., 2009). Other authors have presented proprietary single-
406 channel seismic data from this area which supports this interpretation, such as reverse-polarity
407 anomalies and flat spots reported by Dunford et al., (2001). However, these anomalies will remain a
408 speculative interpretation until ground truthing is done by geochemical sampling.

1
2
3
4
5
6
7
8
9
10
11
12
13
14
15
16
17
18
19
20
21
22
23
24
25
26
27
28
29
30
31
32
33
34
35
36
37
38
39
40
41
42
43
44
45
46
47
48
49
50
51
52
53
54
55
56
57
58
59
60
61
62
63
64
65

409 Evidence for shallow gas is also observed in Quaternary sediments (i.e. the PF and SSF) from shallow,
410 sub-bottom acoustic data in the Lambay Deep causing enhanced reflection (Fig. 8). The PF has also been
411 observed to be gas-bearing in the CFZ (Van Landeghem et al., 2015). Whilst we infer a thermogenic
412 origin for the gas/fluids in this area, a biogenic component cannot be discounted. Isotope analysis of
413 MDAC at the CFZ SAC by O'Reilly et al. (2014) suggests possible mixing of biogenic and thermogenic
414 sourced gas. Based on the present data, it is not possible to estimate the timescales for the migration of
415 these fluids. The Croker Carbonate Slab SAC is located 12-15 kms NE of the CFZ SAC area (Fig. 1). Judd et
416 al. (2019) place the formation of MDACs in the Croker Carbonate Slab SAC between 17 ka BP to 5 ka BP,
417 with evidence for present day gas seepage. The MDAC cements the PF, which is inferred as being
418 deposited in a glaciomarine environment between approximately 20 ka and 10 ka BP (Judd et al., 2019).
419 It is also assumed that, prior to the deposition of the PF as the ISIS retreated, gas accumulated beneath
420 the ice sheet (Judd et al., 2019). Gas accumulations below ice-sheets has also been proposed for other
421 locations globally during the Devensian (Crémière et al., 2016; Fichler et al., 2005; Portnov et al., 2016).
422 This spatial correlation of seabed features with the Codling Fault Zone implies that at least a portion of
423 the fluids responsible for their formation will be bedrock-sourced thermogenic gas, with the Codling
424 Fault Zone acting as the main conduit for the migration of hydrocarbon fluids to the shallow subsurface.

425 Western Irish Sea Mud Belt (including Queenie Corner)

426 Shallow gas accumulations have been observed in the MF in the WISMB, acoustically blanking the layers
427 below (Coughlan et al., 2019) (Fig. 10). Similar accumulations of shallow gas in the WISMB have
428 previously been linked with a biogenic origin, given the organic rich nature of the MF sediments (Yuan et
429 al., 1992). Stable isotope data in Woods et al. (2019) presents evidence for methane seeps in the WISMB
430 during the Mid Holocene age (post 8.2 ka). Considering the Holocene age of the MF and the estimated
431 volume of gas present (Supplementary Material; S2), it is difficult to envision a solely biogenic source.
432 This study has provided credible evidence of shallow gas accumulation directly above a Permo-Triassic
433 infilled basin with its boundaries defined by the graben-bounding faults (Fig. 3 and Fig. 14). These faults,
434 which were reactivated during the Cenozoic and are observed offsetting the Base-Cenozoic
435 Unconformity, would provide pathways for fluid flow from the Carboniferous source rocks below (Fig.
436 14). The gas is seen to be hosted in the PF, below the base of the MF (Fig. 10). This suggests upward fluid
437 migration through the underlying CF (glacial outwash sediments) and UT member (subglacial till). Whilst
438 the UT in the Irish Sea is often over-consolidated, it is highly heterogeneous comprising a range of
439 sediment classes that would facilitate fluid migration through it (Fig. 14) (Coughlan et al., 2019; Van

1
2
3
4
5
6
7
8
9
10
11
12
13
14
15
16
17
18
19
20
21
22
23
24
25
26
27
28
29
30
31
32
33
34
35
36
37
38
39
40
41
42
43
44
45
46
47
48
49
50
51
52
53
54
55
56
57
58
59
60
61
62
63
64
65

440 Landeghem et al., 2015). The top of the shallow gas is typically within 10-12 m of the seabed-surface and
441 has a sharp boundary with the surrounding non-gas bearing sediments (Fig. 10). Pockmarks P14, P15,
442 P16 and P17 were found to coincide with the lateral extent of underlying shallow gas accumulation,
443 previously identified by Coughlan et al. (2019) (Fig. 9 and Fig. 15). Episodic or continuous migration of
444 this shallow gas accumulation to the seafloor would allow for fluid seepage at the seafloor, and the
445 formation of features such as mounds and pockmarks, which will be discussed in more detail in the next
446 section. Pockmarks occurring outside this accumulation of shallow gas form a strong, linear trend
447 coincident with the prognosed extension of the Codling Fault Zone (Fig. 15), implying that fluid migrating
448 from deeper source rocks along the main fault of CFZ possibly seep out from these pockmarks.

449 *Formation mechanisms of seep-related seafloor features*

451
452 We can classify seep-related seafloor morphological features observed in this study into two different
453 types: mounds and pockmarks (Fig. 15). Mounds can be further classified into mounds formed from
454 MDACs and mounds formed due to mud-diapirism. Mounds described here in association with the CFZ
455 have collectively been described extensively in the literature as carbonate mounds formed from MDACs
456 (Judd et al., 2019; O'Reilly et al., 2014; Van Landeghem et al., 2015). Alternatively, the mound located
457 within Lambay Deep was described by Croker et al. (2005) as the Lambay Deep Mud Diapir (LDMD). Judd
458 and Hovland (2007) defined a mud diapir as a sediment structure that has risen through a sediment
459 sequence due to upward migrating fluids, piercing or deforming younger sediments. Mud diapirs can be
460 recognised on seismic profiles as an acoustically amorphous piercement structure, as documented in the
461 East China Sea (Xing et al., 2016), SW Taiwan (Chen et al., 2014), and the Mediterranean Ridge
462 (Camerlenghi et al., 1992). In this section we focus on the formation mechanisms of the remaining
463 seabed features in the WISMB, which are poorly understood in an Irish Sea context.

464
465 The pockmarks identified in this study are concentrated in the western part of the WISMB (Fig. 15).
466 Within this set of pockmarks (P1-P17) there are two different morphologies: pockmarks with a central
467 mound and pockmarks without a central mound. All the pockmarks are located in an area of sandy-mud
468 to muddy-sand according to the British Geological Survey DigSBS250 database (Fig. 15). This
469 differentiates them from pockmarks previously documented by Yuan et al. (1992), which were located in
470 areas dominated by mud class sediments and were related to a zone of “acoustically turbid sediments”
471 (ATZ) (Fig. 15). Yuan et al. (1992) offers no explanation for the mechanism for their formation, although

1
2
3
4
5
6
7
8
9
10
11
12
13
14
15
16
17
18
19
20
21
22
23
24
25
26
27
28
29
30
31
32
33
34
35
36
37
38
39
40
41
42
43
44
45
46
47
48
49
50
51
52
53
54
55
56
57
58
59
60
61
62
63
64
65

472 Croker et al. (2005) does highlight the requirement of clay- to silt-grade substrate for the formation of
473 pockmarks. The fluids escaping from these pockmarks could either be biogenic- or thermogenic-sourced
474 or of mixed origin. We further suggest that pore-water escape from the shallow glacial marine deposits
475 could have also led to the formation of pockmarks, as suggested in other glacial marine settings
476 (Harrington, 1985; Roy et al., 2019), however, pore-water escape would not support the formation of
477 mounds within pockmarks.

478
479 Low-relief seabed mounds are found in Queenie Corner in the eastern part of the WISMB, which is
480 characterised by sandy-mud seafloor sediments (Fig. 15). Mounds mapped by Croker et al. (2005) occur
481 in areas of mud and sandy mud (Fig. 15). The near surface sediments in the WISMB are often under-
482 consolidated, and so likely to be highly permeable (Coughlan et al., 2019; Mellet et al., 2015), which is
483 unsuitable for the mechanism of formation proposed by Croker et al. (2005). In this study, described
484 mounds and pockmarks are located in distinct areas and separated from each other.

485
486 The distribution of these seep-related seafloor morphological features varies over differing seafloor
487 sediment types, which indicates differing formation mechanisms. Based on previous studies (Brothers et
488 al., 2011; Crémière et al., 2018; Hammer et al., 2009; Hovland, 2002; Loher et al., 2018) and
489 observations made in this study, we discuss two conceptual models for:

- 490 (i) The formation of central mounds within pockmarks in muddy sediment areas with a sand-
491 component, and;
- 492 (ii) The formation of seabed mounds in muddy sediments, leading to the formation of collapsed
493 pockmarks.

494
495 The formation of central mounds within pockmarks in sediments with a sand component

496
497 Initially fluid seepage at a relatively flat seafloor facilitates the development of microbial mats and an
498 initial MDAC crust, which reduces the seepage rate at that location (Fig. 16A; Stage 1). Over time, this
499 MDAC crust develops further, forming a consolidated seal at the seafloor (Fig. 16A; Stage 2). A
500 combination of seepage of fluids from, and bottom currents at, the seafloor around the mounds
501 preferentially erodes the surrounding un-cemented seafloor sediments, partially exposing the MDAC
502 crust (Fig. 16A; Stage 3). Further seepage of fluids around the perimeter of the carbonate crust along
503 with reworking and winnowing of sediments finally exposes the mound completely, which resembles a

1
2
3
4
5
6
7
8
9
10
11
12
13
14
15
16
17
18
19
20
21
22
23
24
25
26
27
28
29
30
31
32
33
34
35
36
37
38
39
40
41
42
43
44
45
46
47
48
49
50
51
52
53
54
55
56
57
58
59
60
61
62
63
64
65

504 mound at the centre of a pockmark (Fig. 16A; Stage 4). This is in agreement with the formation
505 mechanism of carbonate mounds within pockmarks on a relatively flat seabed whereby a combination
506 of fluid seepage and bottom currents erode the surrounding un-cemented seafloor sediments, partially
507 exposing the mound in the centre of the pockmarks as has been suggested by Crémière et al. (2018).
508 Similar carbonate crusts have been observed within pockmarks in the Harstad Basin in the Barents Sea
509 (Crémière et al., 2018) and offshore Norway (Hovland et al., 2010), where several satellite pockmarks
510 surrounding the 'mother pockmark' have been documented with a carbonate mound in the centre.

511

512 The formation of seabed mounds, leading to pockmarks in muddy sediments

513

514 Initially, prolonged seepage of methane gas at the seafloor leads to the formation of thin fragments of
515 MDAC, followed by cementation of these thin MDAC fragments just beneath the seabed (Fig. 16B; Stage
516 1). The thin MDAC crust beneath the seabed acts as an impermeable seal at the seabed sediment-water
517 interface and redirects fluid seepage around the MDAC crust perimeter (Fig. 16B; Stage 2). Gas starts to
518 accumulate and build up pore-pressure beneath the crust, while also increasing the pore-volume. The
519 build-up of pore pressure and increase of pore volume within the unconsolidated sediments underlying
520 the MDAC crust is facilitated by the combined effect of upward fluid migration and sealing capacities of
521 mud-rich sediments and the MDAC crust. The sealing effect of the MDAC crust, along with the buoyant
522 force of the upward migrating gas and increase in pore-volume, results in the bulging outward of the
523 unconsolidated sediments and the MDAC crust (Fig. 16B; Stage 3). At this point, the MDAC crust has
524 been modified to a carbonate mound due to the outward bulging of the sediments underneath, such as
525 the mounds at Queenie Corner (Fig. 13). The gradual increase in the buoyant force of the gas further
526 leads to the formation of fractures within the deformed MDAC mound, to the point when the MDAC
527 mound ruptures and collapses under its own weight after the underlying pressurised gas has dissipated
528 (Fig. 16B; Stage 4). The collapsed mound resembles a crater-like depression like a pockmark. A single
529 grab sample taken from the area of seafloor mounds in the southwestern section of Queenie Corner
530 revealed cemented muds, with a strong odour, which would suggest hardened substrates caused by
531 oxidation of methane forming carbonate precipitates (Supplementary Material; S3). However, this
532 hypothesis assumes that the initial MDAC crust formation is thin enough to be deformed by the increase
533 in pore pressure and volume due to the upward migrating fluids.

1
2
3
4
5
6
7
8
9
10
11
12
13
14
15
16
17
18
19
20
21
22
23
24
25
26
27
28
29
30
31
32
33
34
35
36
37
38
39
40
41
42
43
44
45
46
47
48
49
50
51
52
53
54
55
56
57
58
59
60
61
62
63
64
65

534

535 *Data interpretation and geological model limitations*

536

537 The identification, characterisation and assessment of geohazards such as shallow gas, fluid flow and
538 seepage involves a multidisciplinary approach utilising a range of site investigation techniques
539 (Cevatoglu et al., 2015; Clare et al., 2017; Vanneste et al., 2014). This study aims to integrate multi-scale
540 geophysical datasets in order to develop a geological framework to study potential fluid migration
541 pathways from deeper stratigraphy or source rocks to shallow gas accumulations, and thereafter
542 seepage at seafloor in the Irish Sea. Characterising and describing shallow gas acoustic features on
543 shallow seismic data in particular depends on the acquisition system and frequencies used (Tóth et al.,
544 2014). The shallow sub-bottom data used to characterise shallow sub-seabed features were gathered as
545 part of regional surveys, without the express intention of studying shallow gas and fluid flow. The
546 systems used to gather shallow sub-bottom data (i.e. sparker and pinger) transmit a signal within a
547 frequency range of 0.5 – 4 kHz, which can be attenuated through scattering by fluid bubbles in gas
548 charged sediments, the result of which is acoustic turbidity and blanking (Tóth et al., 2014). Both these
549 phenomena are recognised in this study (Fig. 10) and are common at depth in such areas of mud to
550 sandy mud on single-channel datasets (e.g. Laier and Jensen, 2007). As a result, only the top of the gas
551 front is identified on shallow sub-bottom data, and there is ambiguity with regards to the depth of
552 shallow gas and details of the underlying geology. However, low-frequency 2D-multichannel seismic
553 provides information on underlying bedrock geology and tectonics. Ultimately, some studies show
554 amplitude versus offset (AVO) analysis on 2D-multichannel seismic data to further affirm the presence
555 of gas in the sediments (e.g. Kim et al., 2020)

556

557 At the seafloor, geomorphological features synonymous with fluid migration and seepage can be
558 mapped using multibeam echosounder (e.g. Roelofse et al., 2020). In this study pockmarks have been
559 identified, characterised and discussed within the context of fluid migration and seepage. However,
560 there is a current lack of geochemical data from these pockmarks to ascertain the nature of fluids
561 seeping from them. Analysis of cores taken in the vicinity of the pockmarks in the WISMB and the LDMD
562 discussed here proved inconclusive in terms of determining the composition of sub-surface fluids due to
563 a lack of depth penetration (O'Reilly, S. pers. Comms.). As this study has identified several areas within
564 the northern Irish Sea where there is compelling evidence for the presence of gas in the shallow
565 subsurface, we anticipate future research cruises will acquire sediment and pore-water samples to
566 confirm the nature of origin or fluids seeping from these locations.

1
2
3
4
5
6
7
8
9
10
11
12
13
14
15
16
17
18
19
20
21
22
23
24
25
26
27
28
29
30
31
32
33
34
35
36
37
38
39
40
41
42
43
44
45
46
47
48
49
50
51
52
53
54
55
56
57
58
59
60
61
62
63
64
65

567

Implications of shallow gas and fluid seepage

569

570 The presence of gas accumulations in shallow sub-surface sediments can have engineering implications
571 for the construction of offshore infrastructure and is considered a geohazard within the hydrocarbon
572 and maritime industry (Evans, 2011; Hovland et al., 2002; Sun et al., 2017) as well as for renewable
573 energy developments (Society for Underwater Technology, 2005). When gas occurs in solution in the
574 pore-water, or free gas-filled voids between sediment grains, it can affect the compressibility of the
575 sediment and negatively influence the engineering properties (Sills and Wheeler, 1992; Sultan et al.,
576 2012). Where fluid seeps to the seafloor, it can impact the ground-conditions by: (i) forming a hard
577 surface (i.e. MDAC), which may be difficult to pile or penetrate, or; (ii) causing changes in seabed
578 bathymetry (e.g. doming or pockmarks), which would create seabed instability. Hence, it is vital to do a
579 marine baseline study of an area of interest before installation of submarine engineering structures. This
580 study, inter alia, has mapped a widespread occurrence of shallow gas throughout the north Irish Sea as
581 well as included previous studies in the area, which overlies a variety of geological and tectonic settings
582 (Fig. 1 and 15). More research is required to better understand the migration of fluids along proposed
583 fault-routes, their sealing versus leaking capabilities, and the true nature and timing of the seeping
584 fluids. At the very least, it is possible to anticipate where certain shallow gas and fluid escape structures
585 may be encountered based on regional geology and mitigating site investigation techniques planned
586 accordingly.

587

588 Studies have shown that MDAC harbours different benthic communities to surrounding sediments in the
589 Irish Sea: whether this is due to the formation of complex three-dimensional reef-like structures in
590 otherwise fairly homogeneous sedimentary habitats, thereby allowing colonisation by taxa common on
591 hard rocky substrates, or due to the unique characteristics of MDAC which are as yet unclear (Judd et al.,
592 2019; Noble-James et al., 2020). Pockmarks have been shown to harbour exclusive fauna in the North
593 Sea (Webb et al., 2009), characterised by species with endosymbiotic sulphur-oxidising bacteria, as well
594 as the structures providing shelter for specific fish species (Dando, 2001). (Dando, 2010) reviewed 62
595 shallow-water hydrothermal vent and cold seep sites and found that obligate species are rare at such
596 sites, however higher species diversity was often found in the immediate vicinity of seeps often due to
597 the heterogeneity of the bathymetry, compared with surrounding more homogeneous areas. As yet,
598 the pockmarks and seabed doming in this study have not had targeted biological sampling, but at

1
2
3
4
5
6
7
8
9
10
11
12
13
14
15
16
17
18
19
20
21
22
23
24
25
26
27
28
29
30
31
32
33
34
35
36
37
38
39
40
41
42
43
44
45
46
47
48
49
50
51
52
53
54
55
56
57
58
59
60
61
62
63
64
65

599 Queenie Corner cemented sediment was retrieved by Day-grab from one seabed dome area with faunal
600 excavation of the cemented sediment by bivalves and gastropods (Supplementary Material; S3).
601 Whether the fauna in such structures is unique compared to surrounding sedimentary areas would
602 require further investigation; however, substrata-boring fauna could be viewed as a functionally
603 significant component of the local ecosystem (Noble-James et al., 2020). An understanding of this,
604 coupled with accurate mapping of the extent and potential ecological connectivity of such features
605 throughout the Irish Sea, is required to underpin effective management of these habitats.

606

607 **CONCLUSIONS AND FUTURE WORK**

608 High-resolution geophysical datasets from the Irish Sea reveal sub-seabed shallow gas accumulations in
609 Quaternary sediments and a range of seafloor expressions of fluid seepage. Based on the integrated
610 geophysical investigation of seafloor geomorphologies, shallow sub-surface sediments and deeper
611 geological and tectonic features, this study generated a geological framework from which the following
612 can be made summarised.

613 In both the Codling Fault Zone and Western Irish Sea Mud Belt, there is compelling evidence linking
614 shallow gas accumulation within Quaternary sediments with major structural lineaments (i.e. faults) in
615 the bedrock geology. These faults can act as pathways for hydrocarbon fluids to migrate from deeply
616 seated source rocks to shallow stratigraphic layers. This supports earlier geochemical studies which
617 found a thermogenic component to the shallow gas and seafloor seepage features in both these areas.

618 In the Western Irish Sea Mud Belt, both pockmarks and seabed mounds were recorded in areas of mud
619 with a varying sand component. Pockmarks display two morphologies consisting of regular, circular
620 types and pockmarks with a central mound, typically less than 0.5 m in relief. Pockmark centres often
621 exhibit high backscatter reflectance values suggesting some degree of sediment consolidation due to the
622 formation of MDAC. Mounds are typically 1 m in height above the regular seabed and are associated
623 with gas chimneys rooted to an underlying shallow gas accumulation. These mounds, and surrounding
624 seabed, exhibit high back backscatter reflectance values, again, suggesting the formation of MDAC. This
625 is supported by a grab sample from a mound containing cemented, MDAC-like material.

1
2
3
4
5
6
7
8
9
10
11
12
13
14
15
16
17
18
19
20
21
22
23
24
25
26
27
28
29
30
31
32
33
34
35
36
37
38
39
40
41
42
43
44
45
46
47
48
49
50
51
52
53
54
55
56
57
58
59
60
61
62
63
64
65

626 We propose two mechanisms for the formation of pockmarks; one in muddy seafloor settings with a
627 sand component, which accounted for the formation of a central mound, and one for the formation of
628 thin MDAC mounds as pre-cursors to pockmarks in muddy seafloor settings.

629 Based on our findings, we make the following concluding statements and recommendations for future
630 work:

- 631 ● The revised geological models for the Codling Fault Zone and Western Irish Sea Mud Belt allow
632 for a better understanding of the role of existing and re-activated faults as a potential pathway
633 for fluid (e.g. gas) migration from kilometre-scale depth to the shallow sub-seabed. In future,
634 this will help quantify the contribution of thermogenic-sourced gas to ongoing shallow sub-
635 seabed gas accumulation and seafloor seepage in these areas. Geochemical analysis of targeted
636 seabed seepage and shallow gas accumulation locations from the Western Irish Sea Mud Belt is
637 required to constrain the origin of shallow gas definitively and is a proposed area of further
638 work.
- 639 ● To validate the model linking the creation of MDAC to pockmark formation, repeat survey data
640 over the mounds at Queenie Corner is required to record their evolution over time.
- 641 ● The presence of shallow gas accumulations in the Western Irish Sea Mud Belt, along with gas
642 chimneys and mounds, suggests that fluid seepage at the seafloor is an on-going process. This
643 has significant implications for seabed infrastructure development and seabed ecological and
644 conservation efforts. Based on the results of this study and models presented, our
645 understanding of the geological controls on fluid migration and seafloor seepage is greatly
646 improved, making it increasingly possible to predict the extent of shallow gas and location of
647 certain gas seepage structures in the Irish Sea. Future data collection surveys (e.g. INFOMAR)
648 will further improve this understanding.
- 649 ● To better constrain gas content and extent of gas front in areas of acoustic blanking, we
650 recommend the acquisition of multichannel seismic data and the application of AVO analysis.
- 651 ● Ground-truthing and further geotechnical analysis of Quaternary sediments is required to better
652 understand how fluids migrate through, and are hosted in, these sediments.

- 1
2
3
4 653 ● Biological data available from the Western Irish Sea Mud Belt pockmarks and mounds are
5
6 654 limited in determining the range of biodiversity at these sites at present. Epibenthic surveys
7
8 655 consisting of drop-frame or towed camera platforms or ship-based grab sampling are typically
9
10 656 unable to spatially target and sample chemoautotrophic communities, so it is recommended
11 657 that ROV techniques are used for such purposes.

14 658 **Acknowledgements**

15
16 659
17
18 660 This research is funded in part by a research grant from Science Foundation Ireland (SFI) under Grant
19
20 661 Number 13/RC/2092 and is co-funded under the European Regional Development Fund, and by the
21
22 662 Petroleum Infrastructure Programme (PIP) and its member companies. SR is funded by the Irish
23
24 663 Research Council Government of Ireland Postdoctoral Fellow Award (GOIPD/2018/17). The authors
25 664 would like to thank the Petroleum Affairs Division (PAD) of the Department of Communications, Climate
26
27 665 Action and Environment (DCCAE), Ireland, for providing access to released borehole, seismic and
28
29 666 potential field datasets. The authors would also like to thank Schlumberger for providing academic
30
31 667 licenses of Petrel to University College Dublin. We are grateful to IHS Markit for providing the academic
32
33 668 licence for the KINGDOM software package to iCrag. This paper contains Irish Public Sector Data
34
35 669 (INFOMAR) licensed under a Creative Commons Attribution 4.0 International (CC BY 4.0) licence. The
36
37 670 authors acknowledge Dr. Matthew Service and Rory O’Loughlin (both Agri-Food and Biosciences
38
39 671 Institute, Northern Ireland) for releasing the MBES data for Queenie Corner, and for support during the
40
41 672 AFBI surveys. The pinger line shown was acquired as part of NERC project NE/H02431/1. The authors
42
43 673 acknowledge Rosie Jebb (GSI) and Andy Trafford (UCD) for assistance processing MBES and sub-bottom
44
45 674 profile data respectively. The authors also acknowledge the crew and scientists onboard all surveys
46
47 675 listed for their work, co-operation and skill in collecting the data. The authors would like to thank 3
48
49 676 reviewers for their feedback and comments which greatly improved this manuscript.

50 678 **References**

- 51
52 679 Anderson, H., 2013. The origin and nature of Cenozoic faulting in north-east Ireland and the Irish Sea.
53 680 University College Dublin.
54
55 681 Andreassen, K., Nilssen, E.G., Ødegaard, C.M., 2007. Analysis of shallow gas and fluid migration within
56 682 the Plio-Pleistocene sedimentary succession of the SW Barents Sea continental margin using 3D
57 683 seismic data. *Geo-Marine Lett.* 27, 155–171. <https://doi.org/10.1007/s00367-007-0071-5>
58 684 Anka, Z., Berndt, C., Gay, A., 2012. Hydrocarbon leakage through focused fluid flow systems in
59 685 continental margins. *Mar. Geol.* 332–334, 1–3.
- 60
61
62
63
64
65

1
2
3
4 686 <https://doi.org/https://doi.org/10.1016/j.margeo.2012.10.012>
5 687 Brothers, L.L., Kelley, J.T., Belknap, D.F., Barnhardt, W.A., Andrews, B.D., Maynard, M.L., 2011. More
6 688 than a century of bathymetric observations and present-day shallow sediment characterization in
7 689 Belfast Bay, Maine, USA: implications for pockmark field longevity. *Geo-Marine Lett.* 31, 237–248.
8 690 <https://doi.org/10.1007/s00367-011-0228-0>
9 691 Bunce, J., 2018. The history of exploration and development of the Liverpool Bay fields and the East Irish
10 692 Sea Basin. *Hist. Eur. Oil Gas Ind.* <https://doi.org/10.1144/SP465.6>
11 693 Camerlenghi, A., Cita, M.B., Hieke, W., Ricchiuto, T., 1992. Geological evidence for mud diapirism on the
12 694 Mediterranean Ridge accretionary complex. *Earth Planet. Sci. Lett.* 109, 493–504.
13 695 [https://doi.org/https://doi.org/10.1016/0012-821X\(92\)90109-9](https://doi.org/https://doi.org/10.1016/0012-821X(92)90109-9)
14 696 Cevatoglu, M., Bull, J.M., Vardy, M.E., Gernon, T.M., Wright, I.C., Long, D., 2015. Gas migration
15 697 pathways, controlling mechanisms and changes in sediment acoustic properties observed in a
16 698 controlled sub-seabed CO₂ release experiment. *Int. J. Greenh. Gas Control* 38, 26–43.
17 699 <https://doi.org/https://doi.org/10.1016/j.ijggc.2015.03.005>
20 700 Charterhouse, 1986. Well 33/17-1 Final Geological Report.
21 701 Chen, S.-C., Hsu, S.-K., Wang, Y., Chung, S.-H., Chen, P.-C., Tsai, C.-H., Liu, C.-S., Lin, H.-S., Lee, Y.-W.,
22 702 2014. Distribution and characters of the mud diapirs and mud volcanoes off southwest Taiwan. *J.*
23 703 *Asian Earth Sci.* 92, 201–214. <https://doi.org/https://doi.org/10.1016/j.jseae.2013.10.009>
24 704 Clare, M.A., Vardy, M.E., Cartigny, M.J.B., Talling, P.J., Himsworth, M.D., Dix, J.K., Harris, J.M.,
25 705 Whitehouse, R.J.S., Belal, M., 2017. Direct monitoring of active geohazards: Emerging geophysical
26 706 tools for deep-water assessments. *Near Surf. Geophys.* 15, 427–444.
27 707 <https://doi.org/10.3997/1873-0604.2017033>
28 708 Clements, A., Service, M., 2016. Alternative Marine Conservation Zones in Irish Sea mud habitat:
29 709 Assessment of habitat extent and condition at “Queenie corner” and assessment of fishing activity
30 710 at potential MCZ sites. Report to Seafish Northern Ireland Advisory Committee.
31 711 Cole, D., Stewart, S.A., Cartwright, J.A., 2000. Giant irregular pockmark craters in the Palaeogene of the
32 712 Outer Moray Firth Basin, UK North Sea. *Mar. Pet. Geol.* 17, 563–577.
33 713 [https://doi.org/https://doi.org/10.1016/S0264-8172\(00\)00013-1](https://doi.org/https://doi.org/10.1016/S0264-8172(00)00013-1)
34 714 Corcoran, D. V., Doré, A.G., 2002. Depressurization of hydrocarbon-bearing reservoirs in exhumed basin
35 715 settings: evidence from Atlantic margin and borderland basins. *Geol. Soc. London, Spec. Publ.* 196,
36 716 457 LP – 483. <https://doi.org/10.1144/GSL.SP.2002.196.01.25>
37 717 Coughlan, M., Wheeler, A.J., Dorschel, B., Long, M., Doherty, P., Mörz, T., 2019. Stratigraphic model of
38 718 the Quaternary sediments of the Western Irish Sea Mud Belt from core, geotechnical and acoustic
39 719 data. *Geo-Marine Lett.* 39, 223–237.
40 720 Crémière, A., Chand, S., Sahy, D., Thorsnes, T., Martma, T., Noble, S.R., Pedersen, J.H., Brunstad, H.,
41 721 Lepland, A., 2018. Structural controls on seepage of thermogenic and microbial methane since the
42 722 last glacial maximum in the Harstad Basin, southwest Barents Sea. *Mar. Pet. Geol.* 98, 569–581.
43 723 <https://doi.org/https://doi.org/10.1016/j.marpetgeo.2018.07.010>
44 724 Crémière, A., Lepland, A., Chand, S., Sahy, D., Condon, D.J., Noble, S.R., Martma, T., Thorsnes, T., Sauer,
45 725 S., Brunstad, H., 2016. Timescales of methane seepage on the Norwegian margin following collapse
46 726 of the Scandinavian Ice Sheet. *Nat. Commun.* 7, 11509. <https://doi.org/10.1038/ncomms11509>
47 727 Croker, P.F., Kozachenko, M., Wheeler, A.J., 2005. Gas-Related Seabed Structures in the Western Irish
48 728 Sea (IRL-SEA6).
49 729 Dando, P.R., 2010. Biological communities at marine shallow-water vent and seep sites, in: Kiel, S. (Ed.),
50 730 *Vent and Seep Biota: Aspects from Microbes to Ecosystems*. Springer Netherlands, Dordrecht, pp.
51 731 333–378. https://doi.org/10.1007/978-90-481-9572-5_11
52 732 Dando, P.R., 2001. A review of pockmarks in the UK part of the North Sea, with particular respect to
53 733 their biology. *Strategic Environmental Assessment – SEA2. Technical Report 001 – Pockmarks*.
54
55
56
57
58
59
60
61
62
63
64
65

1
2
3
4
5
6
7
8
9
10
11
12
13
14
15
16
17
18
19
20
21
22
23
24
25
26
27
28
29
30
31
32
33
34
35
36
37
38
39
40
41
42
43
44
45
46
47
48
49
50
51
52
53
54
55
56
57
58
59
60
61
62
63
64
65

Dondurur, D., Çifçi, G., Drahor, M.G., Coşkun, S., 2011. Acoustic evidence of shallow gas accumulations and active pockmarks in the İzmir Gulf, Aegean sea. *Mar. Pet. Geol.* 28, 1505–1516. <https://doi.org/10.1016/j.marpetgeo.2011.05.001>

Dunford, G.M., Dancer, P.N., Long, K.D., 2001. Hydrocarbon potential of the Kish Bank Basin: integration within a regional model for the Greater Irish Sea Basin. *Geol. Soc. London, Spec. Publ.* 188, 135 LP – 154. <https://doi.org/10.1144/GSL.SP.2001.188.01.07>

Ergün, M., Dondurur, D., Çifçi, G., 2002. Acoustic evidence for shallow gas accumulations in the sediments of the Eastern Black Sea. *Terra Nov.* 14, 313–320. <https://doi.org/10.1046/j.1365-3121.2002.00434.x>

Evans, T.G., 2011. A systematic approach to offshore engineering for multiple-project developments in geohazardous areas, in: *Frontiers in Offshore Geotechnics II - Proceedings of the 2nd International Symposium on Frontiers in Offshore Geotechnics*. pp. 3–32.

Fichler, C., Henriksen, S., Rueslaatten, H., Hovland, M., 2005. North Sea Quaternary morphology from seismic and magnetic data: indications for gas hydrates during glaciation? *Pet. Geosci.* 11, 331 LP – 337. <https://doi.org/10.1144/1354-079304-635>

Floodpage, J., Newman, P., White, J., 2001. Hydrocarbon prospectivity in the Irish Sea area: insights from recent exploration of the Central Irish Sea, Peel and Solway basins. *Geol. Soc. London, Spec. Publ.* 188, 107 LP – 134. <https://doi.org/10.1144/GSL.SP.2001.188.01.06>

Games, K.P., 2001. Evidence of shallow gas above the Connemara oil accumulation, Block 26/28, Porcupine Basin, in: Haughton, P.W., Corcoran, D. V (Eds.), *The Petroleum Exploration of Ireland's Offshore Basins*. The Geological Society of London, Special Publications, London, pp. 361–373. <https://doi.org/10.1144/GSL.SP.2001.188.01.21>

Hammer, Ø., Webb, K.E., Depreiter, D., 2009. Numerical simulation of upwelling currents in pockmarks, and data from the Inner Oslofjord, Norway. *Geo-Marine Lett.* 29, 269–275. <https://doi.org/10.1007/s00367-009-0140-z>

Harrington, P.K., 1985. Formation of pockmarks by pore-water escape. *Geo-Marine Lett.* 5, 193–197. <https://doi.org/10.1007/BF02281638>

Hovland, M., 2002. On the self-sealing nature of marine seeps. *Cont. Shelf Res.* 22, 2387–2394. [https://doi.org/https://doi.org/10.1016/S0278-4343\(02\)00063-8](https://doi.org/https://doi.org/10.1016/S0278-4343(02)00063-8)

Hovland, M., Curzi, P. V, 1989. Gas seepage and assumed mud diapirism in the Italian central Adriatic Sea. *Mar. Pet. Geol.* 6, 161–169. [https://doi.org/https://doi.org/10.1016/0264-8172\(89\)90019-6](https://doi.org/https://doi.org/10.1016/0264-8172(89)90019-6)

Hovland, M., Gardner, J. V, Judd, A.G., 2002. The significance of pockmarks to understanding fluid flow processes and geohazards. *Geofluids* 2, 127–136. <https://doi.org/10.1046/j.1468-8123.2002.00028.x>

Hovland, M., Heggland, R., De Vries, M.H., Tjelta, T.I., 2010. Unit-pockmarks and their potential significance for predicting fluid flow. *Mar. Pet. Geol.* 27, 1190–1199. <https://doi.org/10.1016/j.marpetgeo.2010.02.005>

Hovland, M., Judd, A.G., 1992. The global production of methane from shallow submarine sources. *Cont. Shelf Res.* 12, 1231–1238. [https://doi.org/10.1016/0278-4343\(92\)90082-U](https://doi.org/10.1016/0278-4343(92)90082-U)

Hovland, M., Judd, A.G., 1988. *Seabed Pockmarks and Seepages*. Graham and Trotman, London.

Jackson, D.I., Jackson, A.A., Evans, D., Wingfield, R.T.R., Barnes, R.P., Arthur, M.J., 1995. *United Kingdom offshore regional report: the geology of the Irish Sea*. British Geological Survey, London.

Jackson, D.I., Mullholland, P., 1993. Tectonic and stratigraphic aspects of the East Irish Sea Basin and adjacent areas: contrasts in their post-Carboniferous structural styles. *Geol. Soc. London, Pet. Geol. Conf. Ser.* 4, 791 LP – 808. <https://doi.org/10.1144/0040791>

Jordan, S.F., O'Reilly, S.S., Praeg, D., Dove, D., Facchin, L., Romeo, R., Szpak, M., Monteys, X., Murphy, B.T., Scott, G., McCarron, S.S., Kelleher, B.P., 2019. Geophysical and geochemical analysis of shallow gas and an associated pockmark field in Bantry Bay, Co. Cork, Ireland. *Estuar. Coast. Shelf*

1
2
3
4 782 Sci. 225, 106232. <https://doi.org/10.1016/j.ecss.2019.05.014>
5 783 Judd, A., Noble-James, T., Golding, N., Eggett, A., Diesing, M., Clare, D., Silburn, B., Duncan, G., Field, L.,
6 784 Milodowski, A., 2019. The Croker Carbonate Slabs: extensive methane-derived authigenic
7 785 carbonate in the Irish Sea—nature, origin, longevity and environmental significance. *Geo-Marine*
8 786 *Lett.* <https://doi.org/10.1007/s00367-019-00584-0>
9 787 Judd, A.G., Hovland, M., 2007. *Seabed Fluid Flow, the Impact on Geology, Biology, and the Marine*
10 788 *Environment*. Cambridge University Press.
11 789 Judd, A.G., Hovland, M., 1992. The evidence of shallow gas in marine sediments. *Cont. Shelf Res.* 12,
12 790 1081–1095.
13 791 Karisiddaiah, S.M., Veerayya, M., 1994. Methane-bearing shallow gas-charged sediments in the eastern
14 792 Arabian Sea: a probable source for greenhouse gas. *Cont. Shelf Res.* 14, 1361–1370.
15 793 [https://doi.org/https://doi.org/10.1016/0278-4343\(94\)90053-1](https://doi.org/https://doi.org/10.1016/0278-4343(94)90053-1)
16 794 Kiel, S., 2010. The vent and seep biota, in: Landman, N.H., Harries, P. (Eds.), *Topics in Geobiology*.
17 795 Springer, Germany, p. 487.
18 796 Kim, Y.-J., Cheong, S., Chun, J.-H., Cukur, D., Kim, S.-P., Kim, J.-K., Kim, B.-Y., 2020. Identification of
19 797 shallow gas by seismic data and AVO processing: Example from the southwestern continental shelf
20 798 of the Ulleung Basin, East Sea, Korea. *Mar. Pet. Geol.* 117, 104346.
21 799 <https://doi.org/https://doi.org/10.1016/j.marpetgeo.2020.104346>
22 800 Koch, S., Berndt, C., Bialas, J., Haeckel, M., Crutchley, G., Papenberg, C., Klaeschen, D., Greinert, J., 2015.
23 801 Gas-controlled seafloor doming. *Geology* 43, 571–574. <https://doi.org/10.1130/G36596.1>
24 802 Laier, T., Jensen, J.B., 2007. Shallow gas depth-contour map of the Skagerrak-western Baltic Sea region.
25 803 *Geo-Marine Lett.* 27, 127–141. <https://doi.org/10.1007/s00367-007-0066-2>
26 804 Loher, M., Marcon, Y., Pape, T., Römer, M., Wintersteller, P., dos Santos Ferreira, C., Praeg, D., Torres,
27 805 M., Sahling, H., Bohrmann, G., 2018. Seafloor sealing, doming, and collapse associated with gas
28 806 seeps and authigenic carbonate structures at Venere mud volcano, Central Mediterranean. *Deep.*
29 807 *Res. Part I Oceanogr. Res. Pap.* 137, 76–96. <https://doi.org/10.1016/j.dsr.2018.04.006>
30 808 Løseth, H., Gading, M., Wensaas, L., 2009. Hydrocarbon leakage interpreted on seismic data. *Mar. Pet.*
31 809 *Geol.* 26, 1304–1319. <https://doi.org/https://doi.org/10.1016/j.marpetgeo.2008.09.008>
32 810 Mazumdar, A., Peketi, A., Dewangan, P., Badesab, F., Ramprasad, T., Ramana, M. V., Patil, D.J., Dayal, A.,
33 811 2009. Shallow gas charged sediments off the Indian west coast: Genesis and distribution. *Mar.*
34 812 *Geol.* 267, 71–85. <https://doi.org/10.1016/j.margeo.2009.09.005>
35 813 Mellet, C., Long, D., Carter, G., Chiverell, R., Van Landeghem, K., 2015. *Geology of the seabed and*
36 814 *shallow subsurface: The Irish Sea*. British Geological Survey Commissioned Report, CR/15/057.
37 815 52pp.
38 816 National Parks and Wildlife, 2015. *Codling Fault Zone SAC Site Synopsis*. Republic of Ireland.
39 817 Newman, P.J., 1999. The geology and hydrocarbon potential of the Peel and Solway Basins, East Irish
40 818 Sea. *J. Pet. Geol.* 22, 305–324. <https://doi.org/10.1111/j.1747-5457.1999.tb00989.x>
41 819 Noble-James, T., Judd, A., Diesing, M., Clare, D., Eggett, A., Silburn, B., Duncan, G., 2020. Monitoring
42 820 shallow methane-derived authigenic carbonate: Insights from a UK Marine Protected Area. *Aquat.*
43 821 *Conserv. Mar. Freshw. Ecosyst.* 1–18. <https://doi.org/10.1002/aqc.3296>
44 822 O'Reilly, S.S., Hryniewicz, K., Little, C.T.S., Monteys, X., Szpak, M.T., Murphy, B.T., Jordan, S.F., Allen,
45 823 C.C.R., Kelleher, B.P., 2014. Shallow water methane-derived authigenic carbonate mounds at the
46 824 Codling Fault Zone, western Irish Sea. *Mar. Geol.* 357, 139–150.
47 825 <https://doi.org/10.1016/j.margeo.2014.08.007>
48 826 O'Reilly, S.S., 2018, personal communications via email with Mark Coughlan, 04/12/2028.
49 827 Pharaoh, T.C., Smith, N.J.P., Kirk, K., Kimbell, G.S., Gent, C., Quinn, M., Monaghan, A.A., 2016. *Palaeozoic*
50 828 *Petroleum Systems of the Irish Sea Energy and Marine Geoscience Programme*, British Geological
51 829 Survey Commissioned Report.
52
53
54
55
56
57
58
59
60
61
62
63
64
65

- 1
2
3
4 830 Portnov, A., Vadakkepuliymbatta, S., Mienert, J., Hubbard, A., 2016. Ice-sheet-driven methane storage
5 831 and release in the Arctic. *Nat. Commun.* 7, 10314. <https://doi.org/10.1038/ncomms10314>
6 832 Ramprasad, T., Dewangan, P., Ramana, M. V., Mazumdar, A., Karisiddaiah, S.M., Ramya, E.R., Sriram, G.,
7 833 2011. Evidence of slumping/sliding in Krishna–Godavari offshore basin due to gas/fluid
8 834 movements. *Mar. Pet. Geol.* 28, 1806–1816.
9 835 <https://doi.org/https://doi.org/10.1016/j.marpetgeo.2011.02.007>
10 836 Rathburn, A.E., Levin, L.A., Held, Z., Lohmann, K.C., 2000. Benthic foraminifera associated with cold
11 837 methane seeps on the northern California margin: Ecology and stable isotopic composition. *Mar.*
12 838 *Micropaleontol.* 38, 247–266. [https://doi.org/https://doi.org/10.1016/S0377-8398\(00\)00005-0](https://doi.org/https://doi.org/10.1016/S0377-8398(00)00005-0)
13 839 Roelofse, C., Alves, T.M., Gafeira, J., 2020. Structural controls on shallow fluid flow and associated
14 840 pockmark fields in the East Breaks area, northern Gulf of Mexico. *Mar. Pet. Geol.* 112, 104074.
15 841 <https://doi.org/10.1016/j.marpetgeo.2019.104074>
16 842 Roy, S., Hovland, M., Noormets, R., Olausen, S., 2015. Seepage in Isfjorden and its tributary fjords, West
17 843 Spitsbergen. *Mar. Geol.* 363, 146–159.
18 844 <https://doi.org/https://doi.org/10.1016/j.margeo.2015.02.003>
19 845 Roy, S., Senger, K., Braathen, A., Noormets, R., Hovland, M., Olausen, S., 2014. Fluid migration
20 846 pathways to seafloor seepage in inner isfjorden and Adventfjorden, Svalbard. *Nor. Geol. Tidsskr.*
21 847 94, 99–199.
22 848 Roy, S., Senger, K., Hovland, M., Römer, M., Braathen, A., 2019. Geological controls on shallow gas
23 849 distribution and seafloor seepage in an Arctic fjord of Spitsbergen, Norway. *Mar. Pet. Geol.* 107,
24 850 237–254. <https://doi.org/https://doi.org/10.1016/j.marpetgeo.2019.05.021>
25 851 Sills, G.C., Wheeler, S.J., 1992. The significance of gas for offshore operations. *Cont. Shelf Res.* 12, 1239–
26 852 1250.
27 853 Society for Underwater Technology, 2005. Guidance Notes on Site Investigations for Offshore
28 854 Renewable, Guidance notes on site investigations for offshore renewable energy projects.
29 855 Sultan, N., de Gennaro, V., Puech, A., 2012. Mechanical behaviour of gas-charged marine plastic
30 856 sediments. *Geotechnique* 62, 751–766. <https://doi.org/10.1680/geot.12.OG.002>
31 857 Sun, Q., Alves, T., Xie, X., He, J., Li, W., Ni, X., 2017. Free gas accumulations in basal shear zones of mass-
32 858 transport deposits (Pearl River Mouth Basin, South China Sea): An important geohazard on
33 859 continental slope basins. *Mar. Pet. Geol.* 81, 17–32.
34 860 <https://doi.org/https://doi.org/10.1016/j.marpetgeo.2016.12.029>
35 861 Sun, Q., Wu, S., Hovland, M., Luo, P., Lu, Y., Qu, T., 2011. The morphologies and genesis of mega-
36 862 pockmarks near the Xisha Uplift, South China Sea. *Mar. Pet. Geol.* 28, 1146–1156.
37 863 <https://doi.org/https://doi.org/10.1016/j.marpetgeo.2011.03.003>
38 864 Szpak, M.T., Monteys, X., O’Reilly, S., Simpson, A.J., Garcia, X., Evans, R.L., Allen, C.C.R., McNally, D.J.,
39 865 Courtier-Murias, D., Kelleher, B.P., 2012. Geophysical and geochemical survey of a large marine
40 866 pockmark on the Malin Shelf, Ireland. *Geochemistry, Geophys. Geosystems* 13, 1–18.
41 867 <https://doi.org/10.1029/2011GC003787>
42 868 Szpak, M.T., Monteys, X., O’Reilly, S.S., Lilley, M.K.S., Scott, G.A., Hart, K.M., McCarron, S.G., Kelleher,
43 869 B.P., 2015. Occurrence, characteristics and formation mechanisms of methane generated micro-
44 870 pockmarks in Dunmanus Bay, Ireland. *Cont. Shelf Res.* 103, 45–59.
45 871 <https://doi.org/10.1016/j.csr.2015.04.023>
46 872 Thomas, I.W., 1978. Well 33/22-1 Completion Report.
47 873 Tóth, Z., Spieß, V., Jensen, J., 2014. Seismo-acoustic signatures of shallow free gas in the Bornholm
48 874 Basin, Baltic Sea. *Cont. Shelf Res.* 88, 228–239.
49 875 <https://doi.org/https://doi.org/10.1016/j.csr.2014.08.007>
50 876 Van Landeghem, K.J.J., Niemann, H., Steinle, L.I., O’Reilly, S.S., Huws, D.G., Croker, P.F., 2015. Geological
51 877 settings and seafloor morphodynamic evolution linked to methane seepage. *Geo-Marine Lett.* 35,

1
2
3
4
5
6
7
8
9
10
11
12
13
14
15
16
17
18
19
20
21
22
23
24
25
26
27
28
29
30
31
32
33
34
35
36
37
38
39
40
41
42
43
44
45
46
47
48
49
50
51
52
53
54
55
56
57
58
59
60
61
62
63
64
65

878 289–304. <https://doi.org/10.1007/s00367-015-0407-5>

879 Vanneste, M., Sultan, N., Garziglia, S., Forsberg, C.F., L’Heureux, J.S., 2014. Seafloor instabilities and
880 sediment deformation processes: The need for integrated, multi-disciplinary investigations. *Mar.*
881 *Geol.* 352, 183–214. <https://doi.org/10.1016/j.margeo.2014.01.005>

882 Ward, S.L., Neill, S.P., Landeghem, K.J.J. Van, Scourse, J.D., 2015. Classifying seabed sediment type using
883 simulated tidal-induced bed shear stress. *Mar. Geol.* 367, 94–104.
884 <https://doi.org/10.1016/j.margeo.2015.05.010>

885 Webb, K.E., Barnes, D.K.A., Plankea, S., 2009. Pockmarks: Refuges for marine benthic biodiversity.
886 *Limnol. Oceanogr.* 54, 1776–1788. <https://doi.org/10.4319/lo.2009.54.5.1776>

887 Woods, M.A., Wilkinson, I.P., Leng, M.J., Riding, J.B., Vane, C.H., Lopes dos Santos, R.A., Kender, S., De
888 Schepper, S., Hennissen, J.A.I., Ward, S.L., Gowing, C.J.B., Wilby, P.R., Nichols, M.D., Rochelle, C.A.,
889 2019. Tracking Holocene palaeostratification and productivity changes in the Western Irish Sea: A
890 multi-proxy record. *Palaeogeogr. Palaeoclimatol. Palaeoecol.* 532, 109231.
891 <https://doi.org/https://doi.org/10.1016/j.palaeo.2019.06.004>

892 Xing, J., Jiang, X., Li, D., 2016. Seismic study of the mud diapir structures in the Okinawa Trough. *Geol. J.*
893 51, 203–208. <https://doi.org/10.1002/gj.2824>

894 Yilmaz, Ö., 2001. *Seismic Data Analysis: Processing, Inversion, and Interpretation of Seismic Data*. Society
895 of Exploration Geophysicists, Tulsa.

896 Yuan, F., Bennell, J.D., Davis, A.M., 1992. Acoustic and physical characteristics of gassy sediments in the
897 western Irish Sea. *Cont. Shelf Res.* 12, 1121–1134.

898

899 **Figure Captions**

900 **Figure 1** Overview of the location of study areas (A-D) within the Irish Sea along with 2D reflection
901 seismic lines and borehole locations referred to in the text superimposed on previously mapped areas of
902 sub-cropping Carboniferous rocks, Mesozoic sedimentary basins (both accessed from EMODNet) and
903 structural lineaments (Anderson, 2013; Anderson et al., 2016). Also included are Special Areas of
904 Conservation (SAC) and Marine Conservation Zones (MCZ) related to gas features and the extent of the
905 Western Irish Sea Mud Belt. Please note that the Carboniferous potential source rock is present in the
906 Permian-Triassic basins.

907
908 **Figure 2** (A) Simplified lithostratigraphic column of the bedrock geology of the Western Irish Sea. (B)
909 Simplified lithostratigraphic column of the Quaternary section discussed in this study.

910
911 **Figure 3** 2D multichannel seismic line E95IE18-03 and accompanying geoseismic interpretation. Image
912 quality degrades significantly within the Codling Fault Zone due to a combination of structural
913 complexity and shallow gas-related features. **Inset:** Several shallow gas related features are identified
914 within the Codling Fault Zone, including seabed brightening with a sharp boundary above a major, near-

1
2
3
4
5
6
7
8
9
10
11
12
13
14
15
16
17
18
19
20
21
22
23
24
25
26
27
28
29
30
31
32
33
34
35
36
37
38
39
40
41
42
43
44
45
46
47
48
49
50
51
52
53
54
55
56
57
58
59
60
61
62
63
64
65

915 seabed splay of the Codling Fault Zone, and reverse polarity anomalies with associated seismic blanking
916 and signal dispersion.

917
918 **Figure 4** 2D multichannel seismic line IS-12 and accompanying geoseismic interpretation. The graben fill
919 is predicted to be of Permian-Triassic sediment, similar to the stratigraphy of the along-strike Peel Basin.
920 The faults bounding the graben are observed to offset the Base-Cenozoic Unconformity, indicating
921 recent tectonic activity and representing possible fluid-migration pathways.

922
923 **Figure 5** 2D multichannel seismic line JSM92-30 and accompany geoseismic interpretation. Several
924 minor faults are observed offsetting the Base-Cenozoic Unconformity in the Queenie Corner area.

925
926 **Figure 6** Seabed mounds observed at the southern part of the study area (within the Codling Fault Zone)
927 are interpreted as carbonate mounds which form as a result of prolonged seepage at the seafloor.
928 Sediment waves are predominant in this region of the study area. A and B highlight the mound
929 structures in close up (note different water depth scales for better visualization of the mounds). High
930 backscatter is evident at these two locations. Refer to Fig. 1 for location.

931
932 **Figure 7** (A) High-resolution bathymetric data illustrating seafloor morphology at Lambay Deep, along
933 with (B) vertical profile across the 1 km wide depression. (C) Zoom-in of the bathymetric high which is
934 characterized by high-backscatter (D). Refer to Fig. 1 for location.

935
936 **Figure 8** Lambay Deep as imaged by sparker seismic data with interpreted units. Highlighted is the
937 mound referred to as the Lambay Deep Mud Diapir (LDMD) and acoustic evidence for shallow gas
938 (acoustic turbidity and enhanced reflections). 'M' denotes seabed multiple. Unit names are referenced
939 from Figure 2. Yellow line is the top of UT (Upper Till member), blue line is top of PF (Prograded Facies),
940 SSF is Surface Sands Formation. Red line denotes the edge of the LDMD. Dashed black line is the top of
941 the shallow gas.

942
943 **Figure 9** Depth to the top of the gas accumulation (interpreted on a grid of 2D sparker seismic lines
944 shown in Fig. 1 of Coughlan et al., (2019), identified in the Western Irish Sea Mud Belt superimposed on
945 water depth from MBES data. Highlighted are the pockmarks described in Supplementary Material, the
946 location of seismic lines presented in Fig. 10 and the pockmarks presented in detail in Fig. 11.

1
2
3
4
5
6
7
8
9
10
11
12
13
14
15
16
17
18
19
20
21
22
23
24
25
26
27
28
29
30
31
32
33
34
35
36
37
38
39
40
41
42
43
44
45
46
47
48
49
50
51
52
53
54
55
56
57
58
59
60
61
62
63
64
65

947

Figure 10 Sparker seismic lines highlighted in Fig. 9 from the WISMB with interpreted units. Also presented is evidence for shallow gas accumulation (enhanced reflection, acoustic turbidity, acoustic blanking). 'M' denotes seabed multiple. Unit names are referenced from Figure 2. Full black line indicates the top of bedrock. Yellow line is the top of UT (Upper Till member), green line is the top of CF (Chaotic Facies), blue line is top of PF (Prograded Facies). Dashed black line denotes the gas front.

953

Figure 11 High-resolution bathymetric data illustrating (A) a central mound within pockmark P15, and (B) morphology of a circular pockmark P13 without a central mound along with their vertical profiles. (C) Central mounds within pockmarks P10 and P11, which are separated by approximately 1 km. Refer to Fig. 9 for locations.

958

Figure 12 High-resolution multibeam bathymetric data (top) and backscatter data (bottom) of the Queenie Corner area seafloor. Refer to Fig. 1 for location. A closer illustration of the seabed mound structures of various sizes and shapes (sub-circular to elongated) have been shown along with their vertical profiles.

963

Figure 13 Pinger profile highlighted in Fig. 12 from Queenie Corner illustrates acoustic evidence for shallow gas in the form of gas chimneys (a) and acoustic blanking (b). Seabed mounds are observed at the top of gas chimneys (a).

967

Figure 14 Conceptual model proposed for fluid migration from deeper thermogenic source rocks via recently reactivated fault conduits to shallow gas-charged Quaternary sediments in the Western Irish Sea Mud Belt. Subsequently, some of the gas migrates upwards to the seafloor, leading to the formation of pockmarks (due to fluid seepage) and seabed mounds (due to increase of pressure and volume within sediment pores).

973

Figure 15 Overview map of shallow gas accumulations and fluid seepage features identified in this study along with similar features identified from other referenced studies. This information is superimposed on the British Geological Survey DigSBS250 database, which maps seabed sediment distribution according to the Folk Classification, in the Irish Sea at a scale of 1:250,000. Some pockmarks from this study are seen to form above a mapped shallow gas accumulation with mud-dominated sediments,

1
2
3
4
5
6
7
8
9
10
11
12
13
14
15
16
17
18
19
20
21
22
23
24
25
26
27
28
29
30
31
32
33
34
35
36
37
38
39
40
41
42
43
44
45
46
47
48
49
50
51
52
53
54
55
56
57
58
59
60
61
62
63
64
65

979 generally pockmarks (this study) are concentrated in areas with a sandier component. Seabed mound
980 features in this study were found in areas where the seabed sediment is mud-dominated.

981
982 **Figure 16** Conceptual models proposed for (A) the formation of mounds at the centre of pockmarks in
983 sand-rich sediments and (B) seabed mounds in mud-rich sediments as precursors to collapsed
984 pockmarks, , adapted from previous studies (Hovland, 2002; Crémière et al. 2018; Loher et al. 2018).

985
986 **Table Captions**

987 **Table 1** List of surveys from which data were used in this study.

1
2
3
4
5
6
7
8
9
10
11
12
13
14
15
16
17
18
19
20
21
22
23
24
25
26
27
28
29
30
31
32
33
34
35
36
37
38
39
40
41
42
43
44
45
46
47
48
49
50
51
52
53
54
55
56
57
58
59
60
61
62
63
64
65

1 **Geological settings and controls of fluid migration and associated seafloor**
2 **seepage features in the north Irish Sea**

3
4 Mark Coughlan^{1,3*}, Srikumar Roy^{2,3}, Conor O’Sullivan^{2,3}, Annika Clements⁴, Ronan O’Toole⁵, Ruth Plets^{6,7}

5
6 ¹School of Civil Engineering, University College Dublin, Newstead, Belfield, Dublin 4, Ireland.

7 ²School of Earth Sciences, Science Centre West, University College Dublin, Belfield, Dublin 4, Ireland.

8 ³Irish Centre for Research in Applied Geosciences, O’Brien Centre for Science East, University College
9 Dublin, Belfield, Dublin 4, Ireland

10 ⁴Seafish, 18 Logie Mill, Logie Green Road, Edinburgh.

11 ⁵Geological Survey of Ireland, Beggars Bush, Dublin, Ireland

12 ⁶School of Geography and Environmental Sciences, Ulster University, Coleraine, Northern Ireland.

13 ⁷Flanders Marine Institute, Wandelaarkaai 7, 8400 Ostend, Belgium

14
15 **ABSTRACT**

16
17 Shallow gas accumulation in unconsolidated Quaternary sediments, and associated seepage at the
18 seafloor, is widespread in the north Irish Sea. This study integrates high-resolution seafloor bathymetry
19 and sub-surface geophysical data to investigate shallow gas accumulations and possible fluid (gas and/or
20 liquids) migration pathways to the seafloor in the northern part of the Irish Sea. Shallow gas occurs
21 broadly in two geological settings: the Codling Fault Zone and the Western Irish Sea Mud Belt. The gas
22 has been recognised to accumulate in both sandy and muddy Quaternary marine near-surface
23 sediments and is characterised by three characteristic sub-bottom acoustic features: i) enhanced
24 reflections, ii) acoustic turbid zones, and iii) acoustic blanking. The seepage of shallow gas at the
25 seafloor has resulted in the formation of morphological features including methane-derived authigenic
26 carbonates, seabed mounds and pockmarks. In many instances, the evidence for this gas as biogenic or
27 thermogenic in origin is inconclusive. Two distinct types of pockmarks are recorded in the Western Irish
28 Mud Belt: pockmarks with a relatively flat centre, and pockmarks with a central mound. Based on our
29 observation and existing models, we infer that the formation of a ~~thin~~ carbonate crust at the seabed
30 surface, ~~which collapses over time~~, is needed as a precursor for the creation of such mounds within

1
2
3
4
5
6
7
8
9
10
11
12
13
14
15
16
17
18
19
20
21
22
23
24
25
26
27
28
29
30
31
32
33
34
35
36
37
38
39
40
41
42
43
44
45
46
47
48
49
50
51
52
53
54
55
56
57
58
59
60
61
62
63
64
65

pockmarks. The formation processes are interpreted to be different for sandy versus muddy sediments, due to variability in erodibility and sealing capacities of the substrate. We suggest that the origin of these features is linked to the presence of ~~a deeper~~ **potential** hydrocarbon source rocks with existing and reactivated faults forming fluid migration pathways to the surface. This in turn could indicate a **mixed** thermogenic-biogenic origin for seep ~~related locations associated~~ structures in the study area. These features have significant implications for the future development of offshore infrastructure including marine renewable energy as well as for seabed ecology and conservation efforts in the Irish Sea.

Keywords: pockmark, seabed mounds, fluid seepage, MDAC, mud diapir, geohazards, ecological conservation, offshore infrastructure

INTRODUCTION

~~The accumulation of~~ **Shallow** gas in **shallow**, unconsolidated marine sediments is **aa global** ~~phenomenon~~ **globally widespread** (Andreassen et al., 2007; Dondurur et al., 2011; Ergün et al., 2002; Hovland and Judd, 1992; Karisiddaiah and Veerayya, 1994; Mazumdar et al., 2009). It represents an important tool for frontier ~~exploration of~~ hydrocarbon **exploration, while also posing reservoirs, as well as being** a significant geohazard, affecting sediment engineering properties (Andreassen et al., 2007; Hovland et al., 2002; Sills and Wheeler, 1992). The impacts of shallow gas and seepage on seabed ecology has also gained importance **over the recent years** (Jordan et al., 2019; Kiel, 2010; Rathburn et al., 2000). To date in the Irish Sea (Fig. 1), a number of areas associated with shallow gas and fluid seepage have been designated as Special Areas of Conservation (SAC) due to the unique habitats they form as “Submarine structures made by leaking gases”, according to the Annex I / II of the E.U. Habitats Directive (National Parks and Wildlife, 2015). These can form two described habitat types: Bubbling Reefs and Structures within Pockmarks. In the Irish Sea, the SAC areas are predominantly related to Methane-Derived Authigenic Carbonates (MDAC) and are known locally as the Codling Fault Zone (CFZ) SAC and Croker Carbonate Slabs (CCS) SAC (Fig. 1). Further north, Queenie Corner is an offshore site within the Western Irish Sea Mud Belt (WISMB) that was designated as a UK Marine Conservation Zone (MCZ) in 2019 for its subtidal mud habitat and sea-pen and burrowing megafauna communities (Clements and Service, 2016).

1
2
3
4
5
6
7
8
9 61 Shallow gas in unconsolidated marine sediments can have a biogenic or thermogenic origin. Bulk
10 62 isotopic analysis on samples from the CFZ by O'Reilly et al. (2014) indicate a biogenic origin of the
11 63 seeping gas, with some possible thermogenic contribution from underlying Carboniferous coal deposits.
12 64 Methanogenesis of organic-rich Quaternary sediments has been proposed as a source for shallow gas in
13 65 Bantry Bay (Jordan et al., 2019) and Dunmanus Bay (Szpak et al., 2015) elsewhere in Irish waters.
14 66 Evidence for shallow gas accumulations and seepage in the Irish Sea has been detected from geophysical
15 67 observations on seismic lines as gas chimneys, enhanced reflectors and acoustic turbidity (e.g. Judd and
16 68 Hovland (1992)). Where fluids (e.g. methane gas) emanate from the seabed, morphological features
17 69 such as mounds and pockmarks have formed in the Western Irish Sea (Croker et al., 2005).
18 70

19 71 Mounds are elevated ~~bathymetric topographic seafloor~~ features which can ~~either~~ form due to upward
20 72 migrating fluids exerting pressure on overlying relatively impermeable layers or precipitation of
21 73 carbonates due to prolonged methane gas seepage. Owing to their different formation mechanism, they
22 74 are known as seabed domes, mud diapirs, and carbonate mounds, all of which have been found in the
23 75 Irish Sea (Croker et al., 2005). Hovland and Curzi (1989) documented seabed domes and mud diapirs in
24 76 the Adriatic Sea offshore Italy, where gas bubbles concentrating in plastic clay caused local density
25 77 reversals, resulting in the upward buoyant flow of the clay and deformation of overlying unlithified
26 78 layers, thus forming elevated ~~bathymetric topographical~~ features at the seafloor and associated gas
27 79 seepages. Such seabed domes and mud diapirs have also been found offshore India (Ramprasad et al.,
28 80 2011), in Norwegian Arctic fjords (Roy et al., 2014), and offshore New Zealand (Koch et al., 2015). Croker
29 81 et al. (2005) previously mapped mounds (referred to as "seabed doming") in the WISMB, and suggested
30 82 that they may have formed due to the replacement of water in the pore space with gas causing an
31 83 increase in sediment volume in the upper sediment layers. For this to occur, fine-grained, relatively
32 84 impermeable sediments are required. Croker et al. (2005) also suggested that seabed doming might be
33 85 an initial stage of pockmark formation. Mounds can also form when prolonged methane gas seepage at
34 86 the seabed ~~chemically~~ interacts with surrounding minerals to form a carbonate precipitate cement
35 87 (MDAC), binding the sediment matrix and forming hard, ~~resistive rocks rock like substances~~ (Judd et al.,
36 88 2019). With continued seepage over time, MDACs can continue to precipitate and grow into sizeable
37 89 features up to 10 m high and 250 m in length, ~~as found at the CFZ in the western Irish Sea~~ (O'Reilly et al.,
38 90 2014).
39 91

40
41
42
43
44
45
46
47
48
49
50
51
52
53
54
55
56
57
58
59
60
61
62
63
64
65

1
2
3
4
5
6
7
8
9 92 Pockmarks are the most common manifestations of fluid seepage on the seafloor and are formed by
10 93 fluids escaping through the seafloor sediments (Hovland and Judd, 1988). Unconsolidated sediments at
11
12 94 the seafloor are lifted and winnowed by the escaping fluids (pore water or gas) forming crater-like
13 95 depressions. Their shapes are typically circular to sub-circular, however, asymmetric, elongated and
14
15 96 trough-like pockmarks have also been documented (Judd and Hovland, 2007; Roy et al., 2015).
16 97 Pockmark diameters range from < 5m (unit-pockmarks) to > 1500m (mega-pockmarks) (Hovland et al.,
17 98 2010; Sun et al., 2011). Pockmarks found in Irish waters vary in size with smaller features typically 2 – 3
19 99 m in diameter (unit-pockmarks) and tens of centimetres deep. Relatively larger pockmarks offshore
20
21 100 Ireland are approximately 20 m in diameter and up to 2 m in depth (Croker et al., 2005; Games, 2001;
22 101 Szpak et al., 2015, 2012). What is imperative for their formation is a fine-grained, clay to silt, substrate at
23
24 102 the seafloor (Croker et al., 2005).

25 103
26
27 104 Seafloor and sub-seabed evidence for shallow gas and fluid migrationseepage in the Irish Sea,
28 105 specifically the CFZ and WISMB, has been previously documented (e.g. Croker et al. (2005)).
29
30 106 Geochemical analysis of the seep and mound locations suggest mixed biogenic and thermogenic
31 107 signatures (Judd et al., 2019; O'Reilly et al., 2014). However, factors such as structural and stratigraphic
32
33 108 features responsible for the migration of fluids responsible for a thermogenic signature are still poorly
34 109 understood. Furthermore, models applicable to the formation mechanisms of the seep-related seafloor
35
36 110 features in the Irish Sea are lacking. With this in mind, the aims~~The aim~~ of this study are~~is therefore two-~~
37 111 fold:

38
39 112 (i) To spatially map and characterise geophysical evidence for shallow gas, fluid migration and
40 113 seafloor seepage in the north Irish Sea;

41 114 (ii) To establish a geological framework incorporating bedrock geology, hydrocarbon source
42 115 rocks, structural geology (faults), Quaternary geology and seafloor morphology in the Irish
43 116 Sea which will facilitate further studies into subsurface fluid flow mechanisms;

44
45
46 117 ~~To (i) to provide a revised geological model to investigate the potential sources of thermogenic gas in~~
47 118 ~~the north Irish Sea (namely the CFZ and WISMB), as well as the direct fluid pathways and stratigraphic~~
48 119 ~~controls that allow it to migrate to shallow sub-seabed accumulations and form seep-related seafloor~~
49
50 120 ~~features, and;~~

51
52 121 (iii) ~~(ii) to~~ suggest theories of seabed mound and pockmark formation in the WISMB.

Formatted: List Paragraph,
Numbered + Level: 1 + Numbering
Style: i, ii, iii, ... + Start at: 1 +
Alignment: Right + Aligned at:
0.63 cm + Indent at: 1.9 cm

53 122
54
55
56
57
58
59
60
61
62
63
64
65

1
2
3
4
5
6
7
8
9
10
11
12
13
14
15
16
17
18
19
20
21
22
23
24
25
26
27
28
29
30
31
32
33
34
35
36
37
38
39
40
41
42
43
44
45
46
47
48
49
50
51
52
53
54
55
56
57
58
59
60
61
62
63
64
65

To achieve this, we provide an integrated analysis of shallow high-resolution datasets (sub-bottom acoustic, multibeam echosounder bathymetry and backscatter data) and deep 2D multichannel seismic datasets from the north Irish Sea. Inferences are made on the formation mechanisms of seep-related seabed features which can be used to better predict their ~~likely~~ distribution elsewhere in the region. Finally, the implications of shallow gas and fluid-seepage at the seafloor are considered in the context of marine infrastructure siting and ecological conservation.

BACKGROUND GEOLOGY

The bedrock geology of the Irish Sea is characterised by a series of rift basins with several kilometres of Carboniferous, Permian and Triassic sedimentary fill. These basins formed through a series of extensional events in the Carboniferous, Permian and Jurassic, punctuated by episodes of uplift during the Late Carboniferous Variscan Orogeny and more recently the Alpine Orogeny during the Cenozoic. During the Cenozoic event, the Irish Sea experienced kilometre-scale uplift resulting in the present-day configuration of erosional outliers, which are remnants of a much larger rift system (Jackson and Mullholland, 1993). These rift basins include the Kish Bank Basin and Peel Basin, both of which have been the focus of hydrocarbon exploration during the last fifty years (Fig. 1) (Dunford et al., 2001; Newman, 1999). Lithologies capable of generating hydrocarbons have been encountered in the Carboniferous, including the gas-prone Pennine Coal Measures Group and the oil-prone Bowland Shale Formation (Fig. 2). These source rocks have generated significant quantities of hydrocarbons, with an estimated 1.8 BBOE (Billion Barrels of Oil Equivalent) discovered in the East Irish Sea Basin (Bunce, 2018). Similar exploration activities took place in the western Irish Sea, primarily in the Kish Bank Basin, with four wells drilled between 1977 and 1997. While no commercial discoveries were made, the presence of the Pennine Coal Measures Group was proven in the 33/22-1 well on the southern margin of the Kish Bank Basin (Thomas, 1978).

The bedrock in the Irish Sea has largely been blanketed with Quaternary sediments, collectively referred to as the Brython Glacigenic Group (Fig. 2). Subglacial sediments ~~were~~ deposited by the Irish Sea Ice Stream (ISIS) during the Last Glacial Maximum are referred to as the Upper Till (UT) member (Fig. 2), and comprise a till containing stiff or hard clay with clasts ranging in size from sand-grade to boulders up to 1 m (Jackson et al., 1995). Overlying the UT are a series of units deposited in a glaciomarine to marine environment as the ISIS retreated, referred to as the Western Irish Sea Formation (WISMF) (Fig. 2)

1
2
3
4
5
6
7
8
9
10
11
12
13
14
15
16
17
18
19
20
21
22
23
24
25
26
27
28
29
30
31
32
33
34
35
36
37
38
39
40
41
42
43
44
45
46
47
48
49
50
51
52
53
54
55
56
57
58
59
60
61
62
63
64
65

(Jackson et al., 1995). Included in this formation, at the base, is the Chaotic Facies (CF). This unit consists of ice-proximal sediments, dominated by gravels with silts, sands and cobble-grade components (Coughlan et al., 2019; Jackson et al., 1995). The overlying Prograding Facies (PF) is ~~described as being~~ composed of fine- to medium-grained sands that are tabular stratified, having been deposited in a marine environment in front of the retreating Irish Sea Ice Stream (ISIS) (Coughlan et al., 2019; Jackson et al., 1995). The Mud Facies (MF) is characterised by stratified grey-brown muddy sands with silts and clays and is interpreted as being deposited in a fully marine environment (Coughlan et al., 2019; Woods et al., 2019). The organic-rich sediments of the MF have been ~~identified~~suggested as a potential~~the~~ source of shallow gas (biogenic-origin) in the north Irish Sea in the Western Irish Sea Mud Belt. The anaerobic decomposition of the organic-rich sediments followed by rapid burial under high sedimentation rates during marine transgression in the Early Holocene produced biogenic gas in the shallow sediments (Yuan et al., 1992). The UT and WISF deposits have been reworked during marine transgression and sea-level rise in the Holocene forming a complex distribution of sediments and bedforms, collectively referred to as the Surface Sands Formation (SSF) (Fig. 2) (Jackson et al., 1995; Ward et al., 2015)(~~Jackson et al., 1995; Ward et al., 2015~~).

DATA AND METHODS

This study uses a variety of shallow and deep geophysical datasets. The shallow datasets used in this study include multibeam echosounder (MBES) bathymetry and backscatter data as well as shallow sparker and pinger seismic data from a variety of surveys (Table 1). They were acquired primarily as part of the Integrated Mapping for the Sustainable Development of Ireland's Marine Resource (INFOMAR) programme, delivered by the Geological Survey of Ireland (GSI) and Marine Institute of Ireland. Data collected by the Agri-Food and Biosciences Institute (AFBI) in collaboration with GSI and by a Natural Environment Research Council (NERC) sponsored survey (NE/H02431/1) is accessed for Queenie Corner. A combination of ArcGIS, IVS Fledermaus, IHS Kingdom and Petrel software were used to analyse and integrate these datasets for a complete sub-surface to seafloor analysis.

Multibeam echosounder data

The high-resolution multibeam datasets were collected with the EM3002D multibeam echosounder (MBES) onboard the *RV Celtic Voyager* (dual head) and *RV Corystes* (single head) acquiring bathymetry data in the 300 kHz range using dynamically focused beams. The horizontal accuracy (x, y) was usually

1
2
3
4
5
6
7
8
9 186 less than 50 cm with a vertical accuracy (z) of <15 cm obtained for the processed bathymetry data. Data
10 187 processing was performed on board with the CARIS HIPS and SIPS software package to remove
11
12 188 erroneous pings and correcting for tidal and water displacement offsets. The output from the CARIS
13 189 HIPS and SIPS software consisted of un-gridded, tidally corrected XYZ data that was subsequently
14
15 190 gridded using QPS Fledermaus v.7 to a 2 m cell resolution. Gridded raster data was then exported to
16 191 ArcGIS v10 and Fledermaus v.7.7.6 for 3D visualization and morphological analysis of seafloor features.
17
18 192 Relative backscatter values were obtained from the strength of the return signal during MBES
19 193 acquisition. Data were processed using Geocoder in CARIS HIPS and SIPS and exported into ESRI ArcGIS
20
21 194 in gridded formats.

22 195 23 24 196 *Sub-bottom acoustic data*

25 197
26
27 198 Seismic sparker data were gathered using a Geo-Source 400 sparker system. The system consisted of a 6
28
29 199 kJ pulsed power supply operating predominantly at a frequency of 0.5 - 2 kHz ~~predominantly~~. The
30 200 unfiltered return signal was picked up ~~using~~ a Geo-Sense single channel hydrophone array. A
31
32 201 maximum penetration of 50 m below the seabed was achieved with a vertical resolution of up to 30 cm.
33 202 Seismic sparker data were incorporated into IHS Kingdom software in SEG-Y format and merged with
34 203 ASCII navigation data before being processed and interpreted. A trapezoid bandpass filter was applied
35
36 204 (low pass value 0.9 - 1.2 kHz, high pass value 5 - 6 kHz) and an automatic gain control of 50 and 100 ms.
37 205 Horizons were picked manually, and seismic depths were converted from two-way travel time to metres
38
39 206 using an acoustic internal velocity of 1600 m s⁻¹ through shallow marine sediments. Seismic pinger data
40 207 were collected from Queenie Corner using a hull-mounted SES 5000 3.5kHz pinger system with a 200 ms
41
42 208 duration. Data were acquired using the CODA system and processed using IHS Kingdom.

43 209 44 45 210 *2D multichannel seismic data*

46
47 211
48 212 The 2D multichannel reflection seismic data used in this study consisted of a multi-vintage database of
49
50 213 six surveys acquired as part of the hydrocarbon exploration activities in the Irish sea. These seismic
51 214 surveys were acquired between 1983 and 1995, comprising over 2,800 kilometres of data, and
52
53 215 processed as per industry standards (Yilmaz, 2001). The majority of the seismic data are centred on the
54 216 Kish Bank Basin, with five 2D seismic surveys not extending significantly beyond the bounds of the basin.
55
56 217 Coverage of the remainder of the study area is provided by a single reconnaissance survey acquired by

57
58
59
60
61
62
63
64
65

1
2
3
4
5
6
7
8
9
10
11
12
13
14
15
16
17
18
19
20
21
22
23
24
25
26
27
28
29
30
31
32
33
34
35
36
37
38
39
40
41
42
43
44
45
46
47
48
49
50
51
52
53
54
55
56
57
58
59
60
61
62
63
64
65

WesternGeco in 1983, which covers the entirety of the Irish sector of the Irish Sea. Stratigraphic control is provided by four deep boreholes drilled to test for hydrocarbons in the Kish Bank Basin. Data associated with these boreholes consists of wireline logs (gamma ray, caliper, neutron-density, sonic, and resistivity logs), well completion reports, formation tops, and time-depth relationship data in the form of checkshots. Seismic interpretation of key stratigraphic horizons and seismic to well tie was carried out in Petrel software.

RESULTS AND INTERPRETATION

2D multichannel seismic data

A 2D multichannel reflection seismic dataset, consisting of several discrete surveys, was used to investigate the bedrock geology of the region, structural lineaments and gas related features. Six key horizons were mapped in the vicinity of the Lambay Deep and Kish Bank Basin where formation tops from four hydrocarbon exploration boreholes provided stratigraphic control: (i) Seabed; (ii) Base-Quaternary; (iii) Base-Cenozoic; (iv) Top Lower Triassic; (v) Top Permian; (vi) Top Basement (Carboniferous & older) (Fig. 1 and Fig. 3).

Where the Codling Fault Zone transects the Kish Bank Basin, a number of seismic amplitude anomalies are observed in the upper Cenozoic section. These seismic amplitudes are locally distributed, including these include distinct seabed brightening, and widespread reverse-polarity anomalies (Fig. 3). These features are confined to the Codling Fault Zone and are not observed in other areas of the Kish Bank Basin. They ~~These shallow features~~ cause acoustic blanking of the deeper section, either due to absorption or reflection of acoustic energy, significantly reducing seismic image quality at depth. Absorption of acoustic energy can be caused due to presence of gas in the upper stratigraphic sediments, whereas reflection could be attributed to the presence of high-density rocks such as igneous bodies. The latter is unlikely, as igneous bodies have not been documented in the upper Cenozoic sediments in this part of the Irish Sea. These features are confined to the Codling Fault Zone and are not observed in other areas of the Kish Bank Basin.

There is limited stratigraphic control beyond the Kish Bank Basin, towards the Peel Basin (Fig. 1). Data quality is poor ~~also poorer~~ here, owing to the limited reflectivity within the Palaeozoic section.

1
2
3
4
5
6
7
8
9
10
11
12
13
14
15
16
17
18
19
20
21
22
23
24
25
26
27
28
29
30
31
32
33
34
35
36
37
38
39
40
41
42
43
44
45
46
47
48
49
50
51
52
53
54
55
56
57
58
59
60
61
62
63
64
65

Therefore, only the Base-Cenozoic unconformity could be reliably interpreted. A small half-graben was identified in the north of the study area (i.e. the WISMB; Fig. 1 and Fig. 4) which at present remains undrilled. Owing to its location along strike from the Peel Basin in the UK sector of the Irish Sea, this minor graben is interpreted as an erosional outlier, and the stratigraphy is inferred to be Permian and Triassic, similar to that of the Peel Basin (Floodpage et al., 2001). The bounding faults of this small graben are observed to offset the Base-Cenozoic surface, indicating relatively recent tectonic activity, and the areal extent of this graben correlates with the extent of the acoustic turbidity mapped on sub-bottom profiler sections (Fig. 4).

Further east within the WISMB, underlying the Queenie Corner area, a 2D reflection seismic line images folded Carboniferous rocks at depth, overlain by Cenozoic sediments (Fig. 5). Similar to structures observed in Fig. 3, several minor faults are observed offsetting the Base-Cenozoic Unconformity and represent relatively recent tectonic activity (Fig. 5).

Multibeam and Sub-bottom acoustic data

Codling Fault Zone

The seabed in the Codling Fault Zone is dynamic with extensive sediment waves (Croker et al., 2005) (Fig. 6). Also prominent are mounds, which form distinctive bathymetric highs relative to the surrounding seafloor. Approximately 23 mounds have been described previously by O'Reilly et al. (2014) and Van Landeghem et al. (2015) and been interpreted as carbonate mounds. This study identified a further two mounds which exhibit a roughly circular morphology and have an approximate diameter of 60 m approximately (Fig. 6). They protrude 8 and 16 m respectively from the seabed and have a higher backscatter than the surrounding seafloor. Based on their morphological similarity and proximity with the carbonate mounds identified Van Landeghem et al. (2015), we infer that these two mounds are probably also carbonate mounds (MDAC) formed due to prolonged seepage of methane gas from the seafloor. However, geochemical sampling and ROV image grabs would be required to ground-truth their association with gas seepage.

Lambay Deep

1
2
3
4
5
6
7
8
9 281 The Lambay Deep itself is a pronounced bathymetric low on the seabed, forming a linear trough-like
10 282 feature ~~broadly oriented NW-SE~~ that is approximately 11 km long, ~~aligned along NW-SE direction~~. The
11
12 283 Deep is 135 mbsl at its deepest point and is generally 50 m ~~deeper~~ lower than the surrounding seabed
13 284 (Fig. 7). The northern extent of the Lambay Deep is bound by an area of exposed bedrock, identified by
14
15 285 its rugged seafloor morphology and high backscatter. At its southern extent, the Deep is bound by a
16 286 sediment wave field. Located near the centre of the Deep is a prominent mound forming a bathymetric
17
18 287 high with a clear backscatter contrast to the surrounding seabed (Fig. 7).
19 288

20
21 289 The sparker data acquired over the Lambay Deep cover the area above the mound, where we observe
22 290 an acoustically transparent ~~unit with a thickness of about 24 m~~ thick unit, above an enhanced reflection
23
24 291 (LD-1, Fig. 8). The western flank exhibits acoustic turbidity. These acoustic anomalies are possibly
25 292 attributed to the accumulation of shallow gas beneath the mound, which was earlier described by
26
27 293 Croker et al. (2005) as the Lambay Deep Mud Diapir (LDMD). To the east of the LDMD, low-amplitude
28 294 parallel to sub-parallel reflections characterise the sedimentary sequence. The acoustic turbidity zone is
29
30 295 imaged on a second representative seismic line across the Deep, and further illustrates an upper
31 296 acoustic unit displaying an almost transparent seismic signature with faint, horizontal, parallel
32
33 297 laminations overlying an enhanced reflection in the centre of the deep (LD-2, Fig. 8). The enhanced
34 298 ~~reflections imaged in both these sparker lines~~ reflection could be possibly attributed to the sharp
35
36 299 acoustic impedance contrast between the underlying gas charged sediments and the overlying lithology.
37 300 Hence, the enhanced reflections are interpreted as top of shallow gas accumulation. The flanks exhibit a
38
39 301 more complex stratigraphy with chaotic acoustic units bounded by moderate to strong internal
40 302 reflectors. The acoustic turbid zones are possibly caused due to scattering of acoustic energy by gas
41
42 303 which is finely disseminated within impervious clay-rich sediments. The sedimentary strata on either
43 304 side of the LDMD exhibit onlapping structures, which is typical at mud diapir locations (Fig. 8). Onlapping
44
45 305 stratigraphy on either side of the LDMD suggest uplifting due to the structure (Fig. 8).
46 306

47 307 Western Irish Sea Mud Belt

48
49 308
50 309 As described earlier, the enhanced reflection is interpreted as the ~~The~~ top of the shallow gas
51
52 310 accumulation ~~zone~~ in the WISMB, which lies between 8 and 18 mbsf and extends across an area of
53 311 approximately 90 km² (Fig. 9). The accumulation has an inverted bowl topography with the rims climbing
54
55 312 down towards its edges, and an enhanced reflection marks the top (Fig. 10). The upper layers in the gas-

1
2
3
4
5
6
7
8
9 313 charged zone are lenticular, and characterized by an acoustically turbid zone, while exhibiting a sharp
10 314 contrast to the surrounding sediments (Fig. 10). Sub-bottom acoustic anomalies related to shallow gas
11
12 315 accumulation in this area of the WISMB and details on the shallow seismic stratigraphy have previously
13 316 been documented by Coughlan et al. (2019).
14

15 317
16 318 Circular to sub-circular crater like features were identified on bathymetry data, which were interpreted
17
18 319 as pockmarks which are direct indicators of fluid seepage at the seafloor. A total of seventeen
19 320 pockmarks (P1-17) were identified using the slope tool in ArcGIS to highlight slope changes along
20
21 321 pockmark walls. All pockmarks in this study (with the exception of P12) were found in water depths
22 322 greater than 40 m (Fig. 9). Information on calculated dimensions and morphology for each pockmark is
23
24 323 presented in the supplementary material (S1). Two separate morphologies were identified: pockmarks
25 324 with central mounds within them and pockmarks without any central mounds.
26

27 325
28 326 P1, P2 and P3 are clustered with a distance of 355 m between P1 and P2 and a further 420 m between
29
30 327 P2 and P3 in a northerly direction. Other pockmarks along this trend are more widely spaced. Pockmarks
31 328 P1 to P12 are sub-circular in shape, although P5-P8 are more ~~elongate~~elongated. The alignments of the
32
33 329 long-axis of the elongate pockmarks are in different orientations suggesting no influence of bottom
34 330 currents on the morphological evolution of the pockmarks. Relief relative to the seabed varies between
35
36 331 0.6m (P3) and 1.6m (P10) with pockmarks becoming generally larger and deeper to the northwest. P12
37 332 is a typical giant irregular pockmark, as documented in the UK North Sea (Cole et al., 2000). It is elliptical
38
39 333 in plan-view, and at least 5 times larger than any of the other pockmarks in this group, the short and
40 334 long axis being c. 500 m and 1000 m (Fig. 11A). Backscatter data for P12 display higher reflectance
41
42 335 values than the surrounding sediments (Fig. 11B). Higher reflectance could either be due to coarser
43 336 sediments or due to carbonate precipitates near the seabed owing to prolonged seepage. We infer the
44
45 337 later to be a more likely explanation to the high backscatter values from the centre of this giant irregular
46 338 pockmark P12.
47

48 339
49 340 Most pockmarks in this study are between 74 and 153 m wide with P7, P10 and P11 being 171 to 268 m
50
51 341 wide. P4 and the larger P10 and P11 pockmarks contain small mounds at their centre being 0.1 m, 0.2 m
52 342 and 0.4 m high respectively (Fig. 1112). P14, P15, P16 and P17 are all circular with a depth typically of
53
54 343 0.4 m to 1 m relative to the seabed. P15 also has a mound about 0.1 m in height at its centre. Maximum
55 344 diameters vary from 54.5 m to 90 m across with the larger-diameter pockmarks tending to be deeper.
56
57
58
59
60
61
62
63
64
65

1
2
3
4
5
6
7
8
9 345
10
11 346
12 347
13 348
14
15 349
16 350
17
18 351
19 352
20
21 353
22 354
23 355
24
25 356
26 357
27
28 358
29 359
30
31 360
32
33 361
34
35 362
36 363
37
38 364
39 365
40 366
41
42 367
43 368
44 369
45
46 370
47
48 371
49 372
50
51 373
52 374
53
54 375
55
56
57
58
59
60
61
62
63
64
65

Queenie Corner

Analysis of the MBES data from the Queenie Corner MCZ suggests largely the same flat topography as seen in the WISMB with notable mound structures. The mounds occur in isolation as well as part of a linear chain, which is approximately 2 km in length (Fig. ~~1213~~). They exhibit a maximum relief of 1 m compared to the regular seabed (Fig. ~~1213~~). Backscatter data from these mounds also indicate higher reflectance compared to the surrounding sediments (Fig. ~~1213~~).

A single Pinger line from the Queenie Corner site revealed acoustic turbidity, indicating shallow gas, at its western end, coinciding with the mounds observed on MBES data (Fig. ~~1213~~ and 14). The top of the acoustic turbidity occurs within 1 m of the seabed with clear evidence for gas chimneys reaching the seabed rooted from the acoustic turbid zone. The gas chimneys emanating from the acoustic turbid zone precisely underlie the mounds observed on the MBES data. Further east, we observe a sharp boundary of the turbidity zone which is interpreted as the gas front (Fig. ~~13B14B~~).

DISCUSSION

Revised geological model with inferences on gas origin and controls on fluid migration

Structural lineaments (i.e. faults) and the properties of Quaternary sediments in the Irish Sea play a significant role in fluid migration from deep seated hydrocarbon source rocks to the shallow sub-seafloor stratigraphic layers, and eventually in subsequent seepage at the seafloor. In this section we discuss an individual, revised geological model for the CFZ and WISMB to elucidate the potential origins for ~~hydrocarbon fluids~~ thermogenic gas in both areas, and the pathways ~~and controls~~ that would allow for the migration of such fluids to the sub-seabed and seafloor. This is not to suggest that there is no biogenic component to ~~any shallow~~ the gas in these areas. The data presented demonstrates that a thermogenic source cannot be excluded, and it is accepted that mixing of sources can occur.

Codling Fault Zone (incl. Lambay Deep)

1
2
3
4
5
6
7
8
9 376 Gas-prone source rocks have been proven throughout the Irish Sea with the most prolific being the gas-
10 377 prone Pennine Coal Measures Group and the oil-prone Bowland Shale Formation, both of Carboniferous
11 age (Pharaoh et al., 2016). Within the study area, the Pennine Coal Measures Group has been proven in
12 378 the 33/22-1 borehole on the southern margin of the Kish Bank Basin where 17 metres of coal were
13 379 encountered with associated methane gas being detected within these coal horizons (Thomas, 1978).
14
15 380 These coal-bearing horizons are interpreted throughout the Kish Bank Basin and are observed as the
16 381 high-amplitude reflectors visible beneath the Base-Permian Unconformity (Fig. 3). Analysis of vitrinite
17 382 reflectance data at the 33/22-1 borehole indicates these gas-prone source rocks have reached the
18 383 pressure and temperature conditions to generate gas at present-day, suggesting that these same
19 384 horizons at deeper, down-dip positions have generated hydrocarbons (Thomas, 1978). The Bowland
20 385 Shale Formation has not been encountered in the 33/22-1 borehole, where the Pennine Coal Measures
21 386 Group sits unconformably upon Lower Palaeozoic metasediments, although erosional outliers may be
22 387 preserved elsewhere in the study area.
23
24 388

25
26
27
28
29 389 In addition to the presence of gas-prone source rocks, several indicators of an active petroleum system
30 390 have been encountered in the vicinity of the Kish Bank Basin, in the form of both liquid and gaseous
31 391 hydrocarbons. Both the previously mentioned 33/22-1 borehole and the 33/17-1 borehole on the
32 392 eastern margin of the Kish Bank Basin encountered residual oil, the former in Carboniferous sandstones
33 393 and the latter in Triassic sandstones (Charterhouse, 1986; Thomas, 1978). The 33/22-1 borehole
34 394 reported tentative oil-staining in Lower Pleistocene sands which may indicate the remigration of liquid
35 395 hydrocarbons from within the bedrock to these shallow, unconsolidated sediments. Previous authors
36 396 have also presented a proprietary seep dataset which shows the location of present-day oil seeps, with a
37 397 strong correlation between the location of seeps and distribution of both large faults and where source-
38 398 rocks sub-crop at the seabed (e.g. Anderson, 2013; Dunford et al., 2001).

39
40
41
42
43
44
45 399 Remigration of hydrocarbons from the bedrock to the shallow seabed can be facilitated by recent
46 400 tectonic activity, which creates fluid conduits in the form of faults, which either breach existing
47 401 hydrocarbon accumulations at depth or allow hydrocarbons to migrate directly from source rocks to
48 402 seabed sediments (Anka et al., 2012; Corcoran and Doré, 2002). In the study area, the Codling Fault
49 403 Zone is the most recent tectonic feature, being a NNW-SSE trending strike-slip fault and offshore
50 extension of the Newry and Camlough Faults of Northern Ireland (Fig. 1). Kilometre-scale dextral motion
51 404 on the fault has been recorded by several previous studies (e.g. Dunford et al., 2001) with the most
52 405 recent research indicating displacement of 8.7 kilometres, incorporating up to 2 kilometres of normal
53
54
55 406

56
57
58
59
60
61
62
63
64
65

1
2
3
4
5
6
7
8
9
10
11
12
13
14
15
16
17
18
19
20
21
22
23
24
25
26
27
28
29
30
31
32
33
34
35
36
37
38
39
40
41
42
43
44
45
46
47
48
49
50
51
52
53
54
55
56
57
58
59
60
61
62
63
64
65

movement on the basin-bounding fault along the northern margin of the Kish Bank Basin (Anderson, 2013). The timing of this fault activity is poorly constrained due to the attenuated Cenozoic section preserved in the study area but has been inferred to have a component of both Paleocene and Oligocene movement (Anderson, 2013; Dunford et al., 2001).

Several observations from 2D multichannel seismic data recorded in this study correlate spatially with the location of the Codling Fault Zone. Within the confines of the Kish Bank Basin, amplitude brightening is observed above the fault zone within the Quaternary units, with a sharp western boundary directly above the trend of one of main fault splays and a more diffuse contact to the east (Fig. 3). Additionally, reverse polarity anomalies are observed in the Cenozoic section directly above the fault zone. While none of the available boreholes penetrate these anomalies, correlation with those seismic intervals along-strike indicate these sediments consist of poorly consolidated sandstones interbedded with thin layers of mudstone (Charterhouse, 1986; Thomas, 1978). ~~These and these~~ anomalies may represent local charging of these sands with re-migrated gaseous hydrocarbons which have migrated up the main fault plane of the Codling Fault Zone (e.g. e.g. Løseth et al., 2009). ~~Other authors have presented proprietary single-channel seismic data from this area which supports this interpretation, such as reverse-polarity anomalies and flat spots reported by Dunford et al., (2001).~~ However, these anomalies will remain a speculative interpretation until ground truthing is done by geochemical sampling.

Evidence for shallow gas is also observed in Quaternary sediments (i.e. the PF and SSF) from shallow, sub-bottom acoustic data in the Lambay Deep causing enhanced reflection (Fig. 8). The PF has also been observed to be gas-bearing in the CFZ (Van Landeghem et al., 2015). Whilst we infer a thermogenic origin for the gas/fluids in this area, a biogenic component cannot be discounted. Isotope analysis of MDAC at the CFZ SAC by O'Reilly et al. (2014) suggests possible mixing of biogenic and thermogenic sourced gas. Based on the present data, it is not possible to estimate the timescales for the migration of these fluids. The Croker Carbonate Slab SAC is located 12-15 kms NE of the CFZ SAC area (Fig. 1). Judd et al. (2019) place the formation of MDACs in the Croker Carbonate Slab SAC ~~at~~ between 17 ka BP to 5 ka BP, with evidence for present day gas seepage. The MDAC cements the PF, which is inferred as being deposited in a glaciomarine environment between approximately 20 ka and 10 ka BP (Judd et al., 2019). It is also assumed that, prior to the deposition of the PF as the ISIS retreated, gas accumulated beneath the ice sheet (Judd et al., 2019). Gas accumulations below ice-sheets has also been proposed for other locations globally during the Devensian (Crémière et al., 2016; Fichler et al., 2005; Portnov et al., 2016). This spatial correlation of seabed features with the Codling Fault Zone implies that at least a portion of

1
2
3
4
5
6
7
8
9
10
11
12
13
14
15
16
17
18
19
20
21
22
23
24
25
26
27
28
29
30
31
32
33
34
35
36
37
38
39
40
41
42
43
44
45
46
47
48
49
50
51
52
53
54
55
56
57
58
59
60
61
62
63
64
65

the fluids responsible for their formation will be bedrock-sourced thermogenic gas, with the Codling Fault Zone acting as the main conduit for the migration of hydrocarbon fluids to the shallow subsurface.

Western Irish Sea Mud Belt (including Queenie Corner)

Shallow gas accumulations have been observed in the MF in the WISMB, acoustically blanking the layers below (Coughlan et al., 2019) (Fig. 10). Similar accumulations of shallow gas in the WISMB have previously been linked with a biogenic origin, given the organic rich nature of the MF sediments (Yuan et al., 1992). Stable isotope data in Woods et al. (2019) presents evidence for methane seeps in the WISMB during the Mid Holocene age (post 8.2 ka). Considering the Holocene age of the MF and the estimated volume of gas present (Supplementary Material; S2), it is difficult to envision a solely biogenic source.

This study has provided ~~credible~~ evidence of shallow gas accumulation directly above a Permian-Triassic infilled basin with its boundaries defined by the graben-bounding faults (Fig. 3 and Fig. 1415). These faults, which were reactivated during the Cenozoic and are observed offsetting the Base-Cenozoic Unconformity, would provide pathways for fluid flow from the Carboniferous source rocks below (Fig. 1415). The gas is seen to be hosted in the PF, below the base of the MF (Fig. 10). This suggests upward fluid migration through the underlying CF (glacial outwash sediments) and UT member (subglacial till). Whilst the UT in the Irish Sea is often over-consolidated, it is highly heterogeneous comprising a range of sediment classes that would facilitate fluid migration through it (Fig. 1415) (Coughlan et al., 2019; Van Landeghem et al., 2015). The top of the shallow gas is typically within 10-12 m of the seabed-surface and has a sharp boundary with the surrounding non-gas bearing sediments (Fig. 10). Pockmarks P14, P15, P16 and P17 were found to coincide with the lateral extent of underlying shallow gas accumulation, previously identified by Coughlan et al. (2019) (Fig. 9 and Fig. 1516). Episodic or continuous migration of this shallow gas accumulation to the seafloor would allow for fluid seepage at the seafloor, and the formation of features such as mounds and pockmarks, which will be discussed in more detail in the next section. Pockmarks occurring outside this accumulation of shallow gas form a strong, linear trend coincident with the prognosed extension of the Codling Fault Zone (Fig. 15), implying that fluid migrating from deeper source rocks along the main fault of CFZ possibly seep out from these pockmarks.~~16~~

Formation mechanisms of seep-related seafloor features

We can classify seep-related seafloor morphological features observed in this study into two different types: mounds and pockmarks (Fig. 1516). Mounds can be further classified into mounds formed from

1
2
3
4
5
6
7
8
9
10
11
12
13
14
15
16
17
18
19
20
21
22
23
24
25
26
27
28
29
30
31
32
33
34
35
36
37
38
39
40
41
42
43
44
45
46
47
48
49
50
51
52
53
54
55
56
57
58
59
60
61
62
63
64
65

MDACs and mounds formed due to mud-diapirism. Mounds described here ~~in association with~~ from the CFZ have collectively been described extensively in the literature as carbonate mounds formed from MDACs (Judd et al., 2019; O'Reilly et al., 2014; Van Landeghem et al., 2015). Alternatively, the mound located within Lambay Deep was described by Croker et al. (2005) as the Lambay Deep Mud Diapir (LDMD). Judd and Hovland (2007) defined a mud diapir as a sediment structure that has risen through a sediment sequence due to upward migrating fluids, piercing or deforming younger sediments. Mud diapirs can be recognised on seismic profiles as an acoustically amorphous piercement structure, as documented in the East China Sea (Xing et al., 2016), SW Taiwan (Chen et al., 2014), and the Mediterranean Ridge (Camerlenghi et al., 1992). In this section we focus on the formation mechanisms of the remaining seabed features in the WISMB, which are poorly understood in an Irish Sea context.

The pockmarks identified in this study are concentrated in the western part of the WISMB (Fig. 1516). Within this set of pockmarks (P1-P17) there are two different morphologies: pockmarks with a central mound and pockmarks without a central mound. All the pockmarks are located in an area of sandy-mud to muddy-sand according to the British Geological Survey DigSBS250 database (Fig. 1516). This differentiates them from pockmarks previously documented by Yuan et al. (1992), which were located in areas dominated by mud class sediments and were related to a zone of "acoustically turbid sediments" (ATZ) (Fig. 1516). Yuan et al. (1992) offers no explanation for the mechanism for their formation, although Croker et al. (2005) does highlight the requirement of clay- to silt-grade substrate for the formation of pockmarks. The fluids escaping from these pockmarks could either be biogenic- or thermogenic-sourced or of mixed origin. We further suggest that pore-water escape from the shallow glacial marine deposits could have also led to the formation of pockmarks, as suggested in other glacial marine settings (Harrington, 1985; Roy et al., 2019), however, pore-water escape would not support the formation of mounds within pockmarks.

Low-relief seabed mounds are found in Queenie Corner in the eastern part of the WISMB, which is characterised by sandy-mud seafloor sediments (Fig. 1516). Mounds mapped by Croker et al. (2005) occur in areas of mud and sandy mud (Fig. 1516). The near surface sediments in the WISMB are often under-consolidated, and so likely to be highly permeable (Coughlan et al., 2019; Mellet et al., 2015), which is unsuitable for the mechanism of formation proposed by Croker et al. (2005). In this study, described mounds and pockmarks are located in distinct areas and separated from each other.

1
2
3
4
5
6
7
8
9 501
10 502
11
12 503
13 504
14
15 505
16 506
17
18 507
19 508
20
21 509
22
23 510
24 511
25 512
26 513
27
28 514
29 515
30
31 516
32 517
33
34 518
35 519
36
37 520
38 521
39
40 522
41 523
42
43 524
44 525
45
46 526
47 527
48
49 528
50 529
51 530
52
53 531
54 532
55
56
57
58
59
60
61
62
63
64
65

The distribution of these seep-related seafloor morphological features **varies** over differing seafloor sediment types, **which indicates therefore, requires** differing formation mechanisms. Based on previous studies (Brothers et al., 2011; Crémière et al., 2018; Hammer et al., 2009; Hovland, 2002; Loher et al., 2018) and observations made in this study, we discuss two conceptual models for:

- (i) ~~The(i) the~~ formation of central mounds within pockmarks in muddy sediment areas with a sand-component, and;
- (ii) ~~The(ii) the~~ formation of seabed mounds in muddy sediments, leading to the formation of collapsed pockmarks.

The formation of central mounds within pockmarks in sediments with a sand component

Initially fluid seepage at a relatively flat seafloor facilitates the development of microbial mats and an initial MDAC crust, which reduces the seepage rate at ~~that~~the location (Fig. ~~16A-17A~~; Stage 1). Over time, this MDAC crust develops further, forming a consolidated seal at the seafloor (Fig. ~~16A-17A~~; Stage 2). A combination of seepage of fluids from, and bottom currents at, the seafloor around the mounds preferentially erodes the surrounding un-cemented seafloor sediments, partially exposing the MDAC crust (Fig. ~~16A-17A~~; Stage 3). Further seepage of fluids around the perimeter of the carbonate crust along with reworking and winnowing of sediments finally exposes the mound completely, which resembles a mound at the centre of a pockmark (Fig. ~~16A-17A~~; Stage 4). This is in agreement with the formation mechanism of carbonate mounds within pockmarks on a relatively flat seabed whereby a combination of fluid seepage and bottom currents erode the surrounding un-cemented seafloor sediments, partially exposing the mound in the centre of the pockmarks as has been suggested by Crémière et al. (2018). Similar carbonate crusts have been observed within pockmarks in the Harstad Basin in the Barents Sea (Crémière et al., 2018) and offshore Norway (Hovland et al., 2010), where several satellite pockmarks surrounding the 'mother pockmark' have been documented with a carbonate mound in the centre.

The formation of seabed mounds, leading to pockmarks in muddy sediments

Initially, prolonged seepage of methane gas at the seafloor leads to the formation of thin fragments of MDAC, followed by cementation of these thin MDAC fragments just beneath the seabed (Fig. ~~16B-17B~~; Stage 1). The thin MDAC crust beneath the seabed acts as an impermeable seal at the seabed sediment-

Formatted: List Paragraph, Numbered + Level: 1 + Numbering Style: i, ii, iii, ... + Start at: 1 + Alignment: Right + Aligned at: 0.63 cm + Indent at: 1.27 cm

1
2
3
4
5
6
7
8
9 533 water interface and ~~redirects~~~~diverges~~ fluid seepage around the MDAC crust perimeter (Fig. ~~16B-17B~~;
10 534 Stage 2). Gas starts to accumulate and build up pore-pressure beneath the crust, ~~while also increasing~~
11 ~~the as well as leads to increase in~~ pore-volume. The build-up of pore pressure and increase of pore
12 535 volume within the unconsolidated sediments underlying the MDAC crust is facilitated by the combined
13 536 effect of upward fluid migration and sealing capacities of mud-rich sediments and the MDAC crust. The
14 537 sealing effect of the MDAC crust, along with the buoyant force of the upward migrating gas and increase
15 538 in pore-volume, results in the bulging outward of the unconsolidated sediments and the MDAC crust
16 539 (Fig. ~~16B-17B~~; Stage 3). At this point, the MDAC crust has been modified to a carbonate mound due to
17 540 the outward bulging of the sediments underneath, such as the mounds at Queenie Corner (Fig. ~~1314~~).
18 541 The gradual increase in the buoyant force of the gas further leads to the formation of fractures within
19 542 the deformed MDAC mound, to the point when the MDAC mound ruptures and collapses under its own
20 543 weight after the underlying pressurised gas has dissipated (Fig. ~~16B-17B~~; Stage 4). The collapsed mound
21 544 resembles a crater-like depression like a pockmark. A single grab sample taken from the area of seafloor
22 545 mounds in the southwestern section of Queenie Corner revealed cemented muds, with a strong odour,
23 546 which would suggest hardened substrates caused by oxidation of methane forming carbonate
24 547 precipitates (Supplementary Material; S3). However, this hypothesis assumes that the initial MDAC crust
25 548 formation is thin enough to be deformed by the increase in pore pressure and volume due to the
26 549 upward migrating fluids.
27 550
28 551

Data interpretation and geological model limitations

29 552 The identification, characterisation and assessment of geohazards such as shallow gas, fluid flow and
30 553 seepage involves a multidisciplinary approach utilising a range of site investigation techniques
31 554 (Cevatoglu et al., 2015; Clare et al., 2017; Vanneste et al., 2014). This study aims to integrate multi-scale
32 555 geophysical datasets in order to develop a geological framework to study potential fluid migration
33 556 pathways from deeper stratigraphy or source rocks to shallow gas accumulations, and thereafter
34 557 seepage at seafloor in the Irish Sea. Characterising and describing shallow gas acoustic features on
35 558 shallow seismic data in particular depends on the acquisition system and frequencies used (Tóth et al.,
36 559 2014). The shallow sub-bottom data used to characterise shallow sub-seabed features were gathered as
37 560 part of regional surveys, without the express intention of studying shallow gas and fluid flow. The
38 561 systems used to gather shallow sub-bottom data (i.e. sparker and pinger) transmit a signal within a
39 562 frequency range of 0.5 – 4 kHz, which can be attenuated through scattering by fluid bubbles in gas
40 563
41 564
42 565
43 566
44 567
45 568
46 569
47 570
48 571
49 572
50 573
51 574
52 575
53 576
54 577
55 578
56 579
57 580
58 581
59 582
60 583
61 584
62 585
63 586
64 587
65 588

1
2
3
4
5
6
7
8
9 565 charged sediments, the result of which is acoustic turbidity and blanking (Tóth et al., 2014). Both these
10 566 phenomena are recognised in this study (Fig. 10) and are common at depth in such areas of mud to
11
12 567 sandy mud on single-channel datasets (e.g. Laier and Jensen, 2007). As a result, only the top of the gas
13 568 front is identified on shallow sub-bottom data, and there is ambiguity with regards to the depth of
14
15 569 shallow gas and details of the underlying geology. However, low-frequency 2D-multichannel seismic
16 570 provides information on underlying bedrock geology and tectonics. Ultimately, some studies show
17
18 571 amplitude versus offset (AVO) analysis on 2D-multichannel seismic data to further affirm the presence
19 572 of gas in the sediments (e.g. Kim et al., 2020)

20
21 573
22 574 At the seafloor, geomorphological features synonymous with fluid migration and seepage can be
23
24 575 mapped using multibeam echosounder (e.g. Roelofse et al., 2020). In this study pockmarks have been
25 576 identified, characterised and discussed within the context of fluid migration and seepage. However,
26
27 577 there is a current lack of geochemical data from these pockmarks to ascertain the nature of fluids
28 578 seeping from them. Analysis of cores taken in the vicinity of the pockmarks in the WISMB and the LDMD
29
30 579 discussed here proved inconclusive in terms of determining the composition of sub-surface fluids due to
31 580 a lack of depth penetration (O'Reilly, S. pers. Comms.). As this study has identified several areas within
32
33 581 the northern Irish Sea where there is compelling evidence for the presence of gas in the shallow
34 582 subsurface, we anticipate future research cruises will acquire sediment and pore-water samples to
35
36 583 confirm the nature of origin or fluids seeping from these locations.

37 584
38 585 *Implications of shallow gas and fluid seepage*
39

40 586
41 587 The presence of gas accumulations in shallow sub-surface sediments can have engineering implications
42
43 588 for the construction of offshore infrastructure and is considered a geohazard within the hydrocarbon
44 589 and maritime industry (Evans, 2011; Hovland et al., 2002; Sun et al., 2017) as well as for renewable
45
46 590 energy developments (Society for Underwater Technology, 2005). When gas occurs in solution in the
47 591 pore-water, or free gas-filled voids between sediment grains, it can affect the compressibility of the
48
49 592 sediment and negatively influence the engineering properties (Sills and Wheeler, 1992; Sultan et al.,
50 593 2012). Where fluid seeps to the seafloor, it can impact the ground-conditions by: (i) forming a hard
51
52 594 surface (i.e. MDAC), which may be difficult to pile or penetrate, or; (ii) causing changes in seabed
53 595 bathymetrytopography (e.g. doming or pockmarks), which would create seabed instability. Hence, it is
54
55 596 vital to do a marine baseline study of an area of interest before installation of submarine engineering

56
57
58
59
60
61
62
63
64
65

1
2
3
4
5
6
7
8
9
10
11
12
13
14
15
16
17
18
19
20
21
22
23
24
25
26
27
28
29
30
31
32
33
34
35
36
37
38
39
40
41
42
43
44
45
46
47
48
49
50
51
52
53
54
55
56
57
58
59
60
61
62
63
64
65

structures. This study, inter alia, has mapped a widespread occurrence of shallow gas throughout the north Irish Sea as well as included previous studies in the area, which overlies a variety of geological and tectonic settings (Fig. 1 and [1516](#)). More research is required to better understand the migration of fluids along proposed fault-routes, their sealing versus leaking capabilities, and the true nature and timing of the seeping fluids. At the very least, it is possible to anticipate where certain shallow gas and fluid escape structures may be encountered based on regional geology and mitigating site investigation techniques planned accordingly.

Studies have shown that MDAC harbours different benthic communities to surrounding sediments in the Irish Sea: whether this is due to the formation of complex three-dimensional reef-like structures in otherwise fairly homogeneous sedimentary habitats, thereby allowing colonisation by taxa common on hard rocky substrates, or due to the unique characteristics of MDAC which are as yet unclear (Judd et al., 2019; Noble-James et al., 2020). Pockmarks have been shown to harbour exclusive fauna in the North Sea (Webb et al., 2009), characterised by species with endosymbiotic sulphur-oxidising bacteria, as well as the structures providing shelter for specific fish species (Dando, 2001). (Dando, 2010) reviewed 62 shallow-water hydrothermal vent and cold seep sites and found that obligate species are rare at such sites, however higher species diversity was often found in the immediate vicinity of seeps often due to the heterogeneity of the [bathymetrytopography](#), compared with surrounding more homogeneous areas. As yet, the pockmarks and seabed doming in this study have not had targeted biological sampling, but at Queenie Corner cemented sediment was retrieved by Day-grab from one seabed dome area with faunal excavation of the cemented sediment by bivalves and gastropods (Supplementary Material; S3). Whether the fauna in such structures is unique compared to surrounding sedimentary areas would require further investigation; however, substrata-boring fauna could be viewed as a functionally significant component of the local ecosystem (Noble-James et al., 2020). An understanding of this, coupled with accurate mapping of the extent and potential ecological connectivity of such features throughout the Irish Sea, is required to underpin effective management of these habitats.

CONCLUSIONS [AND FUTURE WORK](#)

High-resolution geophysical datasets from the Irish Sea reveal sub-seabed shallow gas accumulations in Quaternary sediments and a range of seafloor expressions of fluid seepage. Based on the integrated geophysical investigation of seafloor geomorphologies, shallow sub-surface sediments and deeper

1
2
3
4
5
6
7
8
9
10
11
12
13
14
15
16
17
18
19
20
21
22
23
24
25
26
27
28
29
30
31
32
33
34
35
36
37
38
39
40
41
42
43
44
45
46
47
48
49
50
51
52
53
54
55
56
57
58
59
60
61
62
63
64
65

geological and tectonic features, this study generated a geological framework from which the following can be made summarised.

In both the Codling Fault Zone and Western Irish Sea Mud Belt, there is compelling evidence linking shallow gas accumulation within Quaternary sediments with major structural lineaments (i.e. faults) in the bedrock geology. These faults can act as pathways for hydrocarbon fluids to migrate from deeply seated ~~potential~~ source rocks to shallow stratigraphic layers. This supports earlier geochemical studies which found a thermogenic component to the shallow gas and seafloor seepage features in both these areas.

In the Western Irish Sea Mud Belt, both pockmarks and seabed mounds were recorded in areas of mud with a varying sand component. Pockmarks display two morphologies consisting of regular, circular types and pockmarks with a central mound, typically less than 0.5 m in relief. Pockmark centres often exhibit high backscatter reflectance values suggesting some degree of sediment consolidation due to the formation of MDAC. Mounds are typically 1 m in height above the regular seabed and are associated with gas chimneys rooted to an underlying shallow gas accumulation. These mounds, and surrounding seabed, exhibit high backscatter reflectance values, again, suggesting the formation of MDAC. This is supported by a grab sample from a mound containing cemented, MDAC-like material.

We propose two mechanisms for the formation of pockmarks; one in muddy seafloor settings with a sand component, which accounted for the formation of a central mound, and one for the formation of thin MDAC mounds as pre-cursors to pockmarks in muddy seafloor settings.

Based on our findings, we make the following concluding statements and recommendations for future work:

- The revised geological models for the Codling Fault Zone and Western Irish Sea Mud Belt allow for a better understanding of the role of existing and re-activated faults as a potential pathway for fluid (e.g. gas) migration from kilometre-scale depth to the shallow sub-seabed. In future, this will help quantify the contribution of thermogenic-~~sourced~~~~origin~~ gas to ongoing shallow sub-seabed gas accumulation and seafloor seepage in these areas. Geochemical analysis of targeted seabed seepage and shallow gas accumulation locations from the Western Irish Sea Mud Belt is required to constrain the origin of shallow gas definitively and is a proposed area of further work.

1
2
3
4
5
6
7
8
9 657
10 658
11
12
13 659
14 660
15
16 661
17 662
18
19 663
20 664
21
22 665
23 666
24
25
26 667
27 668
28
29 669
30
31 670
32
33 671
34 672
35
36 673
37
38 674
39 675
40
41 676
42
43 677
44
45 678
46 679
47 680
48
49 681
50 682
51
52 683
53 684
54
55 685
56
57
58
59
60
61
62
63
64
65

- To validate the model linking the creation of MDAC to pockmark formation, repeat survey data over the mounds at Queenie Corner is required to record their evolution over time.
- The presence of shallow gas accumulations in the Western Irish Sea Mud Belt, along with gas chimneys and mounds, suggests that fluid seepage at the seafloor is an on-going process. This has significant implications for seabed infrastructure development and seabed ecological and conservation efforts. Based on the results of this study and models presented, our understanding of the geological controls on fluid migration and seafloor seepage is greatly improved, making it increasingly possible to predict the extent of shallow gas and location of certain gas seepage structures in the Irish Sea. Future data collection surveys (e.g. INFOMAR) will further improve this understanding.
- To better constrain gas content and extent of gas front in areas of acoustic blanking, we recommend the acquisition of multichannel seismic data and the application of AVO analysis.
- Ground-truthing and further geotechnical analysis of Quaternary sediments is required to better understand how fluids migrate through, and are hosted in, these sediments.
- Biological data available from the Western Irish Sea Mud Belt pockmarks and mounds are limited in determining the range of biodiversity at these sites at present. Epibenthic surveys consisting of drop-frame or towed camera platforms or ship-based grab sampling are typically unable to spatially target and sample chemoautotrophic communities, so it is recommended that ROV techniques are used for such purposes.

Acknowledgements

This research is funded in part by a research grant from Science Foundation Ireland (SFI) under Grant Number 13/RC/2092 and is co-funded under the European Regional Development Fund, and by the Petroleum Infrastructure Programme (PIP) and its member companies. SR is funded by the Irish Research Council Government of Ireland Postdoctoral Fellow Award (GOIPD/2018/17). The authors would like to thank the Petroleum Affairs Division (PAD) of the Department of Communications, Climate Action and Environment (DCCA), Ireland, for providing access to released borehole, seismic and potential field datasets. The authors would also like to thank Schlumberger for providing academic licenses of Petrel to University College Dublin. We are grateful to IHS Markit for providing the academic

1
2
3
4
5
6
7
8
9
10
11
12
13
14
15
16
17
18
19
20
21
22
23
24
25
26
27
28
29
30
31
32
33
34
35
36
37
38
39
40
41
42
43
44
45
46
47
48
49
50
51
52
53
54
55
56
57
58
59
60
61
62
63
64
65

licence for the KINGDOM software package to iCrag. This paper contains Irish Public Sector Data (INFOMAR) licensed under a Creative Commons Attribution 4.0 International (CC BY 4.0) licence. The authors acknowledge Dr. Matthew Service and Rory O’Loughlin (both Agri-Food and Biosciences Institute, Northern Ireland) for releasing the MBES data for Queenie Corner, and for support during the AFBI surveys. The pinger line shown was acquired as part of NERC project NE/H02431/1. The authors acknowledge Rosie Jebb (GSI) and Andy Trafford (UCD) for assistance processing MBES and sub-bottom profile data respectively. The authors also acknowledge the crew and scientists onboard all surveys listed for their work, co-operation and skill in collecting the data. The authors would like to thank 3 reviewers for their feedback and comments which greatly improved this manuscript.

References

- Anderson, H., 2013. The origin and nature of Cenozoic faulting in north-east Ireland and the Irish Sea. University College Dublin.
- Andreassen, K., Nilssen, E.G., Ødegaard, C.M., 2007. Analysis of shallow gas and fluid migration within the Plio-Pleistocene sedimentary succession of the SW Barents Sea continental margin using 3D seismic data. *Geo-Marine Lett.* 27, 155–171. <https://doi.org/10.1007/s00367-007-0071-5>
- Anka, Z., Berndt, C., Gay, A., 2012. Hydrocarbon leakage through focused fluid flow systems in continental margins. *Mar. Geol.* 332–334, 1–3. <https://doi.org/10.1016/j.margeo.2012.10.012>
- Brothers, L.L., Kelley, J.T., Belknap, D.F., Barnhardt, W.A., Andrews, B.D., Maynard, M.L., 2011. More than a century of bathymetric observations and present-day shallow sediment characterization in Belfast Bay, Maine, USA: implications for pockmark field longevity. *Geo-Marine Lett.* 31, 237–248. <https://doi.org/10.1007/s00367-011-0228-0>
- Bunce, J., 2018. The history of exploration and development of the Liverpool Bay fields and the East Irish Sea Basin. *Hist. Eur. Oil Gas Ind.* <https://doi.org/10.1144/SP465.6>
- Camerlenghi, A., Cita, M.B., Hieke, W., Ricciuto, T., 1992. Geological evidence for mud diapirism on the Mediterranean Ridge accretionary complex. *Earth Planet. Sci. Lett.* 109, 493–504. [https://doi.org/10.1016/0012-821X\(92\)90109-9](https://doi.org/10.1016/0012-821X(92)90109-9)
- Charterhouse, 1986. Well 33/17-1 Final Geological Report. Charterhouse Ireland Exploration Company.
- Chen, S.-C., Hsu, S.-K., Wang, Y., Chung, S.-H., Chen, P.-C., Tsai, C.-H., Liu, C.-S., Lin, H.-S., Lee, Y.-W., 2014. Distribution and characters of the mud diapirs and mud volcanoes off southwest Taiwan. *J. Asian Earth Sci.* 92, 201–214. <https://doi.org/10.1016/j.jseaes.2013.10.009>
- Clements, A., Service, M., 2016. Alternative Marine Conservation Zones in Irish Sea mud habitat: Assessment of habitat extent and condition at “Queenie corner” and assessment of fishing activity at potential MCZ sites. Report to Seafish Northern Ireland Advisory Committee.
- Cole, D., Stewart, S.A., Cartwright, J.A., 2000. Giant irregular pockmark craters in the Palaeogene of the Outer Moray Firth Basin, UK North Sea. *Mar. Pet. Geol.* 17, 563–577. [https://doi.org/10.1016/S0264-8172\(00\)00013-1](https://doi.org/10.1016/S0264-8172(00)00013-1)
- Corcoran, D. V., Doré, A.G., 2002. Depressurization of hydrocarbon-bearing reservoirs in exhumed basin settings: evidence from Atlantic margin and borderland basins. *Geol. Soc. London, Spec. Publ.* 196, 457 LP – 483. <https://doi.org/10.1144/GSL.SP.2002.196.01.25>
- Coughlan, M., Wheeler, A.J., Dorschel, B., Long, M., Doherty, P., Mörz, T., 2019. Stratigraphic model of

1
2
3
4
5
6
7
8
9 728 the Quaternary sediments of the Western Irish Sea Mud Belt from core, geotechnical and acoustic
10 729 data. *Geo-Marine Lett.* 39, 223–237.
11 730 Crémière, A., Chand, S., Sahy, D., Thorsnes, T., Martma, T., Noble, S.R., Pedersen, J.H., Brunstad, H.,
12 731 Lepland, A., 2018. Structural controls on seepage of thermogenic and microbial methane since the
13 732 last glacial maximum in the Harstad Basin, southwest Barents Sea. *Mar. Pet. Geol.* 98, 569–581.
14 733 <https://doi.org/https://doi.org/10.1016/j.marpetgeo.2018.07.010>
15 734 Crémière, A., Lepland, A., Chand, S., Sahy, D., Condon, D.J., Noble, S.R., Martma, T., Thorsnes, T., Sauer,
16 735 S., Brunstad, H., 2016. Timescales of methane seepage on the Norwegian margin following collapse
17 736 of the Scandinavian Ice Sheet. *Nat. Commun.* 7, 11509. <https://doi.org/10.1038/ncomms11509>
18 737 Croker, P.F., Kozachenko, M., Wheeler, A.J., 2005. Gas-Related Seabed Structures in the Western Irish
19 738 Sea (IRL-SEA6). January 2005, Tech Rep Strategic Environmental Assessment of the Irish Sea (SEA6),
20 739 UK Department of Trade and Industry.
21 740 Dando, P.R., 2010. Biological communities at marine shallow-water vent and seep sites, in: Kiel, S. (Ed.),
22 741 Vent and Seep Biota: Aspects from Microbes to Ecosystems. Springer Netherlands, Dordrecht, pp.
23 742 333–378. https://doi.org/10.1007/978-90-481-9572-5_11
24 743 Dando, P.R., 2001. A review of pockmarks in the UK part of the North Sea, with particular respect to
25 744 their biology. Strategic Environmental Assessment – SEA2. Technical Report 001 – Pockmarks.
26 745 Dondurur, D., Çifçi, G., Drahor, M.G., Coşkun, S., 2011. Acoustic evidence of shallow gas accumulations
27 746 and active pockmarks in the İzmir Gulf, Aegean sea. *Mar. Pet. Geol.* 28, 1505–1516.
28 747 <https://doi.org/10.1016/j.marpetgeo.2011.05.001>
29 748 Dunford, G.M., Dancer, P.N., Long, K.D., 2001. Hydrocarbon potential of the Kish Bank Basin: integration
30 749 within a regional model for the Greater Irish Sea Basin. *Geol. Soc. London, Spec. Publ.* 188, 135 LP –
31 750 154. <https://doi.org/10.1144/GSL.SP.2001.188.01.07>
32 751 Ergün, M., Dondurur, D., Çifçi, G., 2002. Acoustic evidence for shallow gas accumulations in the
33 752 sediments of the Eastern Black Sea. *Terra Nov.* 14, 313–320. <https://doi.org/10.1046/j.1365-3121.2002.00434.x>
34 753
35 754 Evans, T.G., 2011. A systematic approach to offshore engineering for multiple-project developments in
36 755 geohazardous areas, in: *Frontiers in Offshore Geotechnics II - Proceedings of the 2nd International*
37 756 *Symposium on Frontiers in Offshore Geotechnics.* pp. 3–32.
38 757 Fichler, C., Henriksen, S., Rueslaatten, H., Hovland, M., 2005. North Sea Quaternary morphology from
39 758 seismic and magnetic data: indications for gas hydrates during glaciation? *Pet. Geosci.* 11, 331 LP –
40 759 337. <https://doi.org/10.1144/1354-079304-635>
41 760 Floodpage, J., Newman, P., White, J., 2001. Hydrocarbon prospectivity in the Irish Sea area: insights from
42 761 recent exploration of the Central Irish Sea, Peel and Solway basins. *Geol. Soc. London, Spec. Publ.*
43 762 188, 107 LP – 134. <https://doi.org/10.1144/GSL.SP.2001.188.01.06>
44 763 Games, K.P., 2001. Evidence of shallow gas above the Connemara oil accumulation, Block 26/28,
45 764 Porcupine Basin, in: Houghton, P.W., Corcoran, D. V (Eds.), *The Petroleum Exploration of Ireland's*
46 765 *Offshore Basins.* The Geological Society of London, Special Publications, London, pp. 361–373.
47 766 <https://doi.org/10.1144/GSL.SP.2001.188.01.21>
48 767 Hammer, Ø., Webb, K.E., Depreiter, D., 2009. Numerical simulation of upwelling currents in pockmarks,
49 768 and data from the Inner Oslofjord, Norway. *Geo-Marine Lett.* 29, 269–275.
50 769 <https://doi.org/10.1007/s00367-009-0140-z>
51 770 Hovland, M., 2002. On the self-sealing nature of marine seeps. *Cont. Shelf Res.* 22, 2387–2394.
52 771 [https://doi.org/https://doi.org/10.1016/S0278-4343\(02\)00063-8](https://doi.org/https://doi.org/10.1016/S0278-4343(02)00063-8)
53 772 Hovland, M., Curzi, P. V, 1989. Gas seepage and assumed mud diapirism in the Italian central Adriatic
54 773 Sea. *Mar. Pet. Geol.* 6, 161–169. [https://doi.org/https://doi.org/10.1016/0264-8172\(89\)90019-6](https://doi.org/https://doi.org/10.1016/0264-8172(89)90019-6)
55 774 Hovland, M., Gardner, J. V, Judd, A.G., 2002. The significance of pockmarks to understanding fluid flow
56 775 processes and geohazards. *Geofluids* 2, 127–136. [https://doi.org/10.1046/j.1468-](https://doi.org/10.1046/j.1468-5758.2002.00019.x)

1
2
3
4
5
6
7
8
9 776 8123.2002.00028.x
10 777 Hovland, M., Heggland, R., De Vries, M.H., Tjelta, T.I., 2010. Unit-pockmarks and their potential
11 778 significance for predicting fluid flow. *Mar. Pet. Geol.* 27, 1190–1199.
12 779 <https://doi.org/10.1016/j.marpetgeo.2010.02.005>
13 780 Hovland, M., Judd, A.G., 1992. The global production of methane from shallow submarine sources. *Cont.*
14 781 *Shelf Res.* 12, 1231–1238. [https://doi.org/10.1016/0278-4343\(92\)90082-U](https://doi.org/10.1016/0278-4343(92)90082-U)
15 782 Hovland, M., Judd, A.G., 1988. *Seabed Pockmarks and Seepages*. Graham and Trotman, London.
16 783 Jackson, D.I., Jackson, A.A., Evans, D., Wingfield, R.T.R., Barnes, R.P., Arthur, M.J., 1995. United Kingdom
17 784 offshore regional report: the geology of the Irish Sea. British Geological Survey, London.
18 785 Jackson, D.I., Mullholland, P., 1993. Tectonic and stratigraphic aspects of the East Irish Sea Basin and
19 786 adjacent areas: contrasts in their post-Carboniferous structural styles. *Geol. Soc. London, Pet. Geol.*
20 787 *Conf. Ser.* 4, 791 LP – 808. <https://doi.org/10.1144/0040791>
21 788 Jordan, S.F., O'Reilly, S.S., Praeg, D., Dove, D., Facchin, L., Romeo, R., Szpak, M., Monteys, X., Murphy,
22 789 B.T., Scott, G., McCarron, S.S., Kelleher, B.P., 2019. Geophysical and geochemical analysis of
23 790 shallow gas and an associated pockmark field in Bantry Bay, Co. Cork, Ireland. *Estuar. Coast. Shelf*
24 791 *Sci.* 225, 106232. <https://doi.org/10.1016/j.ecss.2019.05.014>
25 792 Judd, A., Noble-James, T., Golding, N., Eggett, A., Diesing, M., Clare, D., Silburn, B., Duncan, G., Field, L.,
26 793 Milodowski, A., 2019. The Croker Carbonate Slabs: extensive methane-derived authigenic
27 794 carbonate in the Irish Sea—nature, origin, longevity and environmental significance. *Geo-Marine*
28 795 *Lett.* <https://doi.org/10.1007/s00367-019-00584-0>
29 796 Judd, A.G., Hovland, M., 2007. *Seabed Fluid Flow, the Impact on Geology, Biology, and the Marine*
30 797 *Environment*. Cambridge University Press.
31 798 Judd, A.G., Hovland, M., 1992. The evidence of shallow gas in marine sediments. *Cont. Shelf Res.* 12,
32 799 1081–1095.
33 800 Karisiddaiah, S.M., Veerayya, M., 1994. Methane-bearing shallow gas-charged sediments in the eastern
34 801 Arabian Sea: a probable source for greenhouse gas. *Cont. Shelf Res.* 14, 1361–1370.
35 802 [https://doi.org/https://doi.org/10.1016/0278-4343\(94\)90053-1](https://doi.org/https://doi.org/10.1016/0278-4343(94)90053-1)
36 803 Kiel, S., 2010. The vent and seep biota, in: Landman, N.H., Harries, P. (Eds.), *Topics in Geobiology*.
37 804 Springer, Germany, p. 487.
38 805 Koch, S., Berndt, C., Bialas, J., Haeckel, M., Crutchley, G., Papenberg, C., Klaeschen, D., Greinert, J., 2015.
39 806 Gas-controlled seafloor doming. *Geology* 43, 571–574. <https://doi.org/10.1130/G36596.1>
40 807 Loher, M., Marcon, Y., Pape, T., Römer, M., Wintersteller, P., dos Santos Ferreira, C., Praeg, D., Torres,
41 808 M., Sahling, H., Bohrmann, G., 2018. Seafloor sealing, doming, and collapse associated with gas
42 809 seeps and authigenic carbonate structures at Venere mud volcano, Central Mediterranean. *Deep.*
43 810 *Res. Part I Oceanogr. Res. Pap.* 137, 76–96. <https://doi.org/10.1016/j.dsr.2018.04.006>
44 811 Løseth, H., Gading, M., Wensaas, L., 2009. Hydrocarbon leakage interpreted on seismic data. *Mar. Pet.*
45 812 *Geol.* 26, 1304–1319. <https://doi.org/https://doi.org/10.1016/j.marpetgeo.2008.09.008>
46 813 Mazumdar, A., Peketi, A., Dewangan, P., Badesab, F., Ramprasad, T., Ramana, M. V., Patil, D.J., Dayal, A.,
47 814 2009. Shallow gas charged sediments off the Indian west coast: Genesis and distribution. *Mar.*
48 815 *Geol.* 267, 71–85. <https://doi.org/10.1016/j.margeo.2009.09.005>
49 816 Mellet, C., Long, D., Carter, G., Chiverell, R., Van Landeghem, K., 2015. *Geology of the seabed and*
50 817 *shallow subsurface: The Irish Sea*. British Geological Survey Commissioned Report, CR/15/057.
51 818 52pp.
52 819 National Parks and Wildlife, 2015. *Codling Fault Zone SAC Site Synopsis*. Republic of Ireland.
53 820 Newman, P.J., 1999. The geology and hydrocarbon potential of the Peel and Solway Basins, East Irish
54 821 Sea. *J. Pet. Geol.* 22, 305–324. <https://doi.org/10.1111/j.1747-5457.1999.tb00989.x>
55 822 Noble-James, T., Judd, A., Diesing, M., Clare, D., Eggett, A., Silburn, B., Duncan, G., 2020. Monitoring
56 823 shallow methane-derived authigenic carbonate: Insights from a UK Marine Protected Area. *Aquat.*

1
2
3
4
5
6
7
8
9
10
11
12
13
14
15
16
17
18
19
20
21
22
23
24
25
26
27
28
29
30
31
32
33
34
35
36
37
38
39
40
41
42
43
44
45
46
47
48
49
50
51
52
53
54
55
56
57
58
59
60
61
62
63
64
65

Conserv. Mar. Freshw. Ecosyst. 1–18. <https://doi.org/10.1002/aqc.3296>

O'Reilly, S.S., Hryniewicz, K., Little, C.T.S., Monteys, X., Szpak, M.T., Murphy, B.T., Jordan, S.F., Allen, C.C.R., Kelleher, B.P., 2014. Shallow water methane-derived authigenic carbonate mounds at the Codling Fault Zone, western Irish Sea. *Mar. Geol.* 357, 139–150. <https://doi.org/10.1016/j.margeo.2014.08.007>

Pharaoh, T.C., Smith, N.J.P., Kirk, K., Kimbell, G.S., Gent, C., Quinn, M., Monaghan, A.A., 2016. Palaeozoic Petroleum Systems of the Irish Sea Energy and Marine Geoscience Programme, British Geological Survey Commissioned Report.

Portnov, A., Vadakkepuliymbatta, S., Mienert, J., Hubbard, A., 2016. Ice-sheet-driven methane storage and release in the Arctic. *Nat. Commun.* 7, 10314. <https://doi.org/10.1038/ncomms10314>

Ramprasad, T., Dewangan, P., Ramana, M. V., Mazumdar, A., Karisiddaiah, S.M., Ramya, E.R., Sriram, G., 2011. Evidence of slumping/sliding in Krishna–Godavari offshore basin due to gas/fluid movements. *Mar. Pet. Geol.* 28, 1806–1816. <https://doi.org/https://doi.org/10.1016/j.marpetgeo.2011.02.007>

Rathburn, A.E., Levin, L.A., Held, Z., Lohmann, K.C., 2000. Benthic foraminifera associated with cold methane seeps on the northern California margin: Ecology and stable isotopic composition. *Mar. Micropaleontol.* 38, 247–266. [https://doi.org/https://doi.org/10.1016/S0377-8398\(00\)00005-0](https://doi.org/https://doi.org/10.1016/S0377-8398(00)00005-0)

Roy, S., Hovland, M., Noormets, R., Olausson, S., 2015. Seepage in Isfjorden and its tributary fjords, West Spitsbergen. *Mar. Geol.* 363, 146–159. <https://doi.org/https://doi.org/10.1016/j.margeo.2015.02.003>

Roy, S., Senger, K., Braathen, A., Noormets, R., Hovland, M., Olausson, S., 2014. Fluid migration pathways to seafloor seepage in inner isfjorden and Adventfjorden, Svalbard. *Nor. Geol. Tidsskr.* 94, 99–199.

Sills, G.C., Wheeler, S.J., 1992. The significance of gas for offshore operations. *Cont. Shelf Res.* 12, 1239–1250.

Society for Underwater Technology, 2005. Guidance Notes on Site Investigations for Offshore Renewable, Guidance notes on site investigations for offshore renewable energy projects.

Sultan, N., de Gennaro, V., Puech, A., 2012. Mechanical behaviour of gas-charged marine plastic sediments. *Geotechnique* 62, 751–766. <https://doi.org/10.1680/geot.12.OG.002>

Sun, Q., Alves, T., Xie, X., He, J., Li, W., Ni, X., 2017. Free gas accumulations in basal shear zones of mass-transport deposits (Pearl River Mouth Basin, South China Sea): An important geohazard on continental slope basins. *Mar. Pet. Geol.* 81, 17–32. <https://doi.org/https://doi.org/10.1016/j.marpetgeo.2016.12.029>

Sun, Q., Wu, S., Hovland, M., Luo, P., Lu, Y., Qu, T., 2011. The morphologies and genesis of megapockmarks near the Xisha Uplift, South China Sea. *Mar. Pet. Geol.* 28, 1146–1156. <https://doi.org/https://doi.org/10.1016/j.marpetgeo.2011.03.003>

Szpak, M.T., Monteys, X., O'Reilly, S., Simpson, A.J., Garcia, X., Evans, R.L., Allen, C.C.R., McNally, D.J., Courtier-Murias, D., Kelleher, B.P., 2012. Geophysical and geochemical survey of a large marine pockmark on the Malin Shelf, Ireland. *Geochemistry, Geophys. Geosystems* 13, 1–18. <https://doi.org/10.1029/2011GC003787>

Szpak, M.T., Monteys, X., O'Reilly, S.S., Lilley, M.K.S., Scott, G.A., Hart, K.M., McCarron, S.G., Kelleher, B.P., 2015. Occurrence, characteristics and formation mechanisms of methane generated micro-pockmarks in Dunmanus Bay, Ireland. *Cont. Shelf Res.* 103, 45–59. <https://doi.org/10.1016/j.csr.2015.04.023>

Thomas, I.W., 1978. Well 33/22-1 Completion Report. Amoco Ireland Exploration Company.

Van Landeghem, K.J.J., Niemann, H., Steinle, L.I., O'Reilly, S.S., Huws, D.G., Croker, P.F., 2015. Geological settings and seafloor morphodynamic evolution linked to methane seepage. *Geo-Marine Lett.* 35, 289–304. <https://doi.org/10.1007/s00367-015-0407-5>

1
2
3
4
5
6
7
8

9 872 Ward, S.L., Neill, S.P., Landeghem, K.J.J. Van, Scourse, J.D., 2015. Classifying seabed sediment type using
10 873 simulated tidal-induced bed shear stress. *Mar. Geol.* 367, 94–104.
11 874 <https://doi.org/10.1016/j.margeo.2015.05.010>
12 875 Webb, K.E., Barnes, D.K.A., Plankea, S., 2009. Pockmarks: Refuges for marine benthic biodiversity.
13 876 *Limnol. Oceanogr.* 54, 1776–1788. <https://doi.org/10.4319/lo.2009.54.5.1776>
14 877 Woods, M.A., Wilkinson, I.P., Leng, M.J., Riding, J.B., Vane, C.H., Lopes dos Santos, R.A., Kender, S., De
15 878 Schepper, S., Hennissen, J.A.I., Ward, S.L., Gowing, C.J.B., Wilby, P.R., Nichols, M.D., Rochelle, C.A.,
16 879 2019. Tracking Holocene palaeostratification and productivity changes in the Western Irish Sea: A
17 880 multi-proxy record. *Palaeogeogr. Palaeoclimatol. Palaeoecol.* 532, 109231.
18 881 <https://doi.org/https://doi.org/10.1016/j.palaeo.2019.06.004>
19 882 Xing, J., Jiang, X., Li, D., 2016. Seismic study of the mud diapir structures in the Okinawa Trough. *Geol. J.*
20 883 51, 203–208. <https://doi.org/10.1002/gj.2824>
21 884 Yuan, F., Bennell, J.D., Davis, A.M., 1992. Acoustic and physical characteristics of gassy sediments in the
22 885 western Irish Sea. *Cont. Shelf Res.* 12, 1121–1134.
23 886

24

25 887 **Figure Captions**

26 888 **Figure 1** Overview of the location of study areas (A-D) within the Irish Sea along with 2D reflection
27 889 seismic lines and borehole locations referred to in the text superimposed on previously mapped areas of
28 890 sub-cropping Carboniferous rocks, Mesozoic sedimentary basins (both accessed from EMODNet) and
29 891 structural lineaments (Anderson, 2013; Anderson et al., 2016). Also included are Special Areas of
30 892 Conservation (SAC) and Marine Conservation Zones (MCZ) related to gas features and the extent of the
31 893 Western Irish Sea Mud Belt. Please note that the Carboniferous potential source rock is present in the
32 894 Permian-Triassic basins.
33 895

34 895

35 896 **Figure 2** (A) Simplified lithostratigraphic column of the bedrock geology of the Western Irish Sea. (B)
36 897 Simplified lithostratigraphic column of the Quaternary section discussed in this study.
37 898

38 898

39 899 **Figure 3** 2D multichannel seismic line E95IE18-03 and accompanying geoseismic interpretation. Image
40 900 quality degrades significantly within the Codling Fault Zone due to a combination of structural
41 901 complexity and shallow gas-related features. **Inset:** Several shallow gas related features are identified
42 902 within the Codling Fault Zone, including seabed brightening with a sharp boundary above a major, near-
43 903 seabed splay of the Codling Fault Zone, and reverse polarity anomalies with associated seismic blanking
44 904 and signal dispersion.
45 905

46 905

47 906 **Figure 4** 2D multichannel seismic line IS-12 and accompanying geoseismic interpretation. The graben fill
48 907 is predicted to be of Permian-Triassic sediment, similar to the stratigraphy of the along-strike Peel Basin.
49 908

50 908

51 909

52 910

53 911

54 912

55 913

56 914

57 915

58 916

1
2
3
4
5
6
7
8
9
10
11
12
13
14
15
16
17
18
19
20
21
22
23
24
25
26
27
28
29
30
31
32
33
34
35
36
37
38
39
40
41
42
43
44
45
46
47
48
49
50
51
52
53
54
55
56
57
58
59
60
61
62
63
64
65

The faults bounding the graben are observed to offset the Base-Cenozoic Unconformity, indicating recent tectonic activity and representing possible fluid-migration pathways.

Figure 5 2D multichannel seismic line JSM92-30 and accompany geoseismic interpretation. Several minor faults are observed offsetting the Base-Cenozoic Unconformity in the Queenie Corner area.

Figure 6 Seabed mounds observed at the southern part of the study area (within the Codling Fault Zone) are interpreted as carbonate mounds which form as a result of prolonged seepage at the seafloor. Sediment waves are predominant in this region of the study area. A and B highlight the mound structures in close up (note different water depth scales for better visualization of the mounds). High backscatter is evident at these two locations. Refer to Fig. 1 for location.

Figure 7 (A) High-resolution bathymetric data illustrating seafloor morphology at Lambay Deep, along with (B) vertical profile across the 1 km wide depression. (C) Zoom-in of the bathymetric high which is characterized by high-backscatter (D). Refer to Fig. 1 for location.

Figure 8 Lambay Deep as imaged by sparker seismic data with interpreted units. Highlighted is the mound referred to as the Lambay Deep Mud Diapir (LDMD) and acoustic evidence for shallow gas (acoustic turbidity and enhanced reflections). 'M' denotes seabed multiple. Unit names are referenced from Figure 2. Yellow line is the top of UT (Upper Till member), blue line is top of PF (Prograded Facies), SSF is Surface Sands Formation. Red line denotes the edge of the LDMD. Dashed black line is the top of the shallow gas.

Figure 9 Depth to the top of the gas accumulation ([interpreted on a grid of 2D sparker seismic lines shown in Fig. 1 of Coughlan et al., \(2019\)](#)), identified in the Western Irish Sea Mud Belt superimposed on water depth from MBES data. Highlighted are the pockmarks described in Supplementary Material, the location of seismic lines presented in Fig. 10 and the pockmarks presented in detail in Fig. 11 ~~and Fig. 12~~.

Figure 10 Sparker seismic lines highlighted in Fig. 9 from the WISMB with interpreted units. Also presented is evidence for shallow gas accumulation (enhanced reflection, acoustic turbidity, acoustic blanking). 'M' denotes seabed multiple. Unit names are referenced from Figure 2. Full black line

1
2
3
4
5
6
7
8
9 940 indicates the top of bedrock. Yellow line is the top of UT (Upper Till member), green line is the top of CF
10 941 (Chaotic Facies), blue line is top of PF (Prograded Facies). Dashed black line denotes the top of the
11 shallow-gas front.
12 942

13 943
14
15 944 **Figure 11** ~~Figure 11 (A) The largest irregular elongated pockmark (P12) is shown on high resolution~~
16 945 ~~bathymetric data. A smaller circular pockmark is located NE of P12. (B) High backscatter at the centre of~~
17 ~~the pockmark is indicative of possible carbonate precipitates or coarse sediments due to prolonged~~
18 946 ~~seepage. (C) Bathymetric contour lines illuminated the rim of the irregular elongated pockmark (P12),~~
19 947 ~~string pockmarks at its centre and the surrounding seafloor morphology. Vertical profiles across the~~
20 ~~short and long axis of the elongated pockmark (P12) illustrate the small depth change (1–1.2 m) across~~
21 948 ~~the P12 pockmark. Refer to Fig. 9 for location. WD: Water depth.~~
22 949
23
24 950

25 951
26
27 952 **Figure 12** High-resolution bathymetric data illustrating (A) a central mound within pockmark P15, and
28 953 (B) morphology of a circular pockmark P13 without a central mound along with their vertical profiles. (C)
29
30 954 Central mounds within pockmarks P10 and P11, which are separated by approximately 1 km. Refer to
31 955 Fig. 9 for locations.
32
33 956

34 957 **Figure 1213** High-resolution multibeam bathymetric data (top) and backscatter data (bottom) of the
35 958 Queenie Corner area seafloor. Refer to Fig. 1 for location. A closer illustration of the seabed mound
36
37 959 structures of various sizes and shapes (sub-circular to elongated) have been shown along with their
38
39 960 vertical profiles.
40 961

41 962 **Figure 1314** Pinger profile highlighted in Fig. 1213 from Queenie Corner illustrates acoustic evidence for
42 963 shallow gas in the form of gas chimneys (a) and acoustic blanking (b). Seabed mounds are observed at
43 964 the top of gas chimneys (a).
44
45 965

46 965
47
48 966 **Figure 1415** Conceptual model proposed for fluid migration from deeper thermogenic source rocks via
49 967 recently reactivated fault conduits to shallow gas-charged Quaternary sediments in the Western Irish
50 968 Sea Mud Belt. Subsequently, some of the gas migrates upwards to the seafloor, leading to the formation
51
52 969 of pockmarks (due to fluid seepage) and seabed mounds (due to increase of pressure and volume within
53 970 sediment pores).
54
55 971

56
57
58
59
60
61
62
63
64
65

1
2
3
4
5
6
7
8
9
10
11
12
13
14
15
16
17
18
19
20
21
22
23
24
25
26
27
28
29
30
31
32
33
34
35
36
37
38
39
40
41
42
43
44
45
46
47
48
49
50
51
52
53
54
55
56
57
58
59
60
61
62
63
64
65

Figure 1516 Overview map of shallow gas accumulations and fluid seepage features identified in this study along with similar features identified from other referenced studies. This information is superimposed on the British Geological Survey DigSBS250 database, which maps seabed sediment distribution. according to the Folk Classification, in the Irish Sea at a scale of 1:250,000. Some pockmarks from this study are seen to form above a mapped shallow gas accumulation with mud-dominated sediments, generally pockmarks (this study) are concentrated in areas with a sandier component. Seabed mound features in this study were found in areas where the seabed sediment is mud-dominated.

Figure 1617 Conceptual models proposed for (A) the formation of mounds at the centre of pockmarks in sand-rich sediments and (B) seabed mounds in mud-rich sediments as a precursors to collapsed pockmarks, , adapted from previous studies (Hovland, 2002; Crémière et al. 2018; Loher et al. 2018).

Table Captions

Table 1 List of surveys from which data were used in this study.

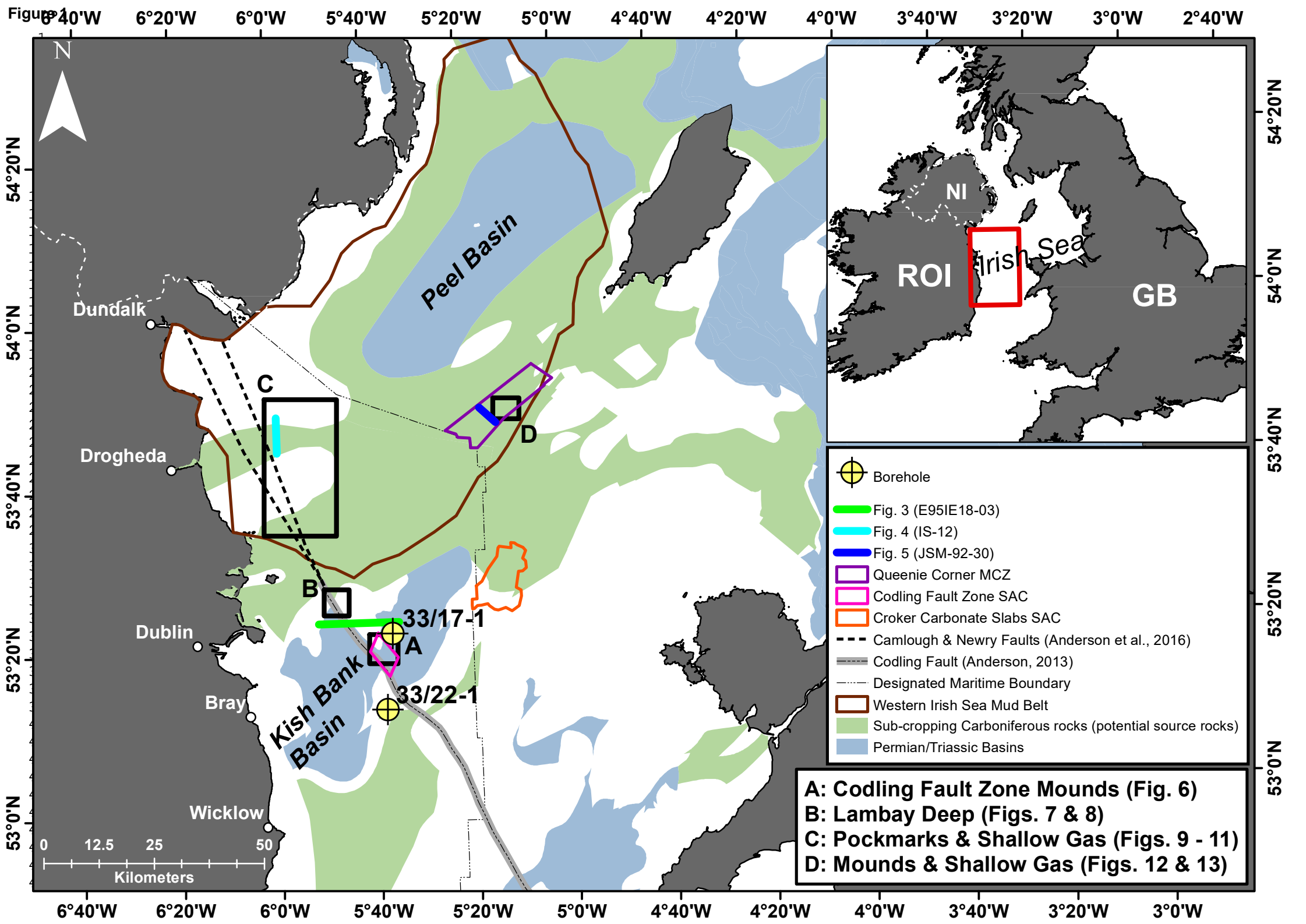


Figure 2

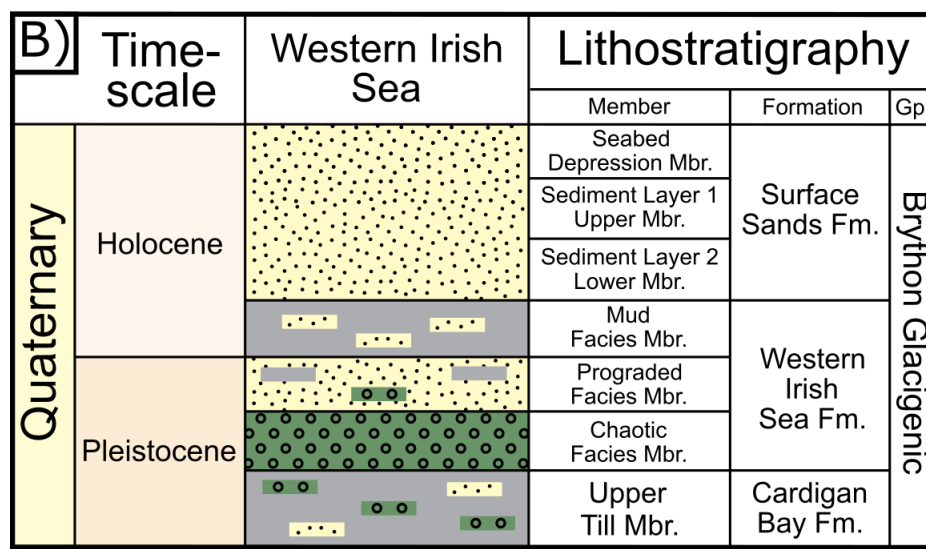
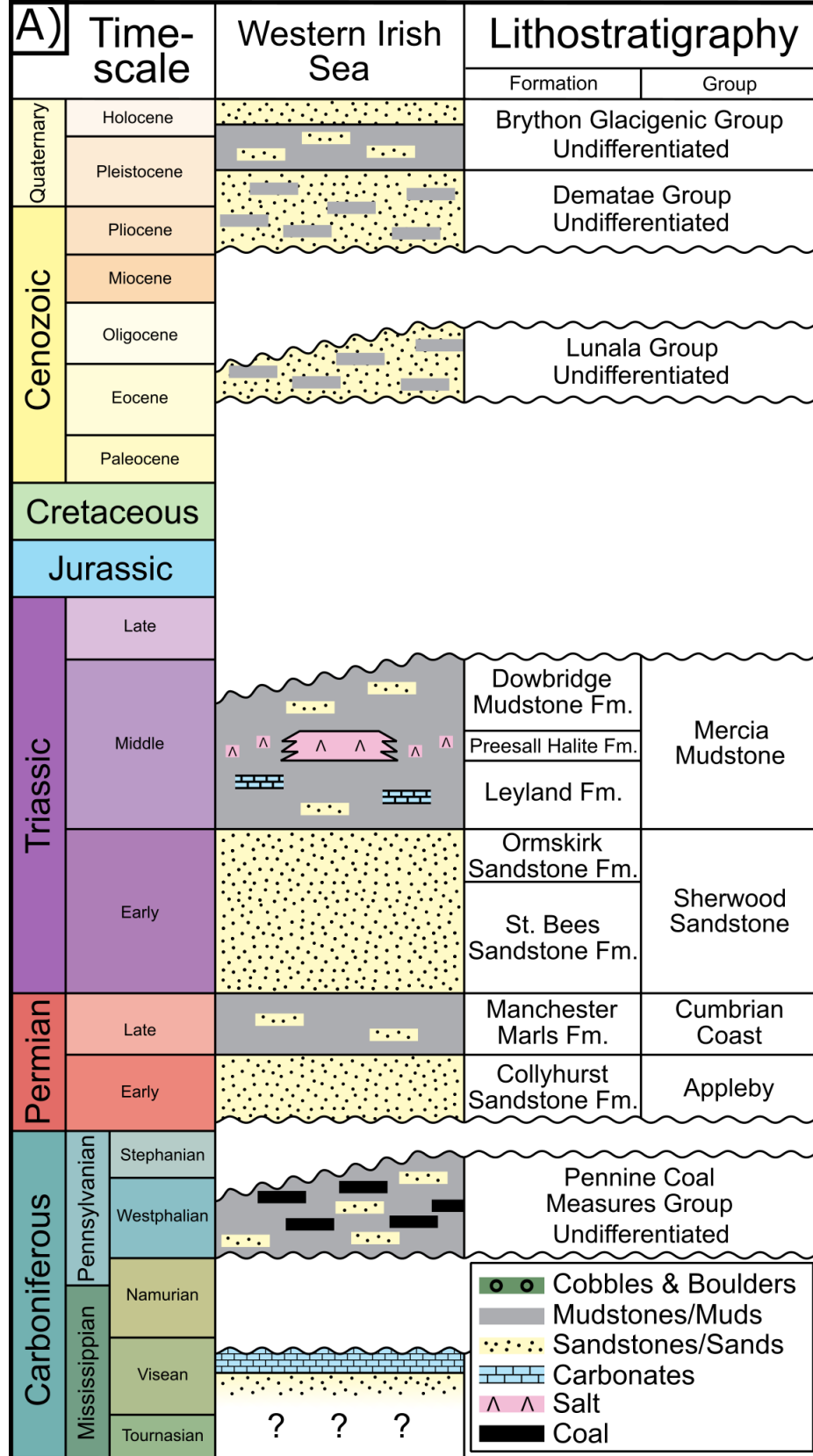


Figure 3

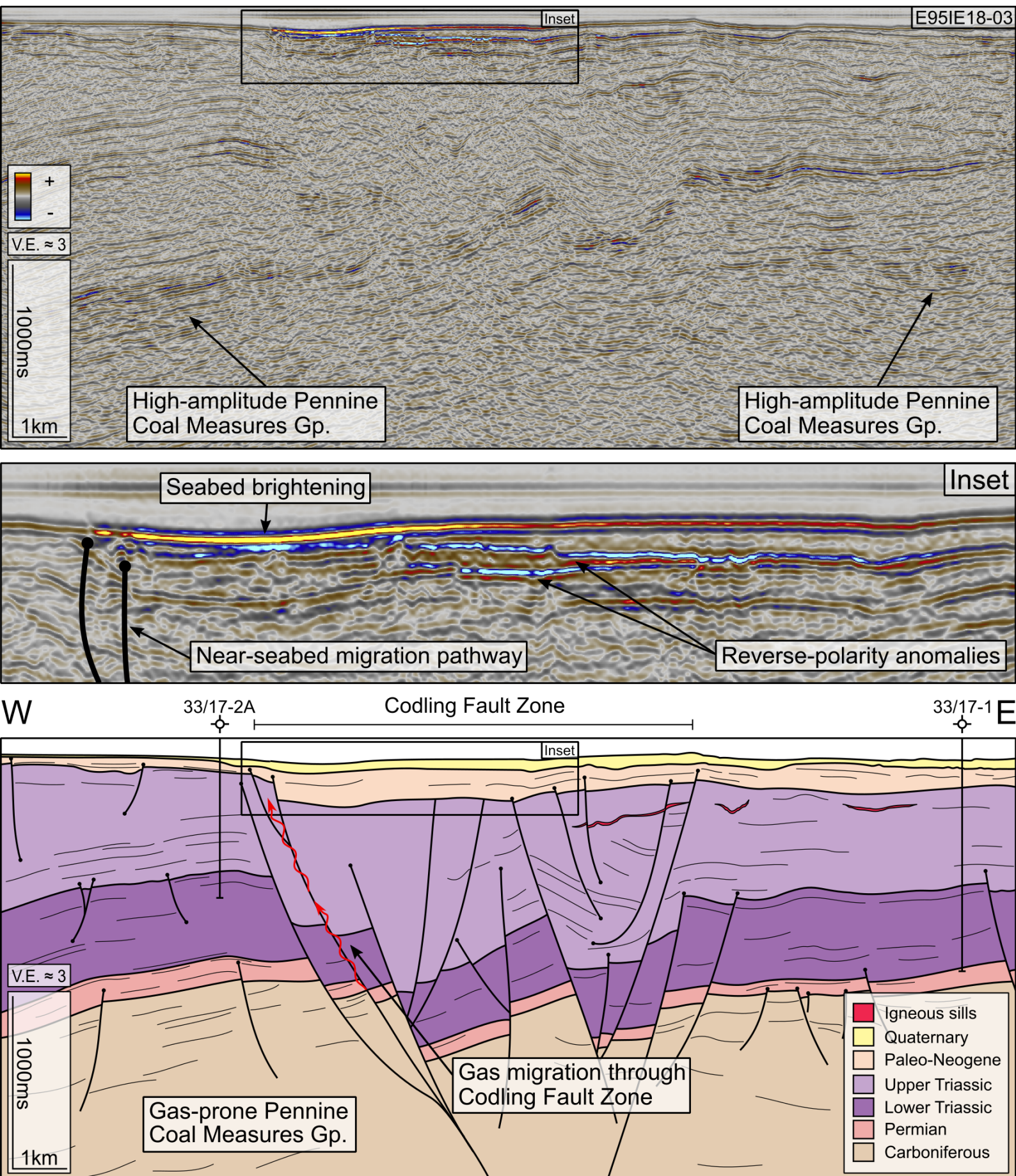


Figure 4

IS-12

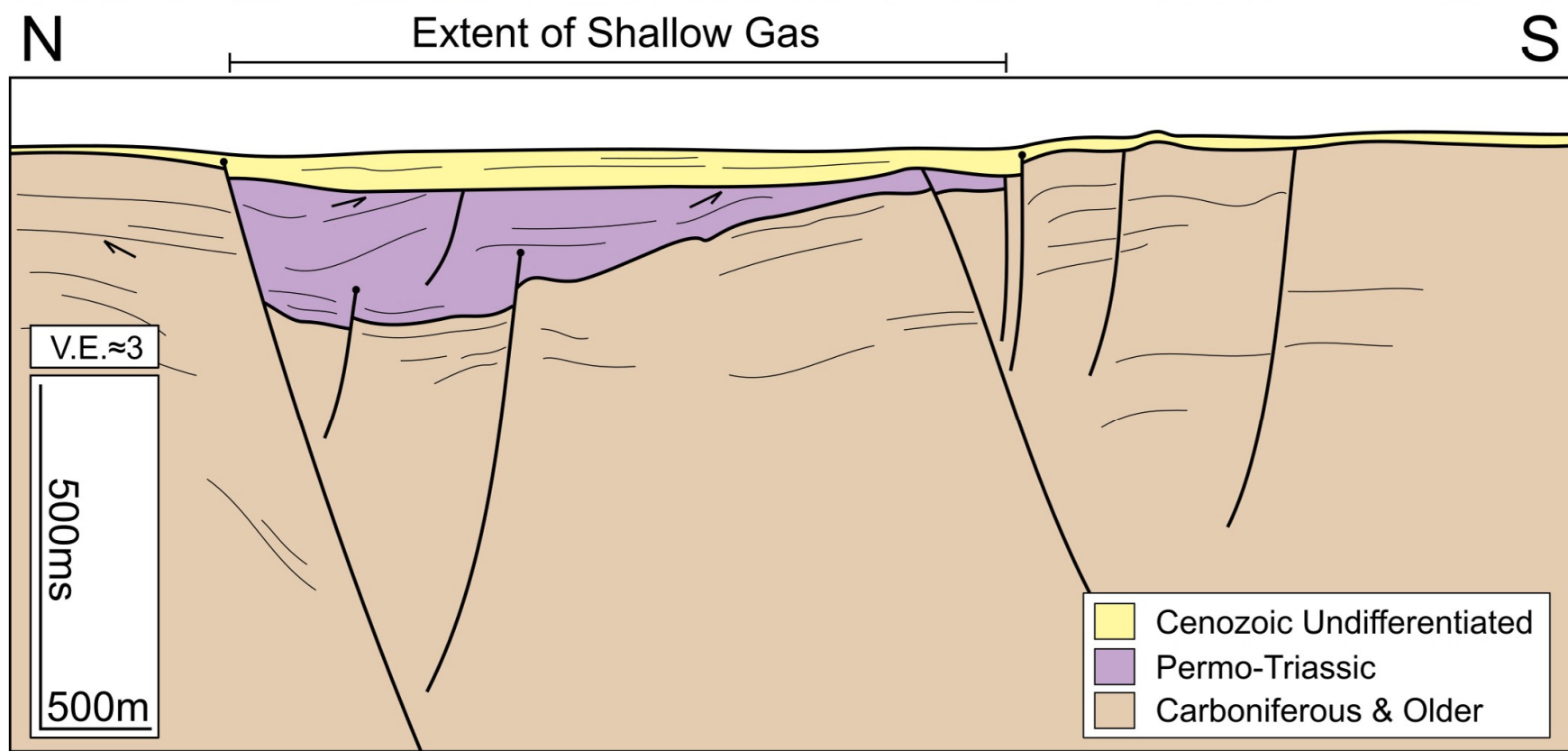
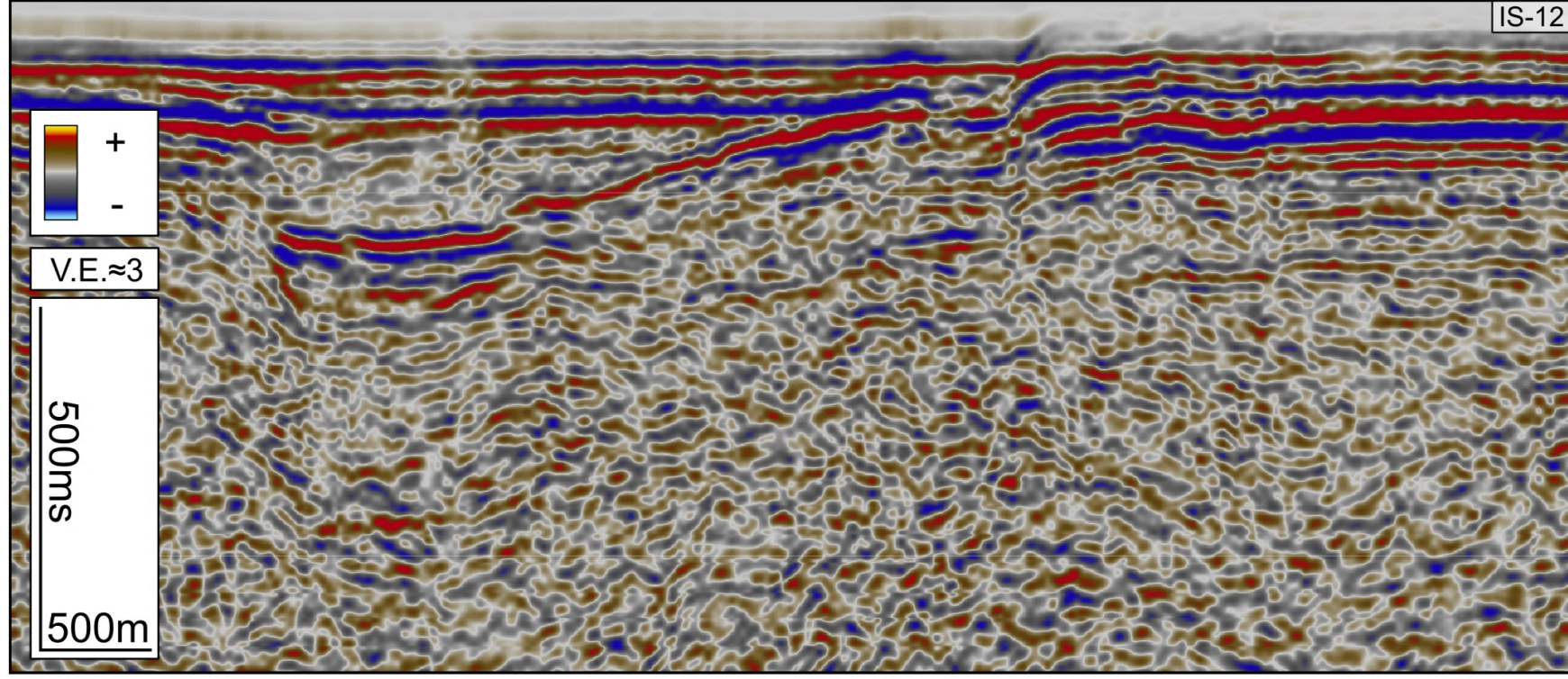
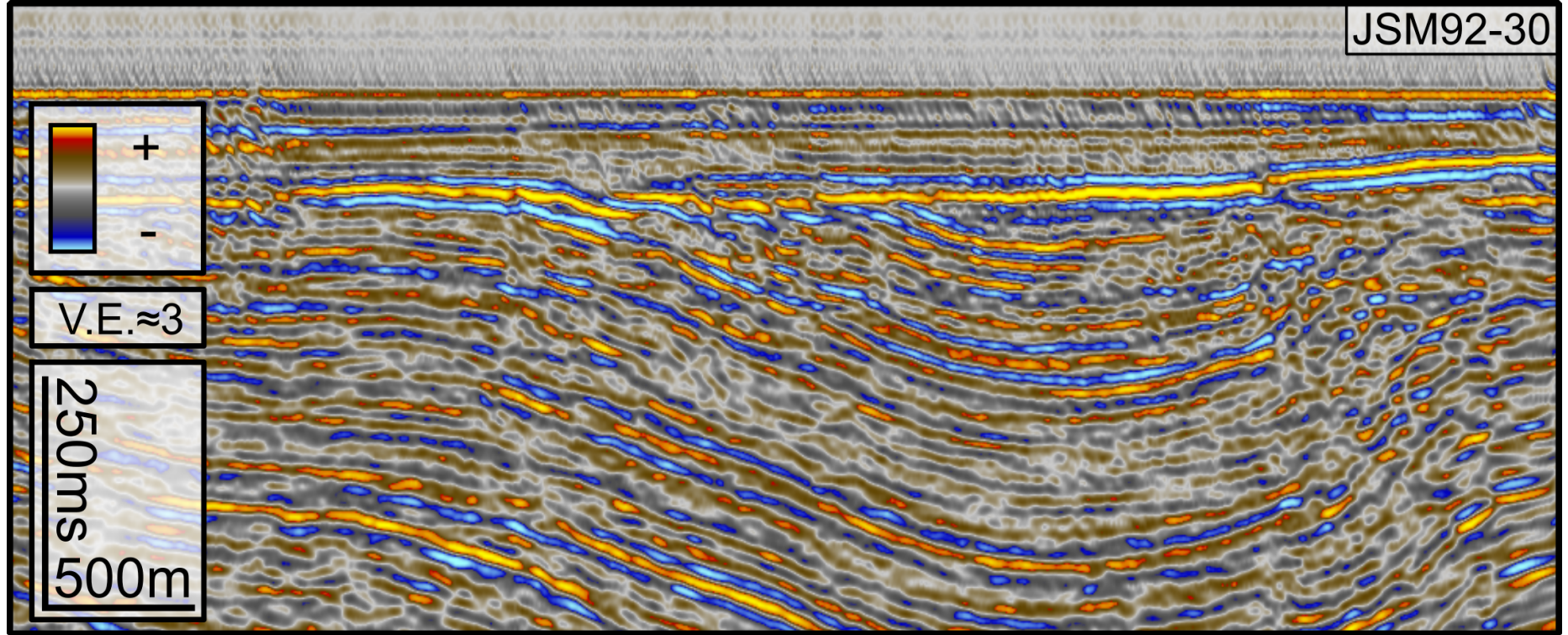


Figure 5



NW

SE

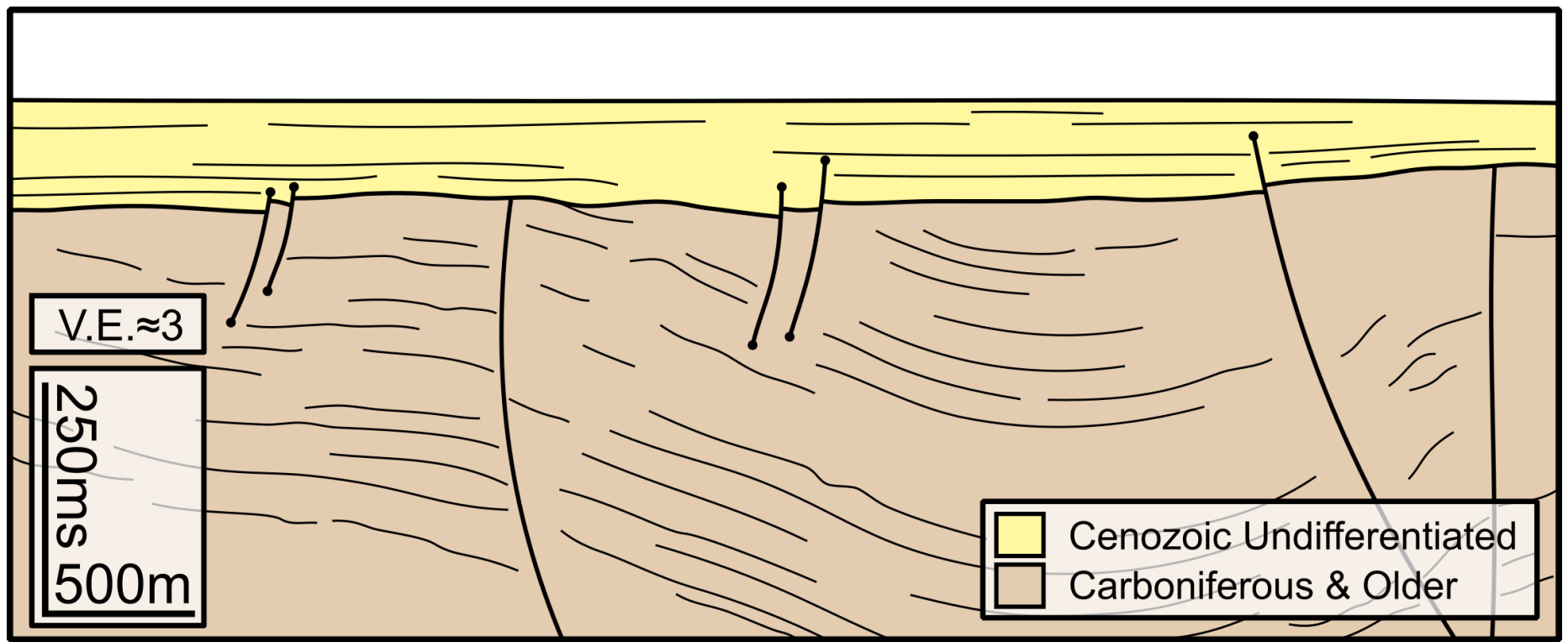


Figure 6

1
2
3
4
5
6
7
8
9
10
11
12
13
14
15
16
17
18
19
20
21
22
23
24
25
26
27
28
29
30
31
32
33
34
35
36
37
38
39
40
41
42
43
44
45
46
47
48
49
50
51
52
53
54
55
56
57
58
59
60
61
62
63
64
65

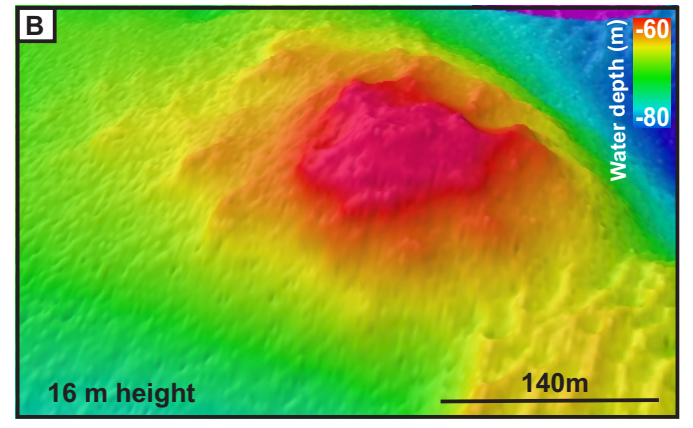
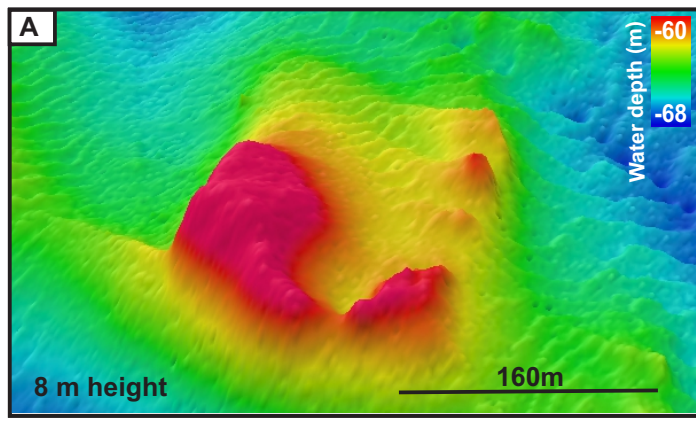
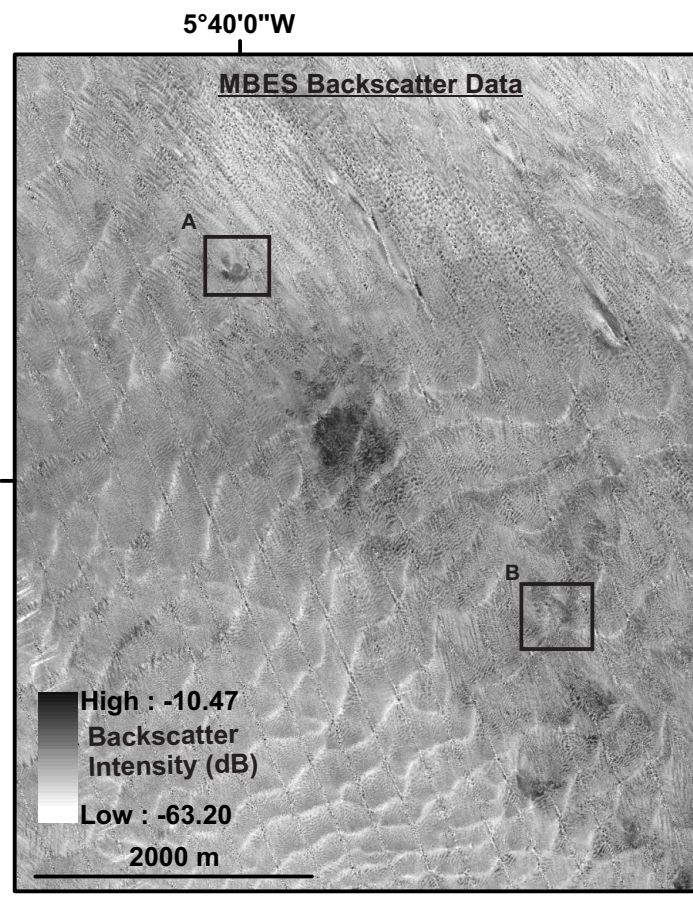
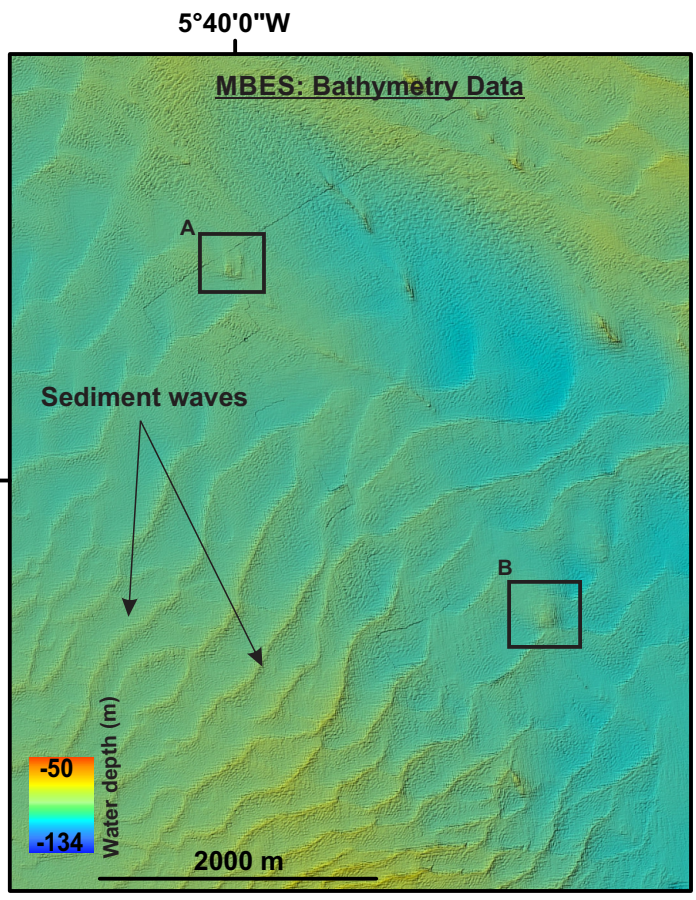
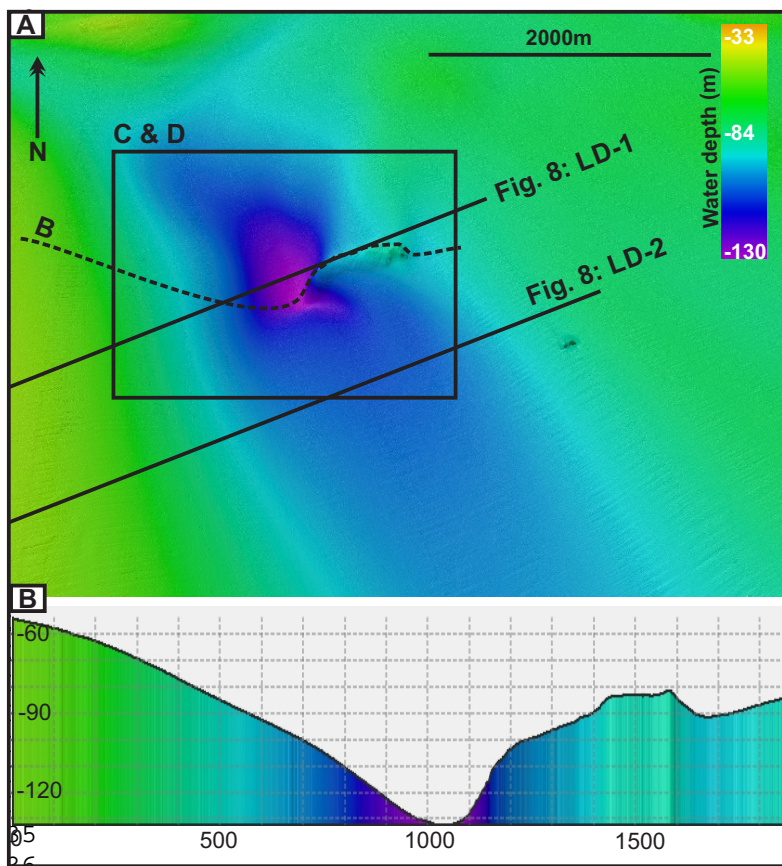


Figure 7

1
2
3
4
5
6
7



36
37
38
39
40
41
42
43
44
45
46
47
48
49
50
51
52
53
54
55
56
57
58
59
60
61
62
63
64
65

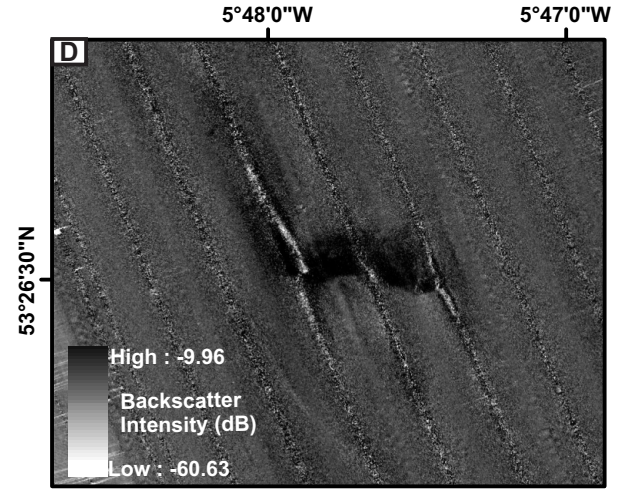
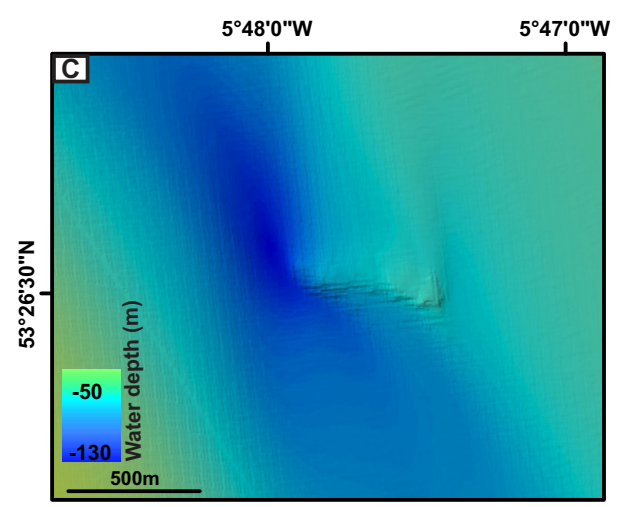


Figure 8

1
2
3
4
5
6
7
8
9
10
11
12
13
14
15
16
17
18
19
20
21
22
23
24
25
26
27
28
29
30
31
32
33
34
35
36
37
38
39
40
41
42
43
44
45
46
47
48
49
50
51
52
53
54
55
56
57
58
59
60
61
62
63
64
65

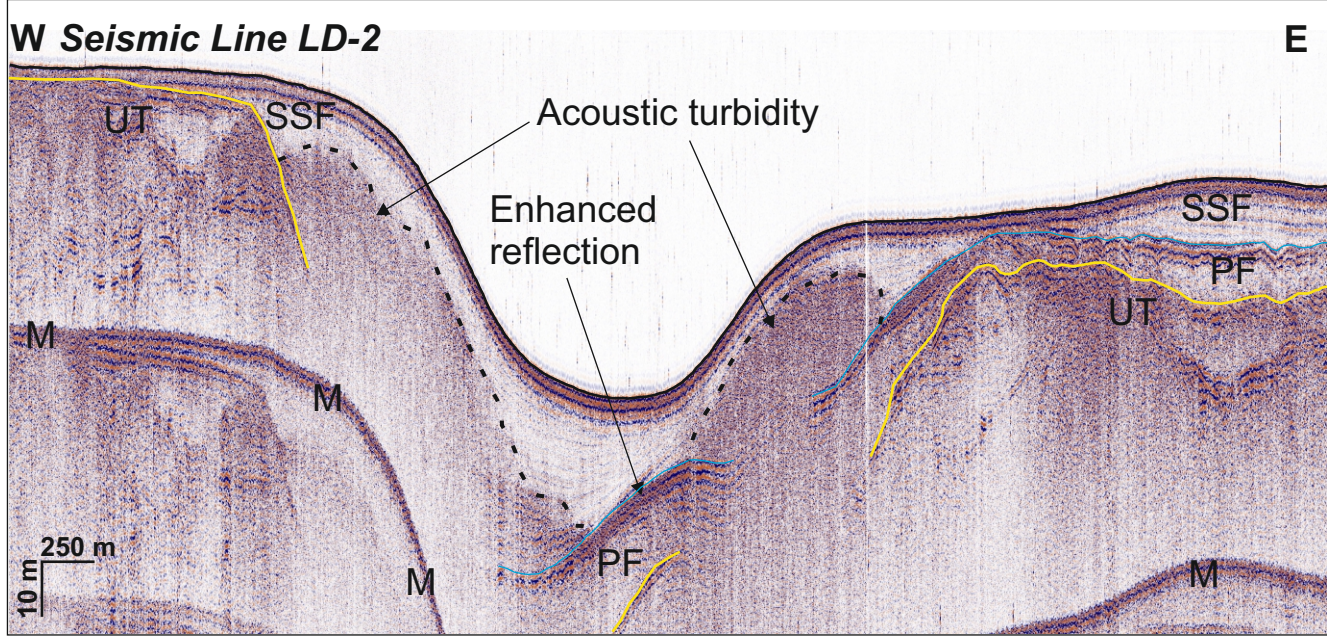
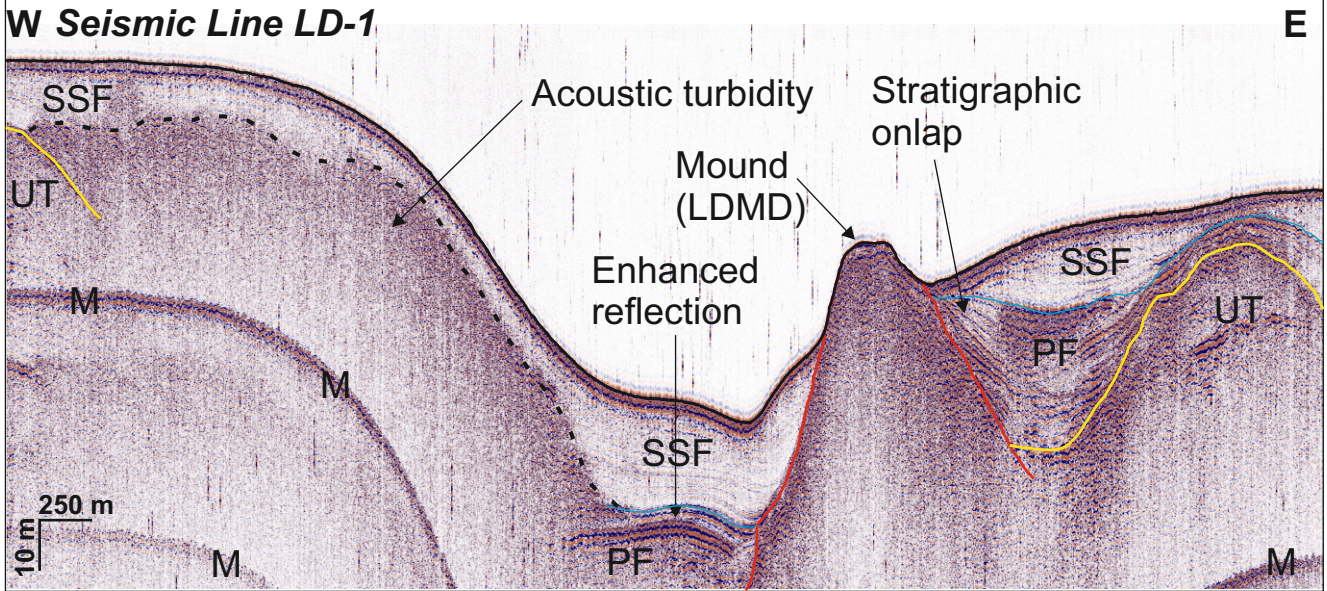


Figure 9

1
2
3
4
5
6
7
8
9
10
11
12
13
14
15
16
17
18
19
20
21
22
23
24
25
26
27
28
29
30
31
32
33
34
35
36
37
38
39
40
41
42
43
44
45
46
47
48
49
50
51
52
53
54
55
56
57
58
59
60
61
62
63
64
65

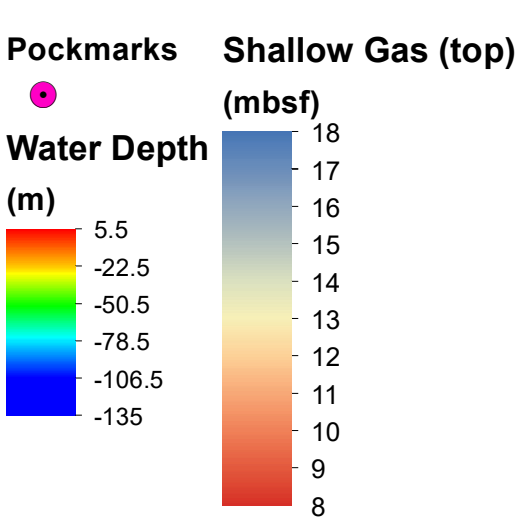
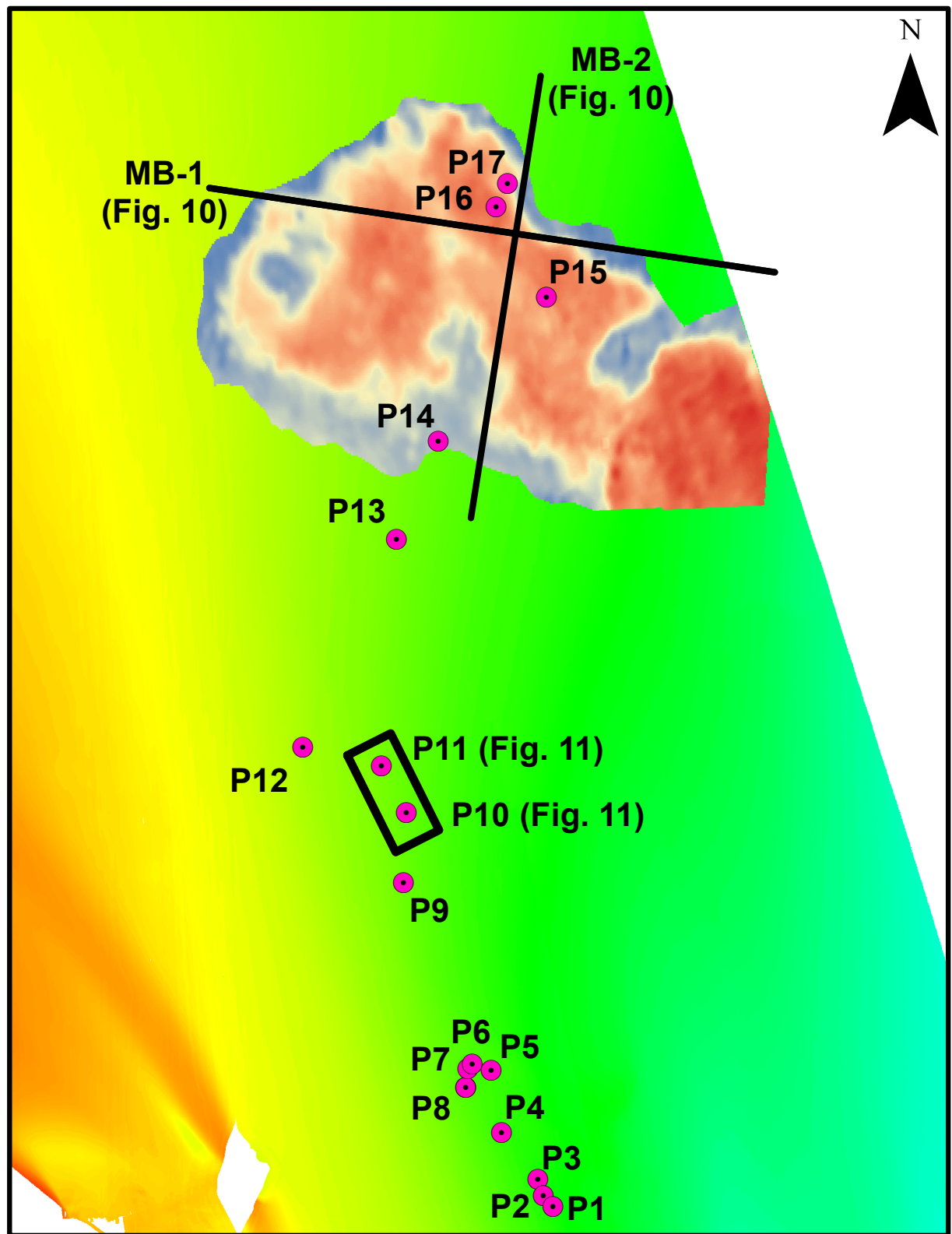


Figure 10

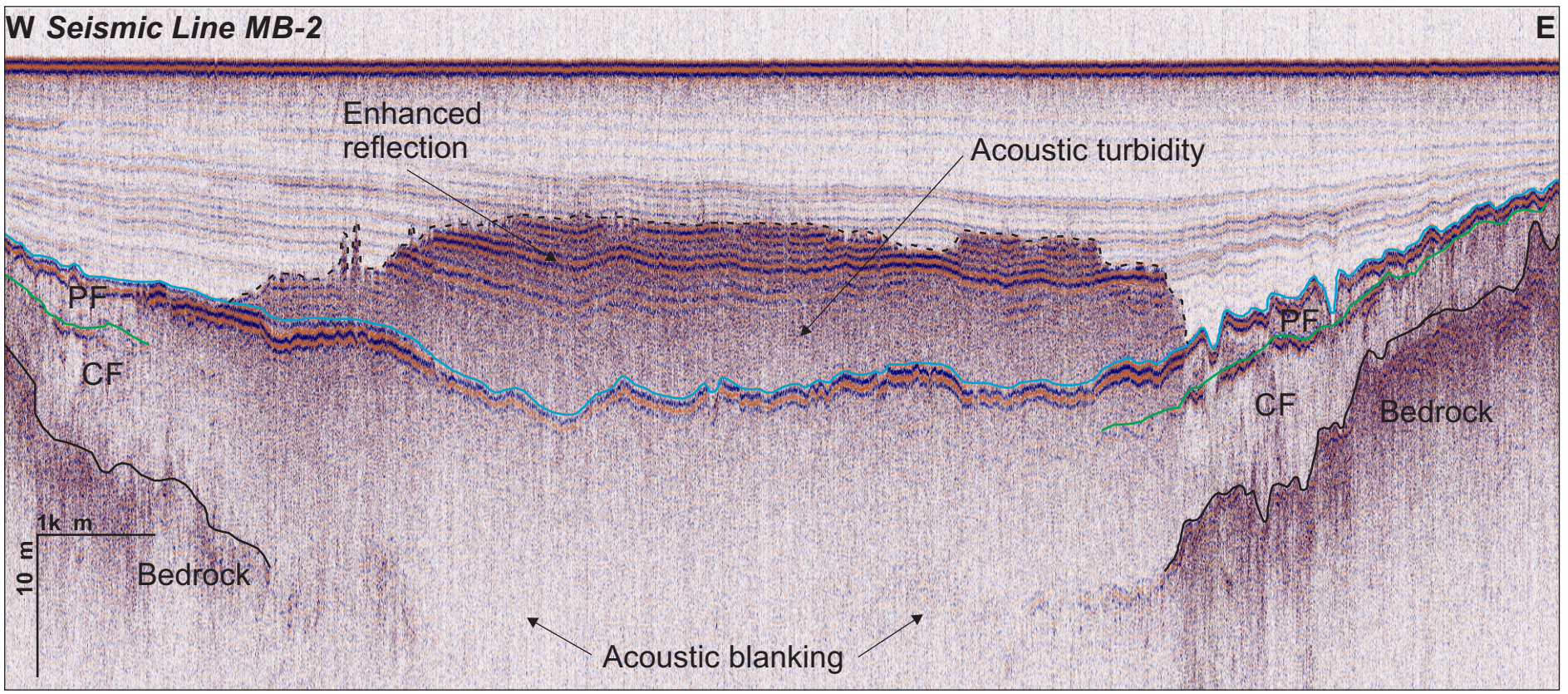
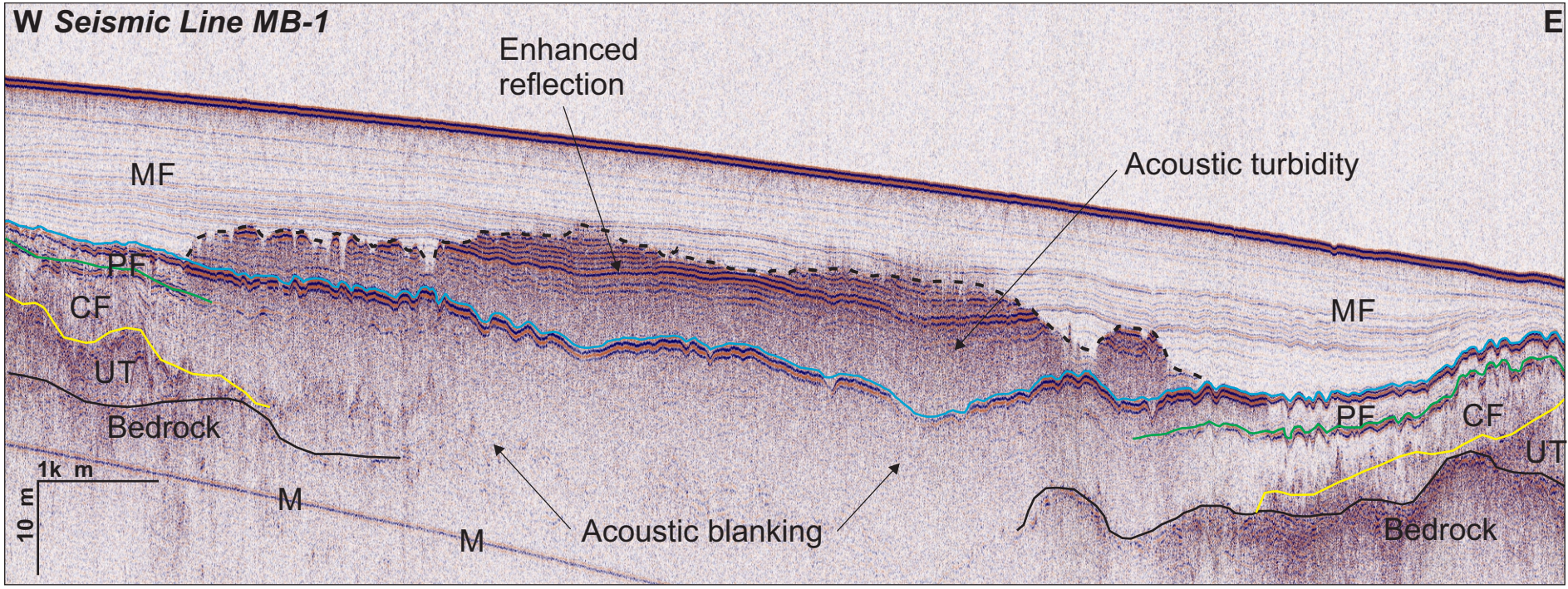
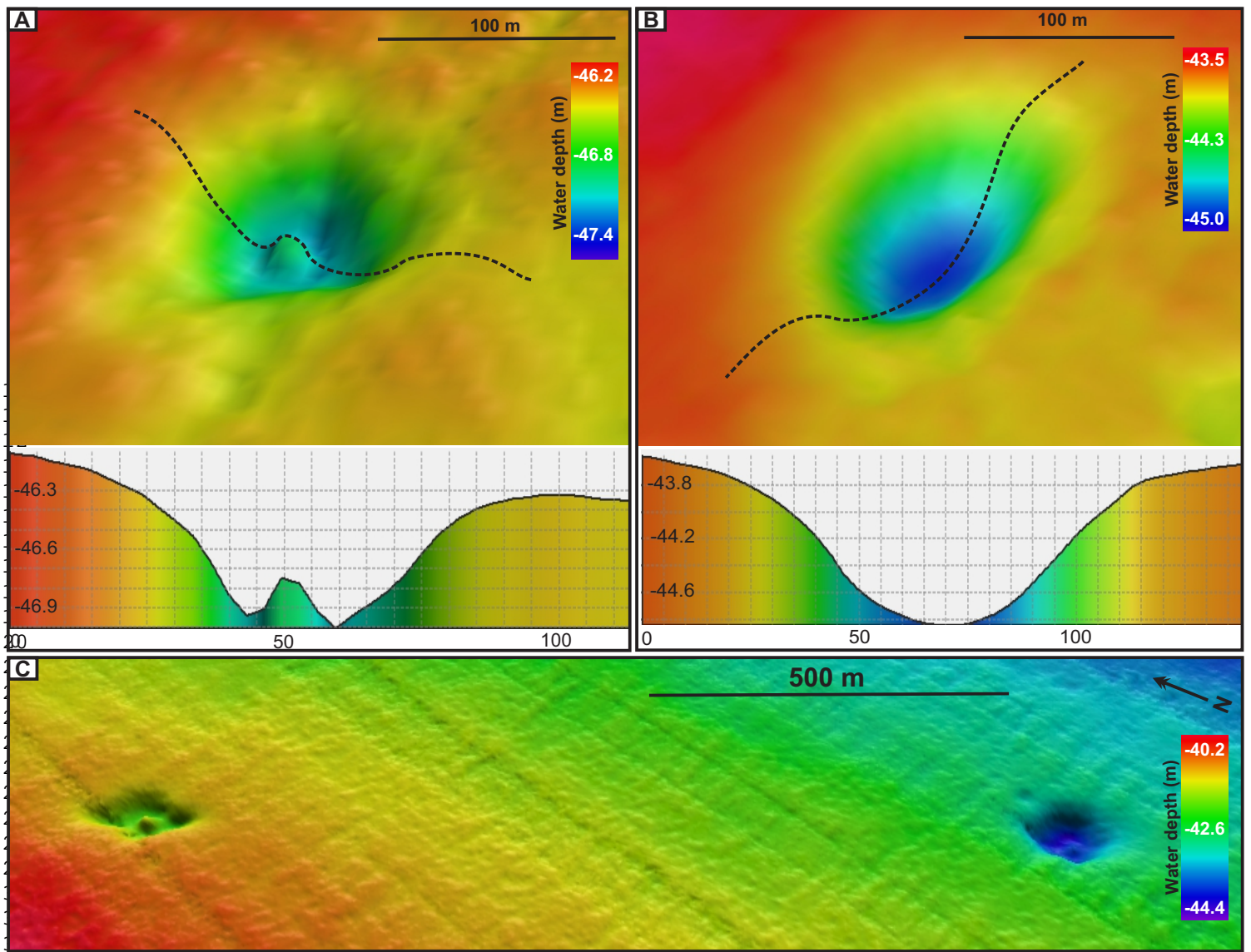
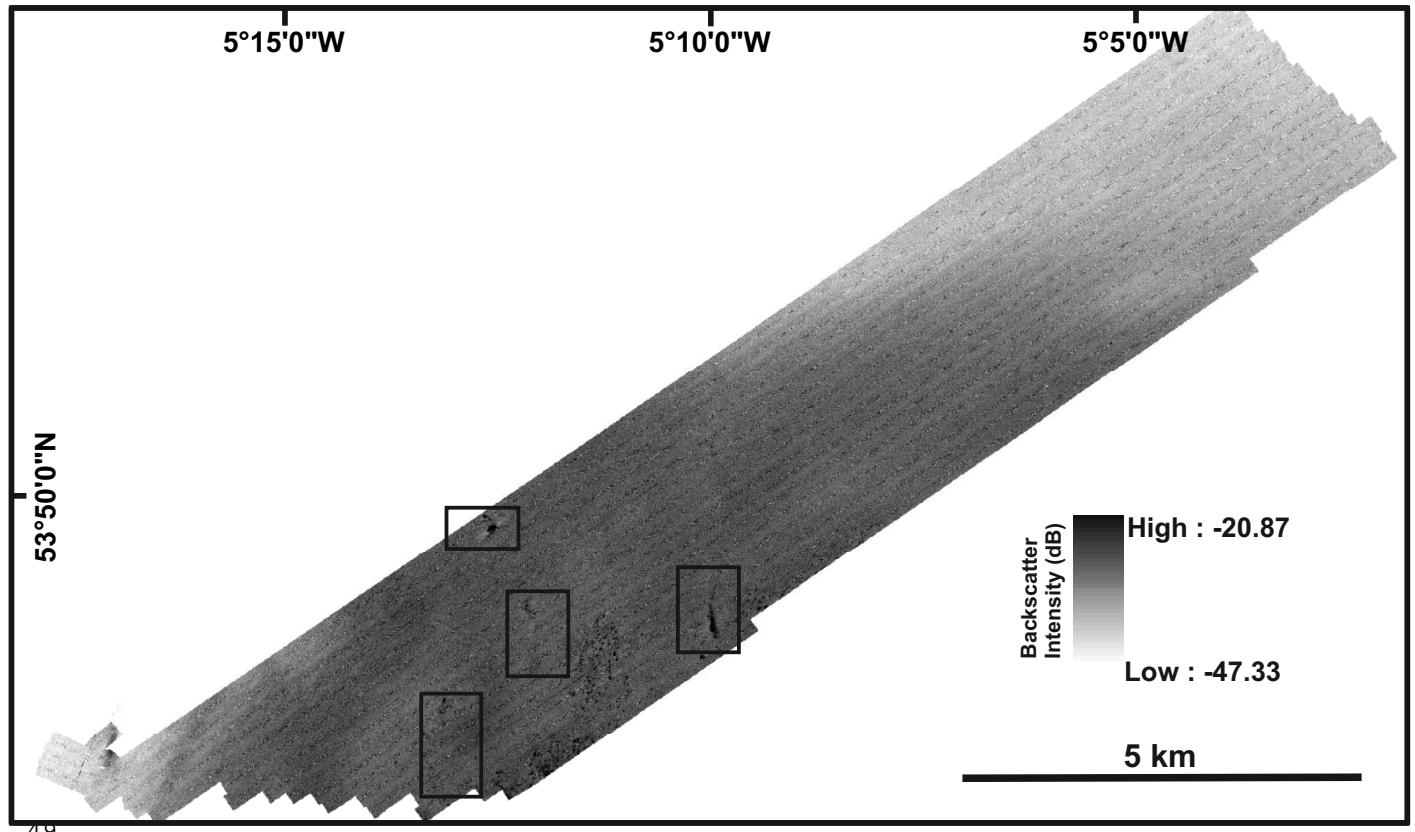
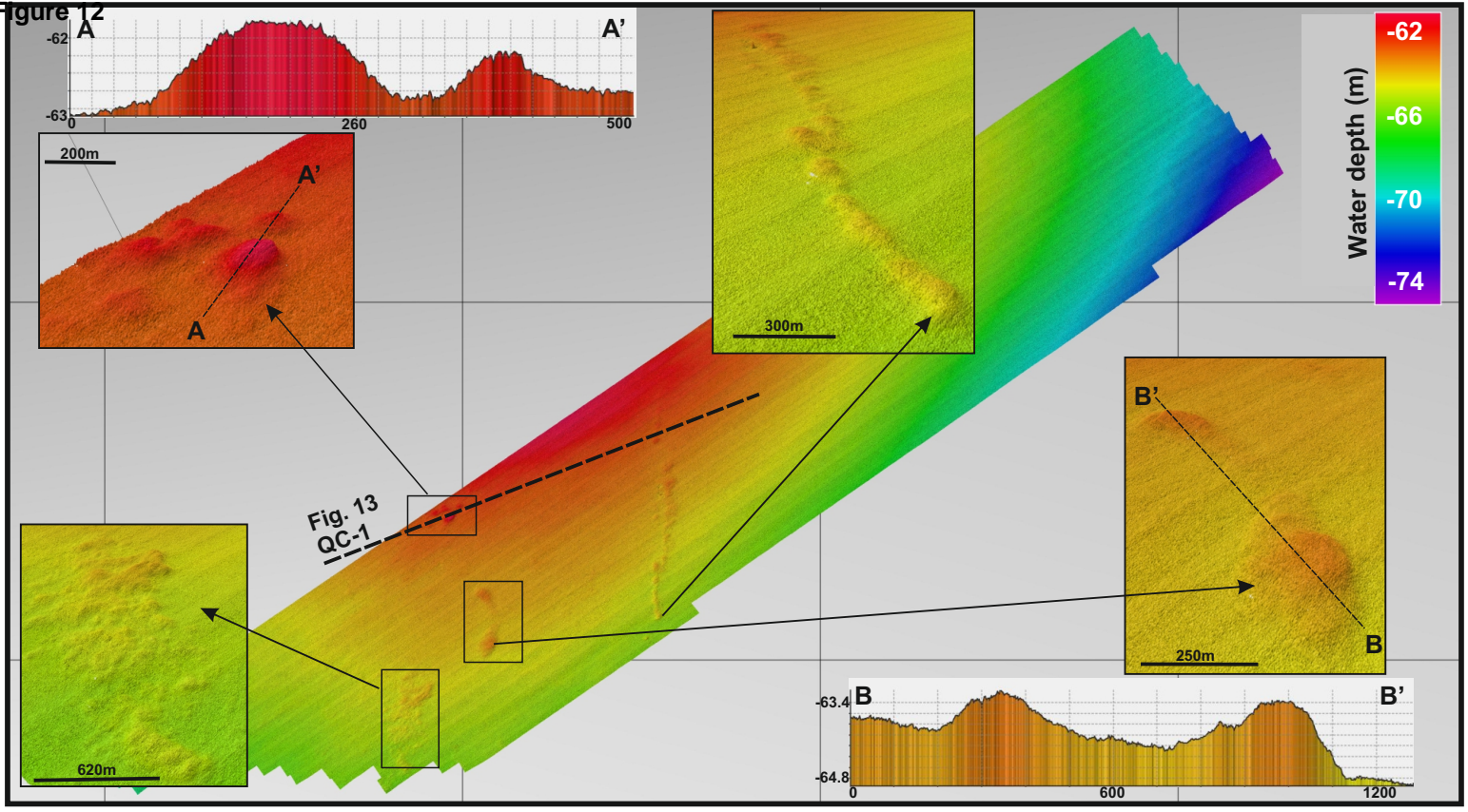


Figure 11



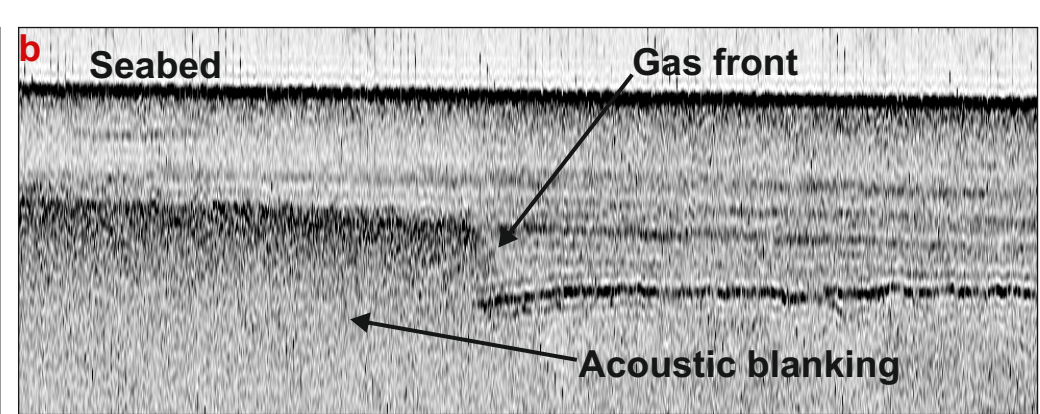
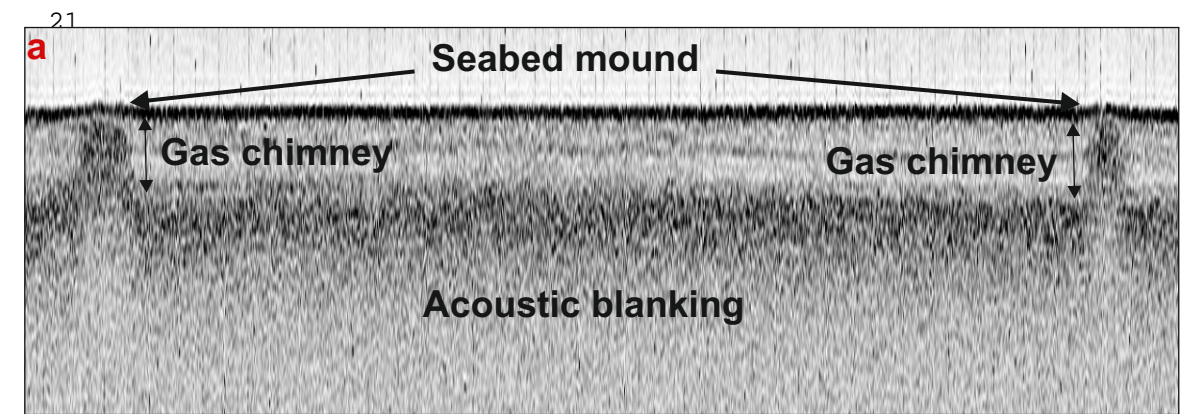
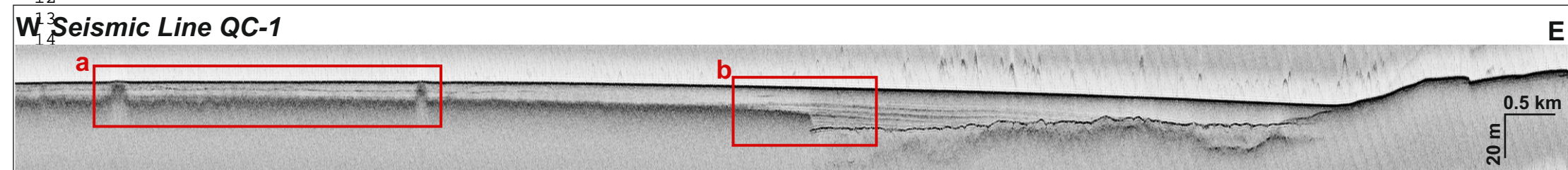
33
34
35
36
37
38
39
40
41
42
43
44
45
46
47
48
49
50
51
52
53
54
55
56
57
58
59
60
61
62
63
64
65



49
50
51
52
53
54
55
56
57
58
59
60
61
62
63
64
65

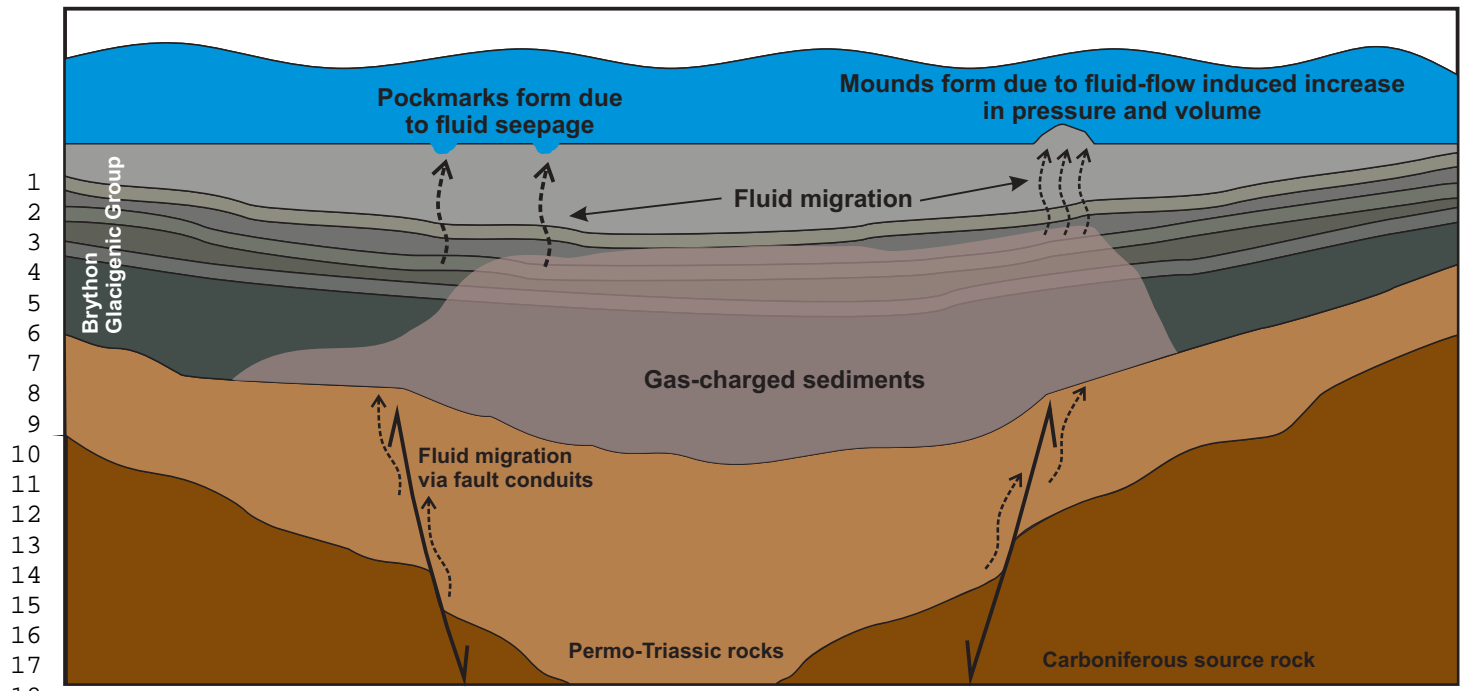
Figure 13

1
2
3
4
5
6
7
8
9
10
11
12



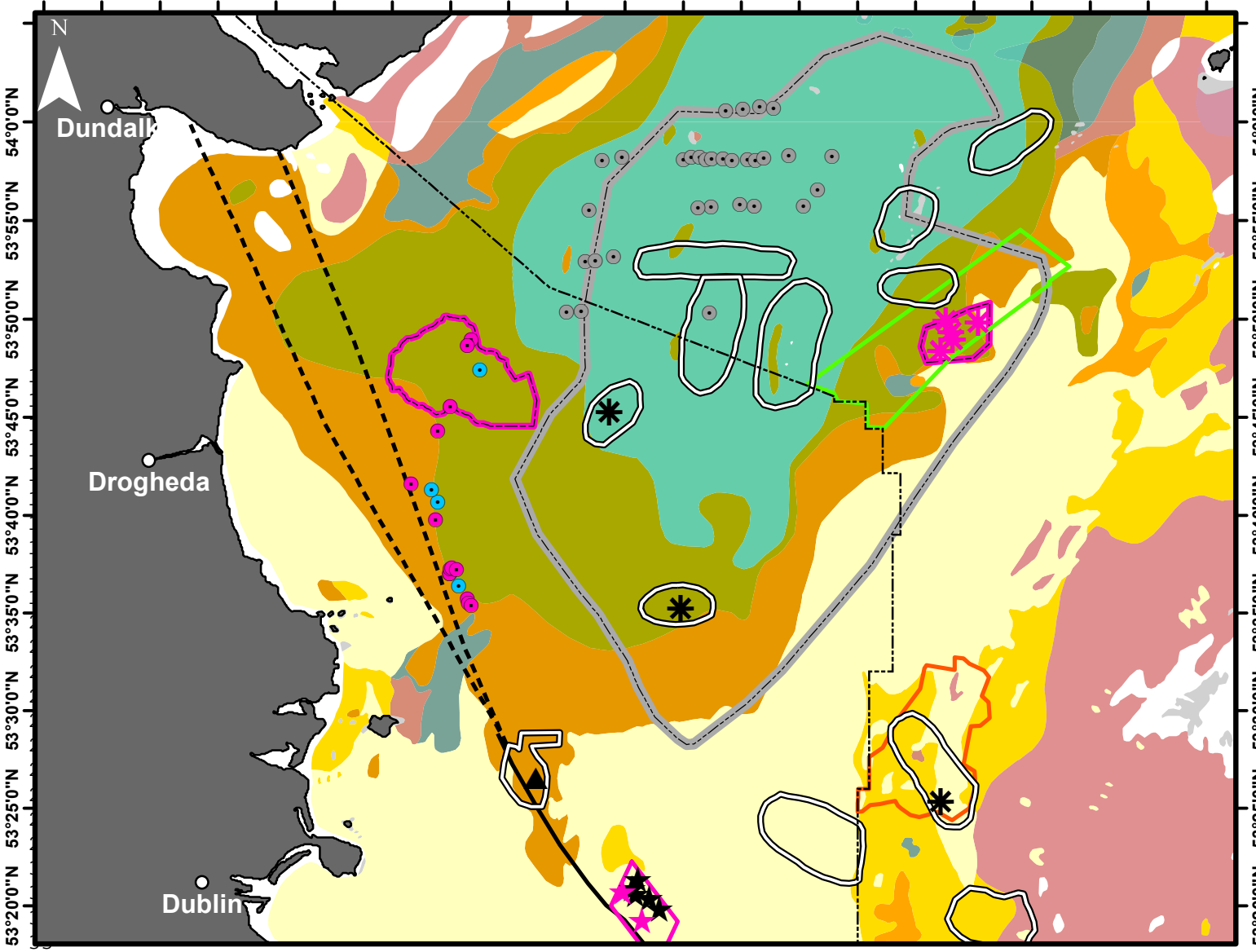
13
14
21
35
36
37
38
39
40
41
42
43
44
45
46
47
48
49

Figure 14



- 1
- 2
- 3
- 4
- 5
- 6
- 7
- 8
- 9
- 10
- 11
- 12
- 13
- 14
- 15
- 16
- 17
- 18
- 19
- 20
- 21
- 22
- 23
- 24
- 25
- 26
- 27
- 28
- 29
- 30
- 31
- 32
- 33
- 34
- 35
- 36
- 37
- 38
- 39
- 40
- 41
- 42
- 43
- 44
- 45
- 46
- 47
- 48
- 49
- 50
- 51
- 52
- 53
- 54
- 55
- 56
- 57
- 58
- 59
- 60
- 61
- 62
- 63
- 64
- 65

Figure 15
 6°30'0"W 6°20'0"W 6°10'0"W 6°0'0"W 5°50'0"W 5°40'0"W 5°30'0"W 5°20'0"W 5°10'0"W 5°0'0"W 4°50'0"W



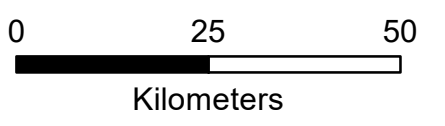
Legend

BGS Marine Sediment

Folk Classification

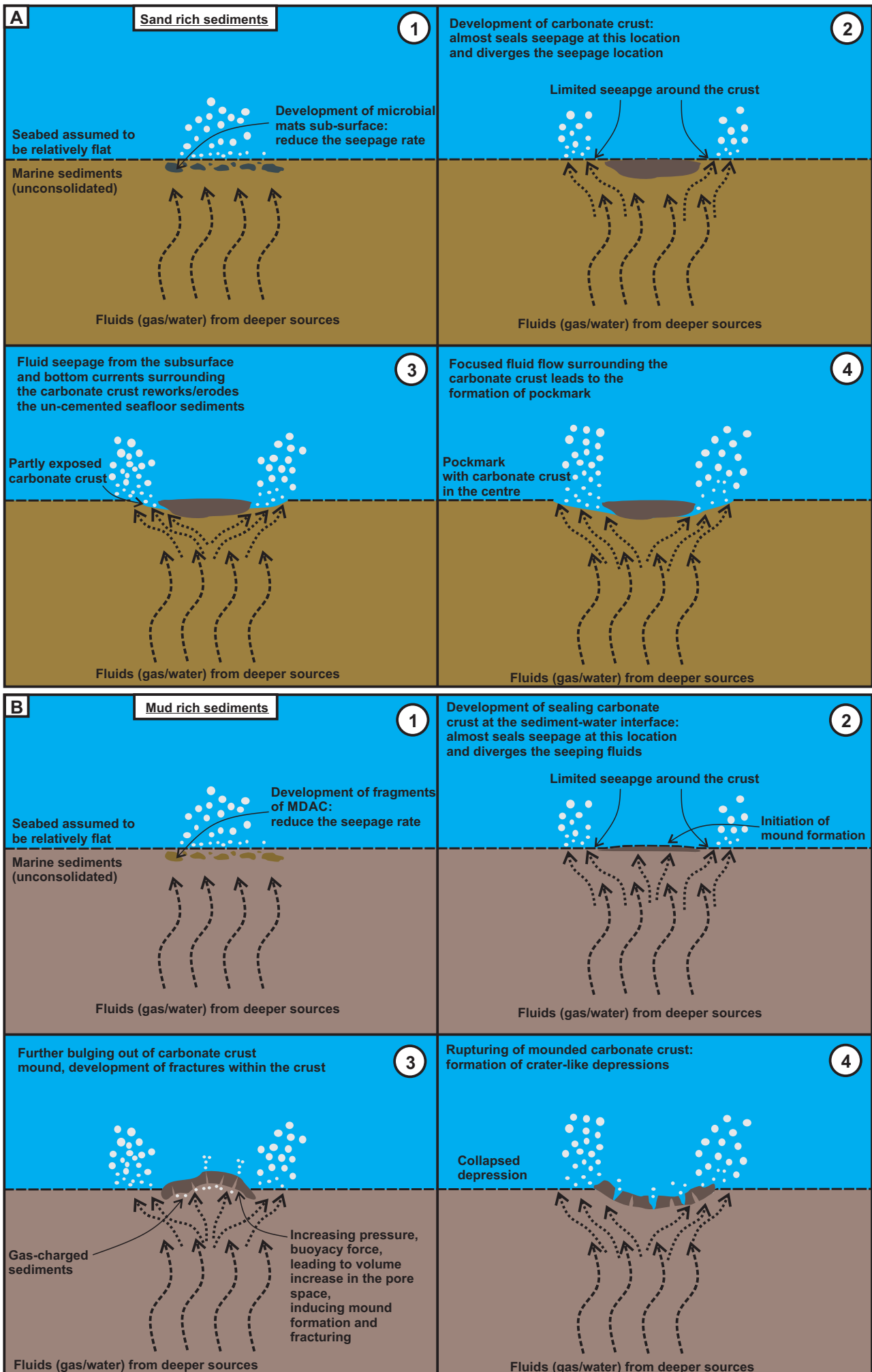
- Mud
- Sandy mud
- Muddy sand
- Sand
- Gravelly mud
- Gravelly muddy sand
- Gravelly sand
- Slightly gravelly sand
- Slightly gravelly mud
- Slightly gravelly muddy sand
- Slightly gravelly sandy mud
- Sandy gravel
- Gravel
- Rock

- Gas Fronts & Plumes (Croker et al., 2005)
- Acoustic Turbid Zone (Yuan et al., 1992)
- Shallow Gas (this study)
- Pockmark (Yuan et al., 1992)
- Pockmark (this study: without mound)
- Pockmark (this study: with mound)
- Seabed Mounds (Croker et al., 2005)
- Seabed Mounds (this study)
- Lambay Deep Mud Diapir (Croker et al., 2005)
- Codling Fault Zone Mounds (Van Landeghem et al., 2015)
- Codling Fault Zone Mounds (this study)
- Queenie Corner MCZ
- Codling Fault Zone SAC
- Croker Carbonate Slabs SAC
- Camrough & Newry Faults (Anderson et al., 2016)
- Codling Fault (Anderson, 2013)
- Ireland/UK EEZ boundary



58
 59
 60
 61
 62
 63
 64
 65

Figure 16



1
2
3
4
5
6
7
8
9
10
11
12
13
14
15
16
17
18
19
20
21
22
23
24
25
26
27
28
29
30
31
32
33
34
35
36
37
38
39
40
41
42
43
44
45
46
47
48
49
50
51
52
53
54
55
56
57
58
59
60
61
62
63
64
65

Table 1

1
2
3
4
5
6
7
8
9
10
11
12
13
14
15
16
17
18
19
20
21
22
23
24
25
26
27
28
29
30
31
32
33
34
35
36
37
38
39
40
41
42
43
44
45
46
47
48
49
50
51
52
53
54
55
56
57
58
59
60
61
62
63
64
65

Survey	Year	Area	Data
CV09_05	2009	WISMB/Lambay Deep	MBES (EM3002D) bathymetry & backscatter
CV09_26	2009	WISMB	MBES (EM3002D) bathymetry & backscatter, Geo-Source 400 sparker
CV10_01	2010	WISMB/Lambay Deep/CFZ	MBES (EM3002D) bathymetry & backscatter
CV11_10	2011	Queenie Corner	SES 5000 pinger
CE14_01	2014	Lambay Deep	Geo-Source 400 sparker
CO24_18	2018	Queenie Corner	MBES (EM3002) bathymetry & backscatter

Pockmark Table

[Click here to download Supplementary Material \(for online publication only\): S1_Pockmark_table.docx](#)

Gas Parameters Table

[Click here to download Supplementary Material \(for online publication only\): S2_Gas_table.docx](#)

Queenie Corner Grab Sample

[Click here to download Supplementary Material \(for online publication only\): S3_Queenie_Corner_grab.jpg](#)

*Credit Author Statement

Mark Coughlan: Conceptualisation, Investigation, Formal analysis, Writing - Original Draft, Visualization

Srikumar Roy: Conceptualisation, Formal analysis, Methodology, Writing - Original Draft, Visualization

Conor O'Sullivan: Methodology, Formal analysis, Writing - Original Draft, Visualization

Annika Clements: Investigation, Writing - Original Draft

Ronan O'Toole: Investigation, Data Curation, Supervision, Writing - Review & Editing

Ruth Plets: Investigation, Supervision, Data Curation, Writing - Review & Editing

Declaration of interests

The authors declare that they have no known competing financial interests or personal relationships that could have appeared to influence the work reported in this paper.

The authors declare the following financial interests/personal relationships which may be considered as potential competing interests: